Towards Resilient Urban Stormwater Management in a Tsunami Reconstruction

A Scenario Discovery Study on Ōtsuchi Town, Japan

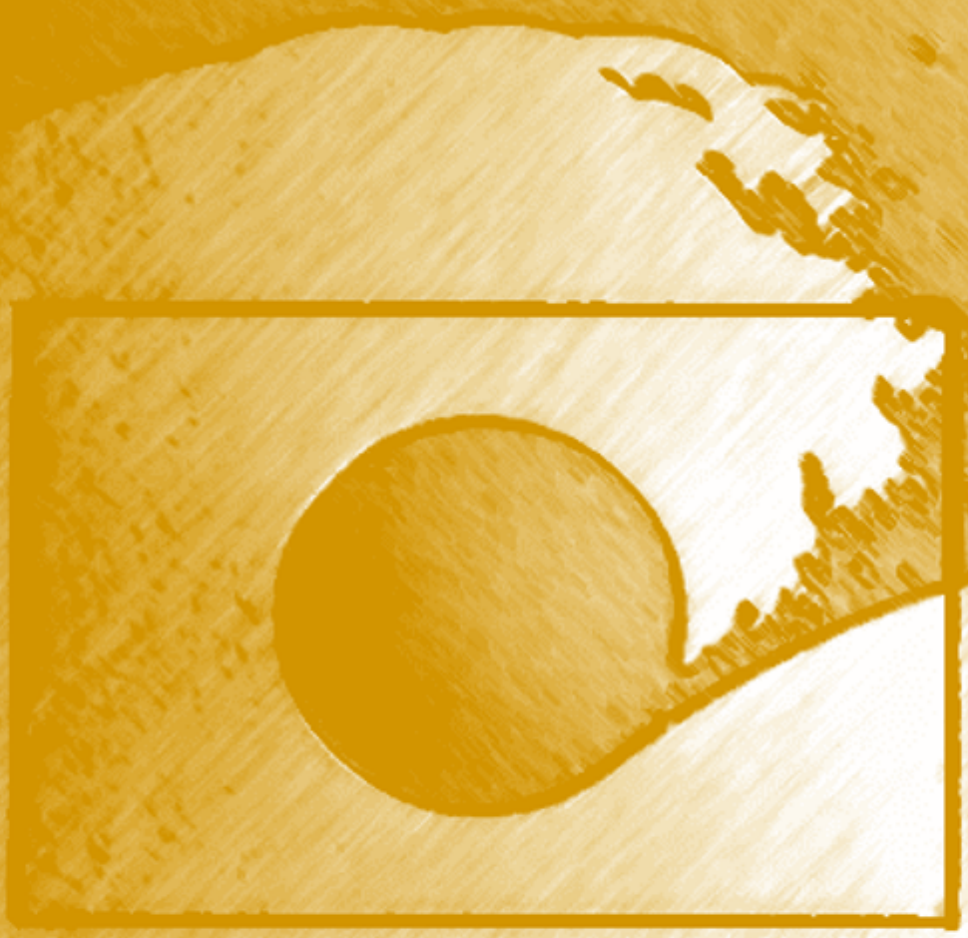

I.A.J. Nederlof

TU Delft

The cover image is adapted with kind permission of the author. The original illustration is titled 'Croix Rouge - Operation Japan Flags, 2011' made by Joel Guenoun, www.joelguenoun.com.

Towards Resilient Urban Stormwater Management in a Tsunami Reconstruction

A Scenario Discovery Study on Ötsuchi Town, Japan

by

I.A.J. Nederlof

to obtain the degree of Master of Science

at the Delft University of Technology,

Student number: 4516818

Date: 28 September 2019

Thesis committee:

Dr. ir. F.H.M. van de Ven	TU Delft, supervisor
Dr. A. Askarinejad	TU Delft
Dr. ir. J.H. Kwakkel	TU Delft
Dr. ir. G. Schoups	TU Delft

An electronic version of this thesis is available at `http://repository.tudelft.nl/`.

TU Delft

金繕い

KINTSUKUROI

the Japanese art
of repairing
broken objects
with gold
making them more
beautiful
after having been broken

Summary

In the face of climate change, urban stormwater management practices are subject to an uncertain context. More frequent and extreme rainfall events are expected in many urban areas. The extent how climate change will affect weather patterns is however uncertain. This challenges contemporary stormwater management practices. A post-disaster reconstruction of an urban area would potentially be an opportunity to anticipate climate change uncertainties from the initial design phase of new urban development. This would allow for taking advantage of the disaster recovery by rebuilding a more resilient stormwater system than was present before, in which the uncertainties are anticipated. A resilient stormwater system would thus be able to cope a wide range of plausible futures, rather than the average. As academic literature lacks insight on re-establishing resilient urban stormwater management in a post-disaster reconstruction, this thesis aims to gain more insights into what extent resilient urban stormwater management has been established in a Tsunami reconstruction, with regard to uncertainties on climate change and urban development.

A case study is conducted in which is focused on a) the conducted design approach, b) the realm of conditions for which the implemented stormwater system would be vulnerable and c) which solutions could be implemented to reduce the vulnerability, and reflected upon opportunities of an interdisciplinary approach from a stormwater management perspective. The selected study area is a town called Ötsuchi Town, in Northern Japan, Iwate Prefecture, which was severely hit during the 2011 Tsunami. The disaster necessitated a comprehensive reconstruction. To gain more insight into what extent a resilient urban stormwater system has been implemented, an exploratory modelling and analysis approach has been applied, which is also known as Scenario Discovery. Prime drivers of Scenario Discovery are exploring the system's performance for wide-ranging plausible futures by sampling the system myriad times with aid of computational modelling, and, the use of regional sensitivity mapping algorithms to understand the dominant factors that lead to insufficient system performance. The latter can be used as input for seeking vulnerability-reducing strategies. In this research, the Patient Rule Induction Method (PRIM) algorithm is used to understand the conditions for which the stormwater drainage system capacity would be exceeded, for an acceptable flooding level of 0.2 meter. Two open-source tools were combined: the conceptual stormwater flow model EPA-SWMM, and, python library EMA-workbench which provides the tools needed for applying Scenario Discovery and supportive analysis.

After the 2011 Tsunami a separate half-open sewer system was established in the reclamation area of Ötsuchi Town. No natural-based solutions, or Blue-Green infrastructure were implemented, even though the residential is adjacent to steep mountain slopes. The uncertainty parameters over which is sampled, include rainfall intensity, rainfall duration, external runoff coefficient, imperviousness, the hydraulic conductivity, Manning's roughness coefficient and depression storage.

The Scenario Discovery results show that the system has been built robust. For almost all locations no flooding occurrence arise from the sampling, even for very extreme rainfall events (>100 mm/hr, for a duration of 60 min). However, when the runoff coefficient of the external runoff from the mountain would be above 0.58, a small area in the northern part would be vulnerable. The dominant factors, are found with PRIM and the relative weights are with very high precision and recall found by pre-processing the sampling data with Principal Component Analysis.

It showed that for the vulnerable area, the hydraulic conductivity of the soil and the proportion of paved area are decisive in whether or not flooding occurs. Paying attention to certain thresholds, would significantly reduce the vulnerability of flooding occurrence. Given the high volumes for which flooding would occur, a preliminary feasibility study has been done for both a vegetative swale and infiltration trenches, in combination with a storage retention area in the lower lying area, such that the pressure on the stormwater drainage system can be released. The vegetative swale reduce the vulnerability significantly. The infiltration trenches seem to be effective for the lower rainfall duration and rainfall intensity. PCA-PRIM outcome showed that when implementing infiltration trenches in the vulnerable area, the impervious rate becomes relatively less sensitive in comparison with outcomes of PRIM with the reference situation.

More information on mountain runoff, soil properties and land use would enhance the accuracy of the results. In addition, since, no information is known yet on initial losses of mountain runoff, more information on runoff flow processes from the mountains would enable to perform joint probability analysis with the results of this research, to better assess whether or not the time is now to implement additional measures.

From the results of this research it seems that the urban stormwater drainage of Ötsuchi Town has been rebuilt very robust, however when the system would fail, no additional measures outside the grey infrastructure are taken. An interdisciplinary approach could have encouraged a more resilient stormwater management.

As this research shows that multiple commutative reconstruction measures could be found from a stormwater management perspective, the obtained information with applying Scenario Discovery, would have been useful to encourage an interdisciplinary approach during the reconstruction process. It is therefore suggested to explore the usage of Scenario Discovery on urban stormwater management even further, such that it enables to take advantage of the disaster reconstruction to establish a resilient urban stormwater management. An example would be to investigate whether the relative sensitivity of the uncertainty parameters would change when a less robust system would be examined. For example, for an urban drainage system for which the threshold would already be exceeded for lower rainfall intensity and duration than 100 mm/hr, and 60 minutes respectively. In addition, a coarse representation of rainfall events are considered in this research. Therefore it would be suggested to examine the applicability of region-specific storm profiles in combination with an exploratory modelling and analysis approach, to better assess the implication of the PRIM outcomes for implementing resilient urban stormwater management strategies.

Preface

This thesis is part of a project from TU Delft's Delta Infrastructure and Mobility Initiative (DIMI), which stimulates interdisciplinary work on the reconstruction of infrastructure in urban deltas. The project involves the investigation of the reconstruction of Ötsuchi Town, Japan, by a group of multidisciplinary professors and students. It gave the opportunity to visit Ötsuchi Town, and to learn lessons from the 2011 Great East Japan and Tsunami aftermath. Being a Water Management student, I looked from the urban water management point of view to the reconstruction of Ötsuchi. The many lessons learned in Ötsuchi were taken as starting point for the topic of this thesis, which is multidisciplinary in nature. Given that this research touch both technical science and social science in combination with learning lessons from a new context, I could not have wished for a better final project to complete the master Water Management at Delft University of Technology.

First of all, my heart goes out to all people who were affected by the 2011 Tsunami. During this project I was fortunate enough to hear the experiences of many people who were closely involved in the disaster and its aftermath. In each interview and lecture the incredible burden of the tsunami was reflected. I would like to pay tribute to all whom were committed to providing help during the disaster recovery and who aim to prevent such a disaster from happening again.

That having been said, I would like to share a story of what has been written down by S. Takezawa in his book 'The aftermath of the 2011 East Japan Earthquake and Tsunami', in which he captured all stories of Ötsuchi Town survivors about their experiences during the tsunami and its aftermath.

On 11 March 2011, the fishermen of Ötsuchi sailed ashore after a morning of fishing just North from Ötsuchi Town. They were amazed: never did they catch that much of fish on their way back to Ötsuchi as that day. Whereas normally the fish move with the current from north to south, this day all shoals of fish seemed to move in northern direction. Not much later, the earthquake happened, about 120 km south to Ötsuchi and the Tsunami warning was issued. Despite that we as humans, have so many tools and sophisticated models to measure and predict natural phenomena, no one could predict the destructive earthquake and tsunami that happened on 11 March 2011, which took the lives of so many people - but it seems that the fish did and swam away from the disaster.

This story underpins the perspective of this thesis. Even though we have so many sophisticated models, we must accept that we are unable to predict all natural phenomena. But what we can do is explore the conditions which would possibly induce a disaster, and seek for vulnerable-reducing strategies to anticipate these conditions. I genuinely believe in taking advantage of a disaster recovery to 'Build Back Better', if only the pieces are brought together. I am happy that during my thesis I could commit to finding these pieces, with the help of many others.

Many people were so kind to help me out to enable me to successfully complete this thesis. Therefore I would like to take the opportunity here to specially thank them.

I would like to thank all people of Ötsuchi Town, and in particularly Mio, who all were so kind to welcome us and share all their experiences with us, to pass on the lessons they had learned from the tsunami aftermath.

In particular, I would like to thank Mr. Higashi-san, for putting a lot of effort in collecting all the information needed to understand the reconstruction process, and for answering my never ending questions. Mr. Sasaki-san, thank you for telling your vivid story on Ötsuchi Town, and bringing me into contact with many researchers who could help me out. Also, Mr. Nakai-san and Mr. Fukushima-san, many thanks for welcoming me to University of Tokyo and providing me new perspectives on the reconstruction project. In addition, I would like to thank all people from the Japanese institutions who provided me with the datasets and helped me out with the Japanese language.

In the course of establishing this thesis, I have learned a lot from my committee members. I would like to thank Amin Askarinejad, for his input from a geotechnical engineering perspective, and for his encouragement throughout the research. His positivity in each meeting, genuinely motivated me to stay on a positive

path forwards. Many thanks to Jan Kwakkel, for providing the right tools to conduct this research and for guiding me in the learning process of Exploratory Modelling and Analysis (EMA). The use of the EMA-workbench, forms the foundation of this thesis and I am very thankful for that. In addition, due to his enthusiasm on the EMA approach, I too have become enthusiastic and could therefore surpass myself on many fronts. I would like to thank Gerrit Schoups, for the great supervision throughout the entire coarse of the thesis. His critical but constructive feedback enhanced this thesis definitely. Finally, I would like to thank my supervisor Frans van de Ven, for bringing me on board to the DIMI project. Thanks for guiding me well in establishing a great thesis. In particular, for giving me space to discover new pathways, for teaching me how to approach urban water management, and for bringing me on the right track in times when I was lost along the way. I think we have done more than well in achieving my goals I had established prior to the thesis. Many thanks for that.

Also, many thanks to all interdisciplinary professors and students involved in the DIMI project. It has been a great experience learning from each other, and to learn so many lessons from another context.

I feel lucky to have had the opportunity to finish my student career with this research, surrounded by many people who supported me. It gave me many new insights, new interests, and even brought me new friendships. After all is said and done, now I can truly say, it has been a great journey. A huge thanks to everyone who made this possible, and for making me ready for the next journey to come.

Arigatou Gozaimasu,

Ilse Nederlof
Delft, 2019

Contents

List of Symbols

The next list describes several symbols that are used in this report:

μ	mean value
σ	standard deviation
b_i	box found during the peeling-trajectory of PRIM, where i represents a step in the peeling process
C	runoff coefficient of external inflow from the mountains [-]
C_u	scaled and normalized runoff coefficient C
coi	cases of interest
Imp	Imperviousness, percentage of surface that is paved
Imp_u	scaled and normalized runoff imperviousness Imp
k	saturated hydraulic conductivity of the soil of the residential area [mm/hr]
k_u	scaled and normalized hydraulic conductivity k
n_p	Manning's roughness coefficient of pervious soil of the residential area [sec/$m^{1/3}$]
$ncoi$	cases not of interest
np_u	scaled and normalized Manning's roughness coefficient n_p
$PC7$	synthetic parameter expressed in a linear combination of scaled and normalized uncertainty parameters $Ri_u, Rd_u, C_u, Imp_u, k_u, np_u, sp_u$
Rd	rainfall duration [min]
Rd_u	scaled and normalized rainfall duration Rd
Ri	rainfall intensity [mm/hr]
Ri_u	scaled and normalized rainfall intensity Ri
s_p	depression storage of pervious soil of the residential area[mm]
sp_u	scaled and normalized rainfall depression storage s_p
x	uncertainty parameter
x_u	scaled and normalized uncertainty parameter x
y	output scalar representing flooding occurrence ($y = 0$ no flooding, $y = 1$ flooding)
$\boldsymbol{B}$	result of PRIM analysis: box set consisting of one or more boxes $\boldsymbol{B_i}$ that represent subspaces of the input domain, mapped to the cases of interest
$\boldsymbol{B_1}$	box 1: user-selected box from the initial peeling-trajectory of PRIM

$\boldsymbol{B_i}$ box *i*: user-selected *i*th-box from the *i*th peeling-trajectory of PRIM

$\boldsymbol{H}$ input domain of uncertainty parameters

$\boldsymbol{H^*}$ input domain of uncertainty parameters of run II, with $\boldsymbol{H^* \subset H}$

$\boldsymbol{H_0}$ input domain of relevant data for PRIM analysis, with $\boldsymbol{H_0 \subset H}$

$\boldsymbol{L}$ sampling data for which each component exists of ($\boldsymbol{X^{(i)}}$, $y_j^{(j)}$) where $\boldsymbol{X^{(i)} \in H}$

$\boldsymbol{L_U}$ normalized and scaled sampling data for which each component exists of ($\boldsymbol{X_u^{(i)}}$, $y_j^{(i)}$))

$\boldsymbol{L_{H0}}$ sampling data for which each component exists of ($\boldsymbol{X^{(i)}}$, $y_j^{(i)}$) where $\boldsymbol{X^{(i)} \in H0}$

$\boldsymbol{L_{PC}}$ rotated sampling data for which each component exists of ($\boldsymbol{X_{pc}^{(i)}}$,$y_j^{(i)}$)

$\boldsymbol{X}$ collection of uncertainty parameters

$\boldsymbol{X^{(i)}}$ experiment (sample) ID, a vector expressed by values for uncertainty parameters $\boldsymbol{X}$, it represents a plausible system state

$\boldsymbol{X_u^{(i)}}$ experiment (sample) ID, a vector expressed by values for scaled and normalized uncertainty parameters $\boldsymbol{X_u}$

$\boldsymbol{X_{pc}^{(i)}}$ experiment (sample) ID, a vector expressed by values for the synthetic parameters $\boldsymbol{X_{pc}}$

$\boldsymbol{X^{H0}}$ rotated set of experiments for which each component exists of $\boldsymbol{X^{(i)}}$

$\boldsymbol{X^{PC}}$ rotated set of experiments for which each component exists of $\boldsymbol{X_{pc}^{(i)}}$

$\boldsymbol{X^{U}}$ rotated set of experiments for which each component exists of $\boldsymbol{X_u^{(i)}}$

$\boldsymbol{X_{pc}}$ collection of synthetic parameters, which are expressed in linear combinations of the scaled and normalized original uncertainty parameters $\boldsymbol{X_u}$

$\boldsymbol{X_u}$ collection of scaled and normalized original parameters

C prefix for conduit

J prefix for node

OUT prefix for outfall

S prefix for subcatchment

List of Figures

List of Tables

1 Introduction

1.1. Stormwater Management in a time of climate change

In the last decades, the need for adaptation within urban stormwater management is increasingly acknowledged. Climate change effects such as droughts, and more frequent and extreme rainfall, are phenomena which are frequently addressed (e.g. IPCC, 2012). These events imply the occurrence of higher rainfall runoff in a shorter time, which puts pressure on the conventional urban stormwater system. In addition, the ongoing development of higher population densities along with highly concentrated economic areas, put areas even at higher risk: when the system fails, the damage will be larger. It is not a straightforward task to anticipate these changing conditions. The frequency and magnitude of extreme events are highly uncertain. Only time will reveal how severe climate will change, and how this would influence weather patterns. Conventional urban drainage systems are designed based on stable, long-term historical rainfall data, on the assumption that the weather is stationary. However, given climate change, engineers and policy-makers are now facing the 'end of weather stationarity' (Milly et al., 2008). Designing an urban drainage system, depending on merely historical data, does not hold water anymore. All these factors mentioned, call for new urban stormwater management approaches, aiming for resilient stormwater management.

Recently, the concept 'resilience' has been widely used among multiple disciplines. Resilience has become a buzzword to denote solutions that anticipate climate change (e.g. Butler et al., 2014; IPCC, 2012; Meerow, Newell, & Stults, 2016). On that account many definitions exist. In the context of urban stormwater management, Butler et al. (2014) define resilience as "*the degree to which the system minimises level of service failure magnitude and duration over its design life when subject to exceptional conditions*" (p. 349). In other words, a system is considered to be resilient when it has a backup mechanism that would reduce the damage it would have caused otherwise. A stormwater drainage system would be resilient if it is capable of enduring a wide range of load conditions, rather than only the average load conditions (Wardekker, de Jong, Knoop, & van der Sluijs, 2010).

Multiple resilient urban flood management strategies are proposed, in which the urban drainage system and its subsystems are considered to play a crucial role (e.g. Butler et al., 2014; Djordjević, Butler, Gourbesville, Mark, & Pasche, 2011; Mugume et al., 2015). Accordingly, different concepts and paradigms have shifted over the past decades (see also Fletcher et al., 2015). Conventional urban stormwater management is characterised by a concrete network of gutters and pipes, called grey infrastructure, that collects and discharges the rainfall runoff as fast as possible. This insinuates shifting problems downstream, and a high risk of system failure during extreme conditions. Nowadays, more resilient approaches are in vogue, to adapt to the increasing range of occurring load conditions. A prominent example is the Sustainable Stormwater Management (SSWM) approach (Goulden, Portman, Carmon, & Alon-Mozes, 2018). It involves concepts such as 'storage', 'retention', and the so-called 'Blue-Green solutions', which are solutions outside the conventional drainage network and focuses more on the root of the rainfall runoff. Examples are rain gardens, green roofs, and open surface water bodies, also referred as Low Impact Development (LID) measures. These interventions allow for reducing the vulnerability to urban floods, while minimizing disturbance of the natural drainage system.

To what extent these 'resilient' measures should be integrated into the urban drainage design, remains dis-

putable. In practice, there seems to be no blueprint how uncertainties concerning (future) system behaviour should be managed, and how it should be transferred into its final design. In academic literature however, a broad range of literature exist on guiding decision making concerning an uncertain context in general. Examples are frameworks as Robust Decision Making (RDM) (Lempert, 2019; Lempert, R.J., Popper, S.W., Bankes, 2003), or Decision Making under Deep Uncertainty (DMUD) techniques (Walker, Haasnoot, & Kwakkel, 2013). In which by use of computational modelling, vulnerability reducing strategies are aimed to find for a wide range of (uncertain) conditions.

In light of urban drainage planning specifically, Geldof, D.G., Kluck (2008) suggested the Three Points Approach: an approach that addresses the importance of considering three domains; 1) the technical guidelines and standards, 2) the day-to-day values and 3) the urban space and spatial planning (see also Fratini, Geldof, Kluck, & Mikkelsen, 2012). Not only is it important that an urban design meets the standards and desired service level (domain 1), also the day-to-day values ought to be maximized (domain 2), and levels that exceed the design standards should be considered to minimize damage of failure (domain 3). Where assessing the second adds to the urban quality of life, the third contributes to the degree of resilience. Nowadays, more regulations and concepts emerge along the same lines. For example in the Netherlands, certain measures (e.g. stresstest) are implemented that encourage municipalities to assess the vulnerabilities in their urban stormwater system with respect to climate change.

Also, just recently, Babovic, Mijic, and Madani (2018) explicitly addresses the need to explore the boundaries of the system behaviour and proposes how it should be assessed. However, not according the traditional scenario planning, where the main aim is to predict what conditions the system would be subject to. Following the viewpoint of RDM and DMDU, he underlines the approach of examining scenarios in a way such that the *what if* question is central. That is; exploring the conditions for which the system would not be sufficient anymore, rather than predicting the conditions that will happen. When even the unexpected situations are considered, a better understanding of the resilience of the system can be obtained. After all, it are the unexpected events, that no one has foreseen, that cause the biggest disruption. Exploring the set of scenarios, could reveal opportunities to make the system more resilient, in an effective way for a range of possible scenarios. Although not much applied on urban stormwater management yet (Babovic et al., 2018; Fischbach et al., 2017), Lempert et al. (2013) proved that applying RDM to be useful in anticipating urban flood risk.

To summarize, it is clear that stormwater management in a time of climate change is a dynamic realm in which academics, policy-makers and engineers are currently very involved in; it has been approached from different perspectives, aiming to reduce vulnerability to urban flooding. Significant new insights were gained, and new approaches have been examined and proposed. Yet, there is much more left to explore.

1.2. Tsunami reconstruction: An opportunity?

Rehabilitating the urban drainage system in existing urban areas can be difficult. Dense urban areas imply high construction cost to adapt the existing situation, which in turn impede the process. Therefore, it is useful to particularly address the importance of embedding resilience into urban drainage systems in new urban development.

This would for example apply to areas that are entirely devastated by a major disaster. Recent examples are cases such as New Orleans by Hurricane Katrina (2005), the coastline of Japan by the Great Eastern Japan Earthquake (2011), and Sint Maarten by hurricane Irma (2017). Devastation of this size necessitates a comprehensive reconstruction. This opens the opportunity to 'Build Back Better'. Build Back Better is referred as: *"The use of the recovery, rehabilitation and reconstruction phases after a disaster to increase the resilience of nations and communities through integrating disaster risk reduction measures into the restoration of physical infrastructure and societal systems, and into the revitalization of livelihoods, economies, and the environment"* (United Nations General Assembly, 2016, p.11) (see also UNISDR, 2017). From an urban water management perspective, Building Back Better would mean that advantage is taken of the possibility to consider resilient urban water management strategies from the very beginning of the urban development in the reconstruction, such that an integrated resilient urban design could be established, in which potential resilient stormwater management measures are embedded.

However, this is a complex task. In a post-disaster setting, it is urgent that recovery and reconstruction occur fast. Multiple disciplines and stakeholders are involved which creates an interplay of both conflicting and complementing objectives. Thus, if only the expertise on resilient urban water management would be

present, its multidisciplinary nature makes decision-making still complex. Mechanisms of the urban water system are integrated over the entire urban space, which makes urban stormwater management strongly dependent on the spatial planning (Goulden et al., 2018). Relatively soft type of interventions, such as street profiles and land use, affect rainfall runoff flows. In addition, physical infrastructures to enhance the resilience against natural hazards, such as tsunamis and earthquakes, could interfere the urban water cycle as well. In this sense, the optimum solution would be to integrate the objectives of multiple disciplines and implement an integrated set of measures. This allows for a high level of resilience on all fronts, potentially. However, this requires a well-integrated planning process of multiple disciplines.

Concerning 'Build Back Better', multiple tools are provided to accomplish integrated policy-making (e.g. UNISDR, 2017). In addition, significant research is done on adaptive water management practices and tools (Bertilsson et al., 2019; Jabareen, 2013; Mugume et al., 2015). However, in academic literature, remarkably little is known on what role the urban stormwater management obtains in the reconstruction design, and to what extent 'resilience' is embedded within the established stormwater management. Insight into this topic creates a better understanding of the challenges and opportunities of establishing resilient urban stormwater management in post-disaster areas. Which in turn, contributes to the aim of 'Build Back Better'.

1.3. Problem statement

It follows that a) the urban drainage sector is urged to adapt to uncertain load conditions in the face of climate change, and b) a post-disaster reconstruction could be an opportunity to include resilient stormwater management from the very beginning. These two worlds combined give rise to the topic of this research. Among urban drainage practitioners and academics, it is still an ongoing process of exploring how to deal best with uncertainties. Also, to date, no research has been conducted on how this is tackled within a post-disaster reconstruction. While the importance of 'Build Back Better' is frequently addressed.

Therefore, this research aims to gain more insight into how resilient stormwater management is approached in a post-disaster reconstruction, addressing climate change and model uncertainties. The scope of the research is limited to tsunami reconstruction, focusing on a case study in Japan that was hit by the 2011 tsunami. Facing multiple natural hazards, Japan is known for its resilience. It is therefore interesting to examine how stormwater management was established after the 2011 tsunami. Focus of research are the design approach of the urban stormwater system, the applied methodology and assumptions, its interdisciplinary character, and the degree of resilience of its final design.

These topics will be examined along the following research questions:

RQ1: How was stormwater management approached as regards its design (method, assumptions, input, criteria, final design)?

RQ2: Under what conditions would the stormwater system not be sufficient (flooded streets > 0.2 m)?

RQ3: What would be feasible measures to improve these conditions?

RQ4: How could these measures be anticipated and/or encouraged by an interdisciplinary approach within the tsunami reconstruction?

Key in answering these questions is the application of exploratory modelling and analysis to a real case. This allows to learn lessons from i) how uncertainties on stormwater load conditions are tackled in a reconstruction context, ii) how exploratory modelling could aid in assessing the resilience of a stormwater system and iii) the complementary interests across disciplines from a stormwater management perspective. The case that is studied is a town called Ötsuchi Town in Northern Japan (Tohoku, Iwate Prefecture). The 2011 Earthquake and Tsunami caused huge destruction of many parts of Ötsuchi Town, including the central district of the town, which used to be a dense residential area. A comprehensive reconstruction was required. In this research, the establishment of the urban stormwater drainage system of the central district of Ötsuchi Town is closer examined.

The opportunities and challenges discovered in this research, contribute to the dynamic scientific research on urban stormwater management. In addition, the lessons learned from Ötsuchi Town could inspire practitioners, by learning from another context.

1.4. Outline

In this report the conducted research and results are discussed. In chapter 2 the theoretical background is elaborated, which is the foundation for the methodology applied. Principles of both urban drainage design and scenario discovery are explained here. An overview of the research approach is given in chapter 3. Characteristics of Ötsuchi Town and the tsunami reconstruction are provided in chapter 4. The first results considering research question 1 are also explained in chapter 4, which serve as input for both the establishment of the SWMM model and experimental design. Accordingly, in 5 the stormwater management model layout and corresponding layout assumptions are elaborated. Also, the input domain for the experimental design is provided here. The outcomes regarding research question 2 and 3 are given in chapter 6. Whereafter the outcomes are discussed in the discussion chapter 7, including the reflection concerning research question 4. Final conclusions and recommendations of this research can be found in chapter 8.

2

Theoretical Background

2.1. Stormwater Management principles

The basic principles stated in this chapter are derived from the urban drainage book of Butler and Davies (2011). This book contains a sophisticated compilation of the fundamentals for urban drainage practices. The basic principles are complemented with recent developments on the concerned topics.

2.1.1. Conceptualization

Defining resilient stormwater management

Stormwater management is closely linked to the urban water cycle. Its aim is to prevent urban flooding which is induced by stormwater. That is runoff generated by precipitation, mainly rainfall. In the natural hydrologic cycle, the majority of the precipitation is infiltrated in the pervious soil. This allows for groundwater recharge. In urban areas, the natural hydrologic cycle is interfered. Large parts are impermeable due to the large proportion of paved surface. This impedes the process of infiltration, and generates more and faster surface runoff, in contrast to rural areas. Stormwater management concerns reducing and managing the peak surface runoff by means of a) urban drainage infrastructure through which runoff is conveyed and b) 'soft measures' that influence how much water end up in the drainage system. In general, these soft measures are related to the concept of resilience. (Butler & Davies, 2011)

Following the definition of resilience mentioned in chapter 1, this study considers resilient stormwater management to be a robust urban drainage system, that is able to endure a wide range of load conditions, in combination with implemented soft measures, that both reduce the runoff peak and the vulnerability of the system, such that damage is limited when exposed to extreme conditions.

Urban drainage system

An urban drainage system consists of a network of channels, either natural or conduits (or both). When urban drainage systems are discussed, usually it is referred to drainage systems consisting of mainly conduits. That applies to this study as well. Two main types of urban drainage systems can be distinguished: 1) Combined sewer system and 2) Separate sewer system. In a combined sewer system, both wastewater and stormwater runoff are collected and conveyed through the same drainage pipe. This water is treated in a treatment plant before it is discharged onto surface water. In a separate system, wastewater and stormwater runoff are distributed separately. Here, the wastewater is conveyed towards the treatment plant. The collected stormwater runoff is usually discharged to a nearby surface water or stored in a retention area. A separate urban drainage system can be beneficial over a combined system, if very high runoff peaks occur regularly. When the design discharge capacity of a combined sewer is exceeded, a so-called combined sewer overflow is required: untreated sewage is discharged onto surface water bodies. This harms the environment. The scope of this study concerns a separate stormwater system.

Soft measures

Soft measures include measures that are more concerned on the root of the problem by increasing infiltration and retention capacity. Dependent factors which can be influenced are the proportion of impervious land use, and the conductivity of the soil by managing the drainage. Also, the water volume that needs to be stored

can be done in LIDS types like rain gardens, infiltration trench, vegetative swales, instead of solid concrete (Rossman, 2006). Which measure is most suitable is dependent on: the root of the load conditions, the extent of the load conditions, and the area characteristics.

Stormwater management in Japan
Stormwater management in Japan is characterized by managing very extreme load conditions. The country is subject to very high precipitation rates regularly. Along this line, almost all urban drainage systems in Japan are separate drainage systems (de Graaf & Matsushita, 2008). In general, the urban drainage consists of a large network of U-shaped half-open gutters that conveys the stormwater throughout the urban area. An example is shown in figure 2.1. To limit the scope of this research, the focus is therefore on stormwater management concerning separate urban drainage systems, with open conduits.

(a)

(b)

Figure 2.1: Examples of semi-open gutters to drain stormwater in Ötsuchi town, Kirikiri district. Source: I. Nederlof

2.1.2. Design approach

In the initial design phase of the urban drainage system, there are two important flows to consider: rainfall and stormwater. (Recall that stormwater is defined as surface runoff generated by rainfall.) Rainfall analysis should be conducted to assess what magnitudes of surface runoff the drainage system could be exposed to. This enables to derive a design storm, that is used as design criteria for the system dimensions. Subsequently, the distribution of stormwater is examined. Finally, when considering resilience, the exceedance of the system should be assessed.

Rainfall analysis
Rainfall analysis concerns deriving relations between the duration, intensity and frequency of extreme annual rainfall events. These relations are captured in a so-called Intensity-Duration-Frequency (IDF) curve. This is done by analysing historical rainfall data. In general, intensity is inversely related to duration. The longer the rainfall event, the lower the average intensity. Also, the lower the probability, the higher the intensity values. The frequency (i.e. probability) of an annual maximum rainfall intensity over a specified duration is determined based on Weibull plotting position plot (Weibull, 1939). This can be fitted with a statistical distribution, for which the log-Gumbel or GEV distribution for extreme values is frequently used (El Adlouni

& Ouarda, 2013).

Based on the IDF-curve, a design storm can be chosen by selecting a specific return period with corresponding intensity and duration. This intensity is thus an average for the considered duration, which implies that the design storm is equally distributed over time. This is called block rainfall. However, in reality a rainfall event is not homogeneous over time. An extreme event has typically a high peak over the course of the event, whereas in the remaining time the intensities are significant lower. Therefore, block rainfall is a coarse representation of a specific rainfall event. However, block rainfall is easy to apply and understand. More sophisticated storm profiles are often country specific, and not further addressed here.

One main assumption of probability theory is that the concerned relations are stationary in time. Considering climate change, it is uncertain how the IDF-relations would possibly change in the future. In light of the end of weather stationarity, Cheng and Aghakouchak (2014) proposed an approach to assess the non-stationarity of IDF-curves, based on Bayesian Interference. This is a method to estimate probability, by iterative adding more 'evidence', or information, to check whether the stationary holds as more information is added. Referring to rainfall data, adding information means, adding data from a sequent year. A changing probability curve by adding that year, would imply a certain degree of non-stationarity within that time-frame, and thus a degree of uncertainty within the considered IDF-curve.

From rainfall to stormwater
How much rainfall results in stormwater, depends on both the rainfall and the subcatchment characteristics. This can be explained according the hydrological processes that are involved. The rainfall-runoff processes are shown in Figure 2.2.

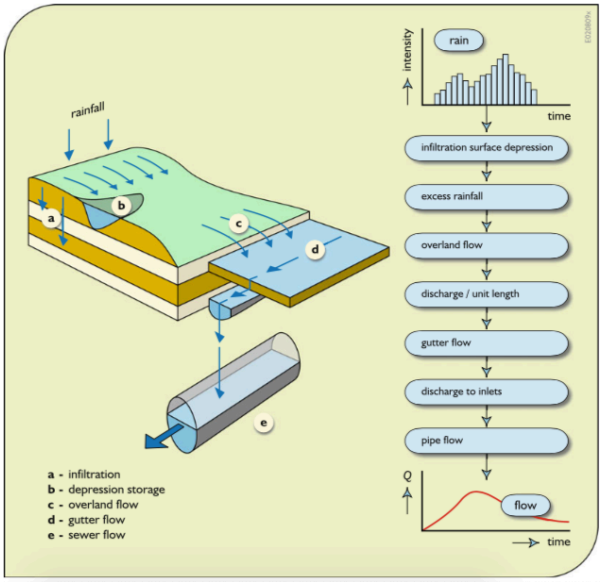

Source: Loucks and van Beek (2017)

Figure 2.2: Rainfall-runoff processes

The initial losses of rainfall are interception and depression storage. Rainfall that is captured on green leaves, and roofs for example, is intercepted from flowing to the surface. This is referred as interception losses. In addition, water that is captured in small holes and cracks between bricks or other surface objects, is restricted to flow elsewhere. This rainfall, that is trapped in multiple small depressions, is considered as depression storage. The quantities of the losses are expressed in mm. When considering a very intense rainfall event, in a very urbanized area, the interception and depression storage losses are relative small in comparison to the other fluxes. However, for an urban subcatchment that has a larger pervious area, the losses are more significant and should be account for. There are no standard rules, however, for when it should be account for or not as this can vary with context. Hence, it is up to the civil engineer to decide. Moreover, rainfall can evaporate as soon as it reaches the surface. When considering only single rainfall events, this is negligible. No evaporation takes place during a heavy rainfall event.

Part of the remaining flow infiltrates into the soil. The proportion depends on the type of soil and antecedent conditions; mainly its infiltration capacity and the moisture content are dominant factors. During the course of the storm the infiltration capacity decreases. This can be represented with the empirical equation of Horton. When applying this equation, maximum and minimum infiltration rates should be estimated with care, as well as the decay rate. Another representative equation for infiltration is the Green-Ampt's equation. This more physical-based approach, assumes a distinct wetting front between the lower soil and the upper soil layer. This equation is based on only three variables, hydraulic conductivity (saturated permeability), initial moisture content and the suction head.

When excess rainfall exceeds the infiltration capacity, surface runoff is generated. How much time it takes to enter the urban drainage system, is dependent on the surface slope, surface roughness, the width of the flow path and the wetted perimeter of the flow. It is method-dependent how overland flow is assessed. This will be explained in more detail in the next paragraph.

Rational Method vs Computational modelling
Flow (or runoff) modelling can be used for either design purposes or analysis of the system. There are two kind of methods distinguished here: the Rational Method and computational modelling.

Key in the Rational Method is the use of a so-called runoff coefficient that translates precipitation to runoff. The runoff coefficient accounts for influential factors on the generation of surface runoff, such as slopes, surface type, initial moisture content. The Japanese guidelines recommend a runoff coefficient between 0.10 to 0.30 for forestry slopes (MLIT, 2015a). For mountains with a steep slope a runoff coefficient of 0.5 is recommended. As many urban areas in Japan are sloped areas above 15%, a long-term experiment research was conducted on the runoff generation for different surface types and rainfall duration in Japan (Masatugu, n.d.). The surface type classified as 'Mostly forested mountain area' showed to have 50-55% runoff for rainfall intensity values from 100-120 mm, after initial losses, where the initial losses are the losses of precipitation until it causes any runoff, interception and infiltration into the soil.

The Rational Method is more simplistic and can only be applied for design purposes, whereas the latter is characterized by using sophisticated computational modelling software based on mathematical equations that represent the flow, and is more appropriate to use for analysis as well.

Secondly, computational software can be used to either design and/or analyse the urban drainage system. This is appropriate for analysing LIDS, and 'what if' conditions. In these applications, flow is described according the Saint-Venant equations: the momentum equation and the continuity equation (see also Chow, 1959). The first relates flow to driving forces and resistance. The second, is the equation of mass conversation. Solving these equations entails high computational cost. Therefore when assessing peak flow, the momentum equation is often simplified, which is acceptable under shallow wave conditions, for which bed slopes are balanced with friction slopes. In this case the Manning's equation can be applied. This approach is known as the Kinematic Wave approximation, characterized by solving the following equations:

$$\frac{\delta d}{\delta t} + \frac{\delta q}{\delta x} = i_e \tag{2.1}$$

$$q = \frac{1}{n} s^{\frac{1}{2}} d^{\frac{5}{3}} \tag{2.2}$$

where: d = flow depth [m]
t = timestep [s]
q = flow rate per unit width [$m^2 s^{-1}$]
x = longitudinal distance [m]
i_e = effective rainfall intensity [$m s^{-1}$]
n = Manning's roughness coefficient [$s m^{-\frac{1}{3}}$]
s = slope [-]

The effective rainfall intensity is the rainfall intensity minus the losses. Equation 2.2 is derived from Manning's equation, under the assumption that the cross-sectional flow width »» depth. The Manning's roughness co-

efficient differs per surface type. 'Rough', or impervious surface are represented with a higher Manning's n, than for example concrete.

Accordingly, flow routing in open channels can be represented with the Kinematic Wave approximation as well. In this case, the continuity equation is applied on the incoming and outgoing channel fluxes.

In the basic urban drainage models, system exceedance is represented as flood volume lost from the drainage system, or simplistically assigned to a 'flood volume storage', and rerouted back when the available capacity allows it to. When particularly interested in flood routing, more advanced software could be used in which the urban drainage system flow routing is combined with surface overland flow for flooding. Such 1D-2D models are increasingly emerging, however, these are very computational and data-intensive.

2.2. Scenario Discovery

2.2.1. Exploratory Modelling & Analysis

As mentioned above, computational modelling can aid in examining the response of the urban drainage system at hand as a computational flow model represents the system's behaviour. It can provide insights that cannot be obtained otherwise. However, a single model consists of many uncertain factors for which a state (parameter value), is chosen based on knowledge about plausible ranges. In addition, certain correlations between factors are assumed which can involve a significant degree of uncertainty too. Reasoning the expectations of future states based on either the outcomes of this one single model, or assumed correlations, can be misleading (Weaver et al., 2013). To illustrate, a single hydraulic conductivity of a soil is chosen from a range of theoretical values, when sufficient observational data is lacking. Also, when a certain design criteria derived from the IDF curve, is the starting point of the analysis for exceedance of the system, certain relevant outcomes could be missed, as these relations may not be so rigid anymore. If in reality the probabilities or assumed correlations are broken, this could generate surprising outcomes. It are these surprising outcomes caused by specific combination of factor states, we are aiming at when establishing a resilient system.

Trying to overcome this problem, when aiming to understand the conditions for certain outcomes of the system, is briefly said, the bottom-line of Exploratory Modelling and Analysis (EMA). It uses computational experiments, to analyze complex and uncertain systems (Bankes, n.d.). Multiple states of the system are generated, which are combinations of varying factors - the uncertainty parameters - within a plausible range that is based on a prior knowledge. Running these scenarios results in multiple model outcomes, and it are these outcomes that should be interpreted to base solutions on. So EMA is not aiming to predict future states, rather it aims to explore the range of possible outcomes, allowing to anticipate the vulnerabilities that are revealed. In contrast to aggregate the possibilities beforehand, it is done later in the process to get a wider understanding of the realm of possibilities. In this way you have the possibility to even consider and interpret these scenarios, which would otherwise be overseen. When applying this approach, it still remains important how the problem is framed, and what ranges are chosen, as this influence the outcomes where reasoning is based on. This can be anticipated by framing the problem at hand in multiple ways, and interpret the results accordingly.

2.2.2. Scenario Discovery

Interpreting the experiment results is done by sub-partitioning the input space (uncertainty parameters) corresponding to a specific region in the output space (system behaviour). This is referred as regional sensitivity analysis (Pianosi et al., 2016). The focus of traditional scenario approaches is merely on capturing the region with the most cases of interest (high coverage). However, to make these captured regions useful for decision-making purposes, it should also be interpretable, and contain mainly cases of interest (high density) (Bryant & Lempert, 2010). This makes effective use of the resulting information more likely. Examining the conditions corresponding to a certain output space, is a very complex task when dealing with a high-dimensional input space. For a two-dimensional plane this could be analysed visually, however for n-dimensions, this is impossible.

On this account, Scenario Discovery was established (Bryant & Lempert, 2010). This regional sensitivity approach is built on the principles of EMA, and involves an assemblage of statistical tools, which together aim to answer the question what combinations of uncertainty factors are decisive in the system's behaviour of interest. It is a frequently used approach to support decision-making concerning an uncertain context ever since (e.g. Lempert et al., 2013; Rozenberg, Guivarch, Lempert, & Hallegatte, 2014; Walker et al., 2013).

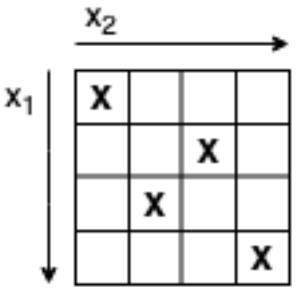

Figure 2.4: Latin Square: each row and column contains only one sample point. Accordingly, for a multi-dimensional dataset, Latin Hyper Cube sampling spans the whole space by generating only one sample point along the axis of a hyper plane

Scenario Discovery is a participatory, computer-assisted scenario development approach that accounts for three criteria of scenario quality: coverage, density and interpretability (Bryant & Lempert, 2010). In Scenario Discovery, a scenario is defined as: "[..] a set of plausible states in the future that represent the vulnerabilities of proposed policies, that is, where a policy fails to meet its performance goals" Bryant and Lempert (2010, p.). The main steps involved in Scenario Discovery are shown in figure 2.3.

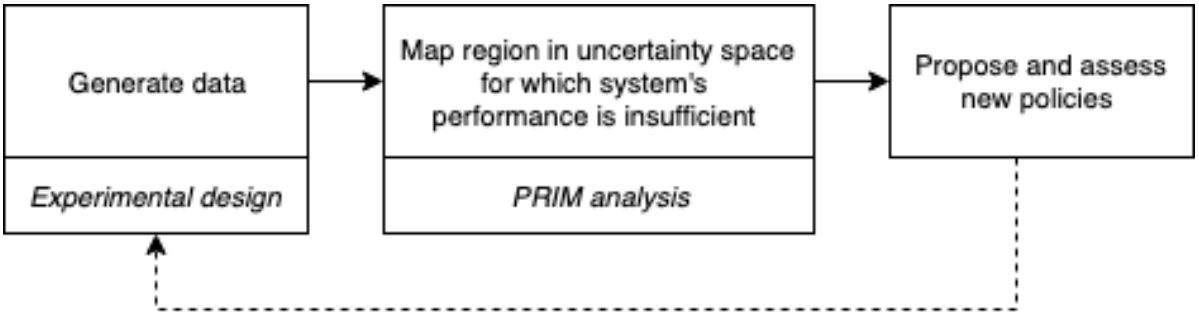

Source: modified from Bryant and Lempert (2010)

Figure 2.3: Steps of Scenario Discovery

Data generation: experimental design
The first step includes data generation. A certain simulation model, that represents the system's behaviour, is runned multiple times in an experimental design, in which the uncertainty parameters at hand are permuted over the input domain ($\boldsymbol{H}$). The input domain is a space defined by the uncertainty parameter bounds. For 2 uncertainty parameters this space can be visualized as a plane, whereas for 4 or more dimension this space can be visualized as a hypercube. Given the basic concept of EMA, the sampling is generally done using a random sampling technique, called Latin Hyper cube Sampling (LHS). LHS assumes a statistical uniform distribution for each uncertainty parameter, hence setting the bounds is critical. This technique is quite similar to Monte Carlo (MC) sampling, which is frequently used in parameter optimization for calibrating hydrologic models. However, LHS enables to span the input domain in a way such that it makes sure the entire input domain is spanned equally, and no subspaces are left behind. Each uncertainty parameter range is divided into equal amount of intervals, and only one sample point is generated per hyperplane within the multidimensional space. For illustration see figure 2.4. The output of the data generation consists of a learning set $L : X^{(i)}, y^{(i)}\}_{i=1}^{N}$, where an N amount of samples ($\boldsymbol{X^{(i)}}$) are sampled over the input domain ($\boldsymbol{H}$), for which each sample is mapped to outcome $y^{(i)}$ that represents the system's behaviour.

Classification
When the objective of the experimental design is to examine whether or not a criteria is met, any model's outcome for each sample is classified into a binary scalar before the data is analyzed; $y = 1$ if the system's performance is not sufficient, $y = 0$ if the system's performance is sufficient. The samples for which the criteria are not met, are the cases of interest (coi), and the samples for which the criteria are met the cases not of interest (ncoi). Given the purpose of stormwater management to avoid disruption caused by stormwater, considering urban drainage problems the binary output could for example be whether or not the urban drainage system's response remains under an acceptable level of flooding (h) at the locations of interest. In Japan an acceptable threshold level for flooding, or 'tatami-level', is about 0.2-0.3 m above surface level in

residential areas (de Graaf & Matsushita, 2008).

Data analysis: PRIM
The second step involves the mapping of the input space assigned to the output space of interest $\boldsymbol{B} \mapsto \boldsymbol{y = 1}$. To do so, either Classification And Regression Trees (CART) or a so-called Patient Rule Induction Method (PRIM) (Friedman & Fisher, 1999) can be used. Here, the focus will be on PRIM and is only briefly explained. More extensive explanations can be found in for example Bryant and Lempert (2010); Friedman and Fisher (1999); Kwakkel and Cunningham (2016).

Firstly, to better understand the key of the PRIM analysis, an overview derived from Greeven, Kraan, Chappin, and Kwakkel (2016) is shown in figure 2.5. It explains the trajectory of capturing the cases of interest (samples shown in black) into a subspace $\boldsymbol{B}$ of input space $\boldsymbol{H}$. The parameters, A, B, and C, represent the uncertainty parameters that are sensitive to the cases of interest. As can be seen, by restricting the parameter ranges, the cases of interest can be 'captured' within a subspace of the input domain. Accordingly, the subspace are described by the restricted parameters intervals. In this case, three parameters are shown. For 4 or more parameters, the input domain and the subspace is a hyper rectangular region.

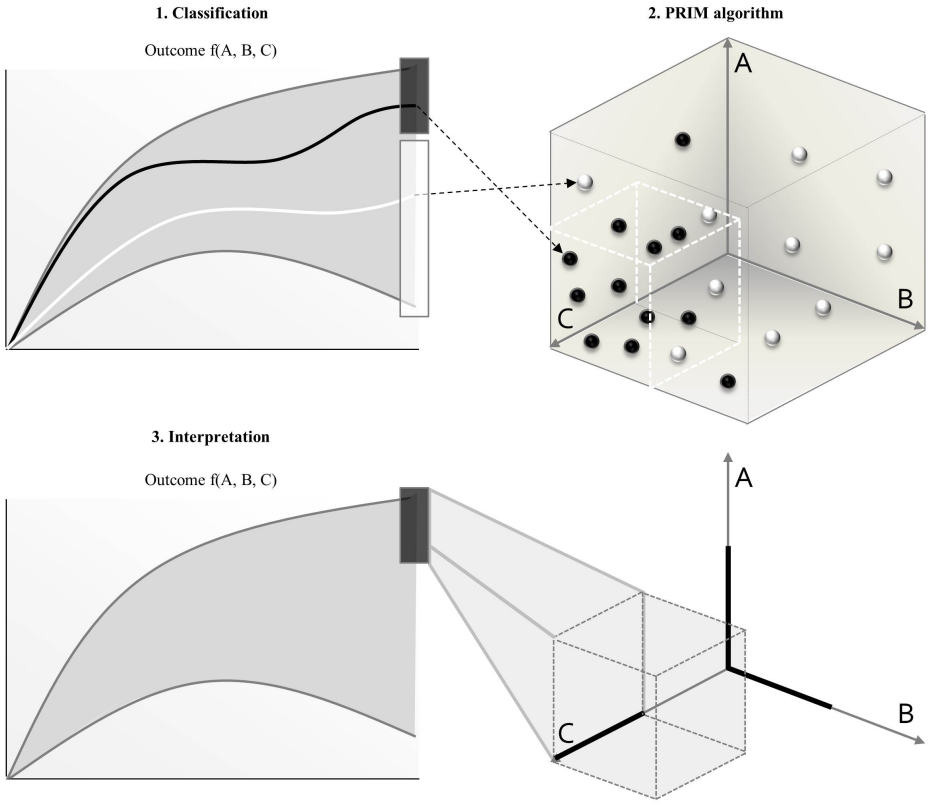

Source: Greeven et al. (2016)

Figure 2.5: Visualisation of mapping the input space to the output space of interest

PRIM is a lenient-hill climbing optimization algorithm in which its objective function seeks for the region in the output space with a higher mean ('the hill'), in comparison to the overall mean of the data-set. In case of binary output, this means that it seeks the region (or 'boxes' $\boldsymbol{B}$) of the input space, corresponding to the highest amount of relevant cases. In case of a 2-dimensional uncertainty space a final box can be visualized like figure 2.6.

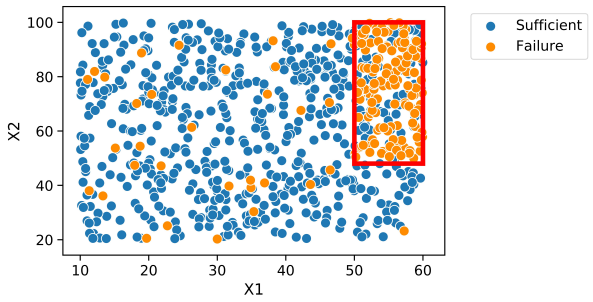

Source: modified from Bryant and Lempert (2010)

Figure 2.6: Thinking inside the box: PRIM

The 'lenient' optimization starts with an initial box $\boldsymbol{b_i}$ that covers all the data, and in each step it 'peels' a small sub box resulting into a new box $\boldsymbol{b_{i+1}}$ (Kwakkel & Cunningham, 2016). This peeling-trajectory is continued until a certain mass within the box is reached which is set by the user. Each box b_i within the peeling-trajectory is characterised by a specific density, coverage and interpretability, which are defined as follows (Bryant & Lempert, 2010):

- *Coverage:* Amount of cases of interest (coi) captured in b_i, out of the total of relevant cases.
- *Density:* Measures how precise b_i is by the ratio of amount of cases of interest captured in b_i to the total number of cases in b_i.
- *Interpretability:* This measure is subjective as it refers to the ease how interpretive b_i is for decision-making purposes. However, the amount of hyper-rectangular spaces, and the amount of parameters that are constrained can be an indication.

Such a peeling-trajectory is visualized in figure 2.7, in which each point represents a resulting box $\boldsymbol{b_i}$ in the peeling process, corresponding to a specific value for each criteria. PRIM is user-interactive, as the user can select the desired hyper rectangular box b_i, along the peeling-trajectory, which is a Pareto-optimum curve of the three criteria, density, coverage and interpretability.

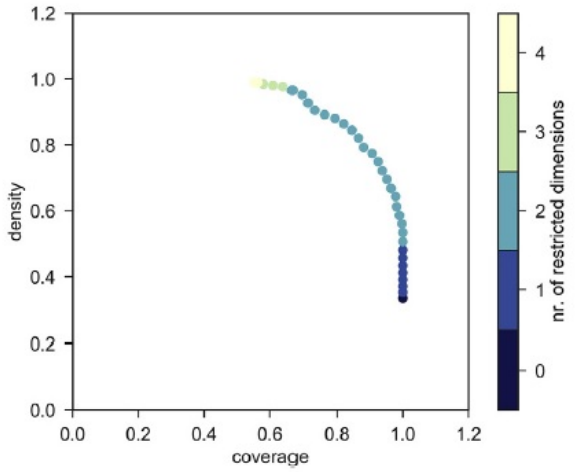

Source: Kwakkel (2017)

Figure 2.7: Visualization of an example peeling-trajectory of PRIM

The user-selected box b_i is the first subspace of $\boldsymbol{H}$ that maps the cases of interest, and is therefore referred as $\boldsymbol{B_1}$. If not all samples of interest are covered within that box, a next peeling-trajectory can be initiated. Accordingly, before initiating a next peeling-trajectory for finding subspaces for the remaining samples not covered by $\boldsymbol{B_1}$, can be done in two ways: either by removal of the samples covered by $\boldsymbol{B_1}$ or classifying the

samples covered by $\boldsymbol{B_1}$ as 'case not of interest' (Guivarch, Rozenberg, & Schweizer, 2016). In which the latter avoids assigning too high density value (false positive) to a box b_i, and is referred to as the 'guivarch method'.

The PRIM output consists of a set of m user-selected boxes $\boldsymbol{B}: \boldsymbol{B_1}, .., \boldsymbol{B_m}$, when all cases of interest have been considered with m distinct peeling-trajectories. Where each B_i, is a hyper-rectangular region within the input domain, defined by constrained intervals of the dominant input parameters, that explain the cases of interest. For each dominant parameter a quasi-p value is given to asses the relative importance of the parameters explaining the outcomes in $\boldsymbol{B}$. Briefly said, it is done by conducting a statistical bi-nominal p-test, whether or not constraining the concerned parameter significantly contributes to explaining $\boldsymbol{B}$ in comparison to the other parameters. A detailed explanation of the quasi-p value can be found in (Bryant & Lempert, 2010).

Since PRIM is an regional sensitivity approach, it also enables dominant control analysis, as the mapping is intrinsically described by the most dominant factors. However, regression analysis should be done if interested in the distinct weights of the factors. Also, Principal Component Analysis (PCA) could potentially aid in this and will be explained later (section 2.2.3).

Scenario Discovery can also be done with Classification Analysis and Regression (CART) methods. However, CART is less user-interactive and less transparent as it lacks the user-interactive option of selection the sub boxes of $\boldsymbol{B}$ that enables the consideration of the three mentioned quality criteria.

The EMA-workbench (Kwakkel, 2017), provides an open-source library package in python which enables to conduct Scenario Discovery, with a user-defined model. Also, it provides different tools that can support Scenario Discovery.

Sequentially, the outcomes of PRIM should be interpreted allowing for decision-making support. Whereafter policies can be explored and vulnerability reduction assessed with the same approach in an iterative way.

2.2.3. PCA-PRIM

The provided scenarios by PRIM, which are represented by hyper-rectangular regions, could possibly be improved when linear correlations between the uncertainty parameters exist. Dalal, Han, Lempert, Jaycocks, and Hackbarth (2013) proved this could be done by using Principal Component Analysis (PCA), to conduct orthogonal rotations on the original data. This induces that a triangular region in the output space, could better be captured when described by a (set of) new parameter(s) (the principal components), consisting of a linear combinations of the original parameters. The principal components represent the (co)variance of the data. For an n-dimensional data-set, n principal components exist.

The concept is clarified in Figure 2.8, with uncertainty parameters $x1$ and $x2$, and corresponding sample points. In (a) the cases of interest are concentrated in a triangular region, suggesting that it can be explained by a linear combination of uncertainty parameters $x1$ and $x2$. When this would be captured by the regular PRIM approach (b), the ranges would also include many cases that are not of interest. The data points are described according our common x-y coordinate system: the data is projected on the $x1$ and $x2$ axes. By finding the principal components of the data-set, $PC1$ and $PC2$, new axes are found to project the data on, each described by a linear combination of the original axes. Accordingly, the data is rotated, with new axes $PC1$ and $PC2$. The PC that represents a lower variance of the data-set, is more likely to improve the scenario quality when it is constrained. As can be seen in (c-e): when constraining $PC1$ would still involve many cases that are not of interest, whereas constraining $PC2$, would capture mainly cases of interest.

Whether this approach will improve the scenarios, is dependent however, to what extent the outcomes can be interpreted. To aim for higher interpretable, the original data-set X, is first centered and normalized for each parameter, as the variables can have different scales. The PCs are thus linear combinations of the scaled and normalized original parameters, which allows for comparison of the relative weights between the original variables.

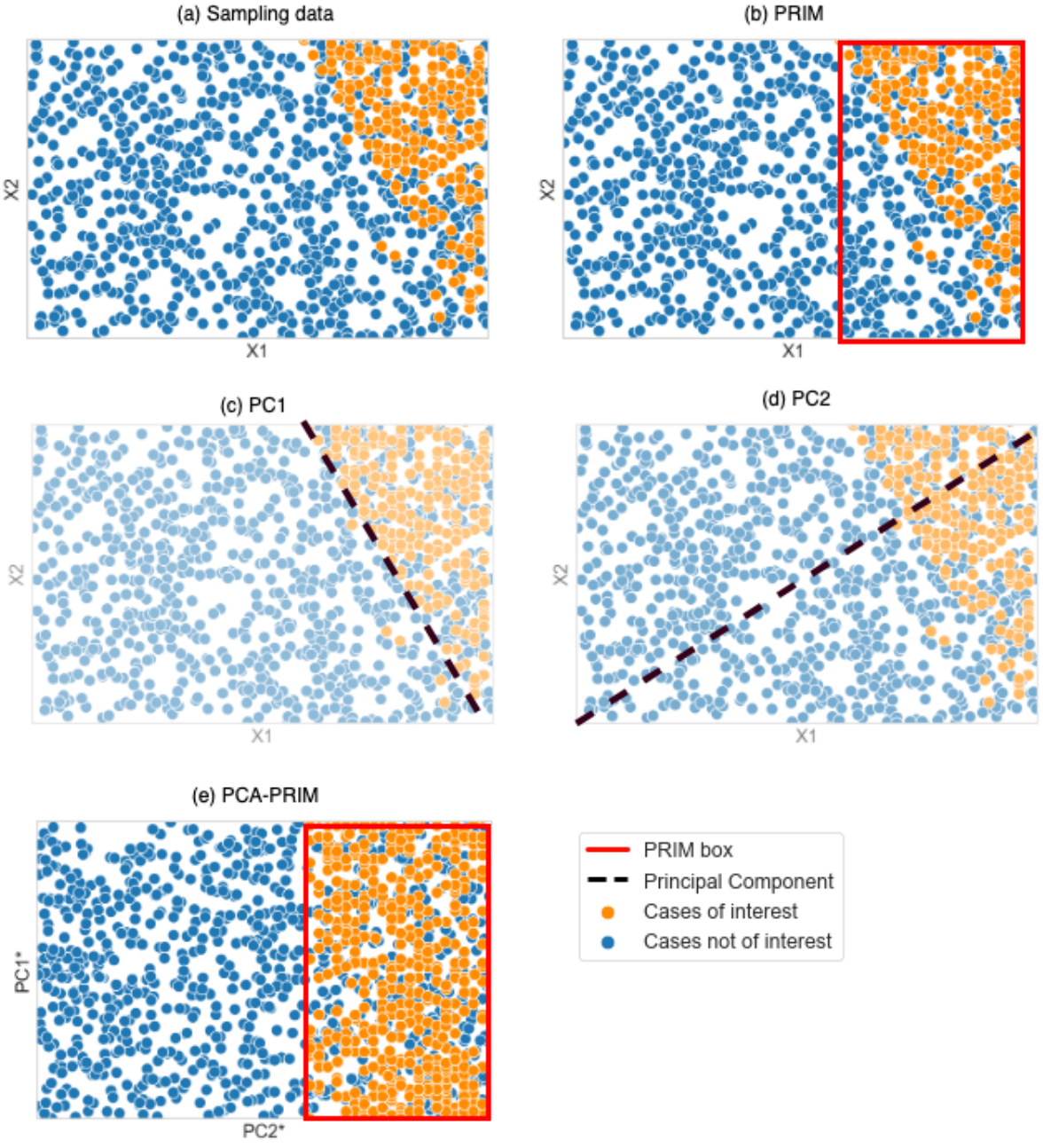

Source: modified from Dalal et al. (2013)

Figure 2.8: PCA-PRIM: Improving PRIM-analysing by rotating the data using Principal Component Analysis

3

Methodology

3.1. Conceptual research framework

It becomes clear from chapter 2, that bringing together Stormwater Management flow modelling with the Scenario Discovery approach would provide very useful insights for evaluating resilient stormwater management in a post-tsunami reconstruction. Therefore, to answer the research questions posed in section 1.3, a case study is conducted in which Scenario Discovery is applied on a real case: an implemented stormwater drainage system within a tsunami reconstruction. The selected case study is the reconstruction of Ötsuchi Town, Japan, and forms the foundation of this research. Applying Scenario Discovery on the stormwater system of Ötsuchi Town allows for evaluating the established system considering a wide range of plausible futures, by mapping the conditions and sensitive factors for which the system would not perform as desired, that is when disruptive flooding would occur. This in turn, will give insight into what extent a resilient system has been established and whether or not decisive factors can be found that serve as input for seeking vulnerability-reducing strategies that either could have been implemented in the initial design phase of the reconstruction, or in the future when the so-called adaptation tipping points are reached.

To enable the application of Scenario Discovery on a stormwater drainage system, two open-source tools are combined: EPA StormWater Management Model (SWMM) (US EPA, 2015) and EMA-workbench (Kwakkel, 2017). In which the first enables Stormwater simulation, and the latter provides all the tools for applying Scenario Discovery.

SWMM is a physically based, conceptual, discrete-time simulation flow model (US EPA, 2015), which enables the simulation of stormwater flow. It includes a conceptual model including Surface runoff, Groundwater, Infiltration, Surface Ponding and Flow Routing. Different infiltration models can be selected (e.g. Horton or Green-Ampt). In the stormwater network of Ötsuchi, water is transported through a network of rectangular semi-open channels. In SWMM this particular geometry can be selected and water flow can be modelled with Manning's equation. Principles of conservation of mass, energy, and momentum are applied wherever appropriate (US EPA, 2015). The software is open source and up to date. Also it includes tools to examine some LID (Low Impact Development) controls, which can be useful in seeking strategies that reduce vulnerability of the system.

The EMA-workbench is increasingly used for model based decision support (Kwakkel, 2017). The EMA-workbench is an python-library package, which can be used to develop an interface for existing simulation models, establish an experimental design for the concerned model, store the results and analyze them accordingly with for example the PRIM-algorithm, and other scenario discovery supportive analysis tools (Kwakkel, 2017).

To successfully evaluate the stormwater drainage system by using Scenario Discovery, multiple inputs are required. First, the set of uncertainty parameters that are possibly sensitive to flooding occurrence ought to be determined prior to establishing the model set up. Given both the research questions posed, and the theory on the design approach of stormwater management, two types of uncertainty parameters are distinguished here: 1) climate change related uncertainty parameters, which are rainfall intensity and rainfall duration of

a single rainfall event, and 2) urban area specific parameters that influence runoff routing which are mainly dependent on land use. The urban land use related parameters are selected to be at least, the percentage of impervious area, depression storage, and, hydraulic conductivity of the soil. Any additional context specific influencing parameters that should also be included in the Scenario Discovery, are determined based on the case specific context within the case study. Within this study the additional parameter is for example the external runoff coefficient from the mountain slopes. The specific uncertainty parameters and ranges that are selected to be relevant in this study are derived from the study area, and are therefore more elaborated later in chapter 5. First the general research approach will be elaborated. In addition to the context-specific uncertainty parameters, also information on the drainage system layout is required to set up a SWMM model: conduits dimensions, slopes, invert levels and if possible discharge data to verify the model. Moreover, information on the design approach are used to put the Scenario Discovery outcomes into context. Accordingly, the mentioned data-collection for a) determining the uncertainty parameter space for which the stormwater drainage system is evaluated, b) the stormwater system layout, and, c) information on what design approach has been applied, brings us to the first step of the research approach. The research approach is represented into a conceptual framework given in figure 3.1, and is further elaborated below.

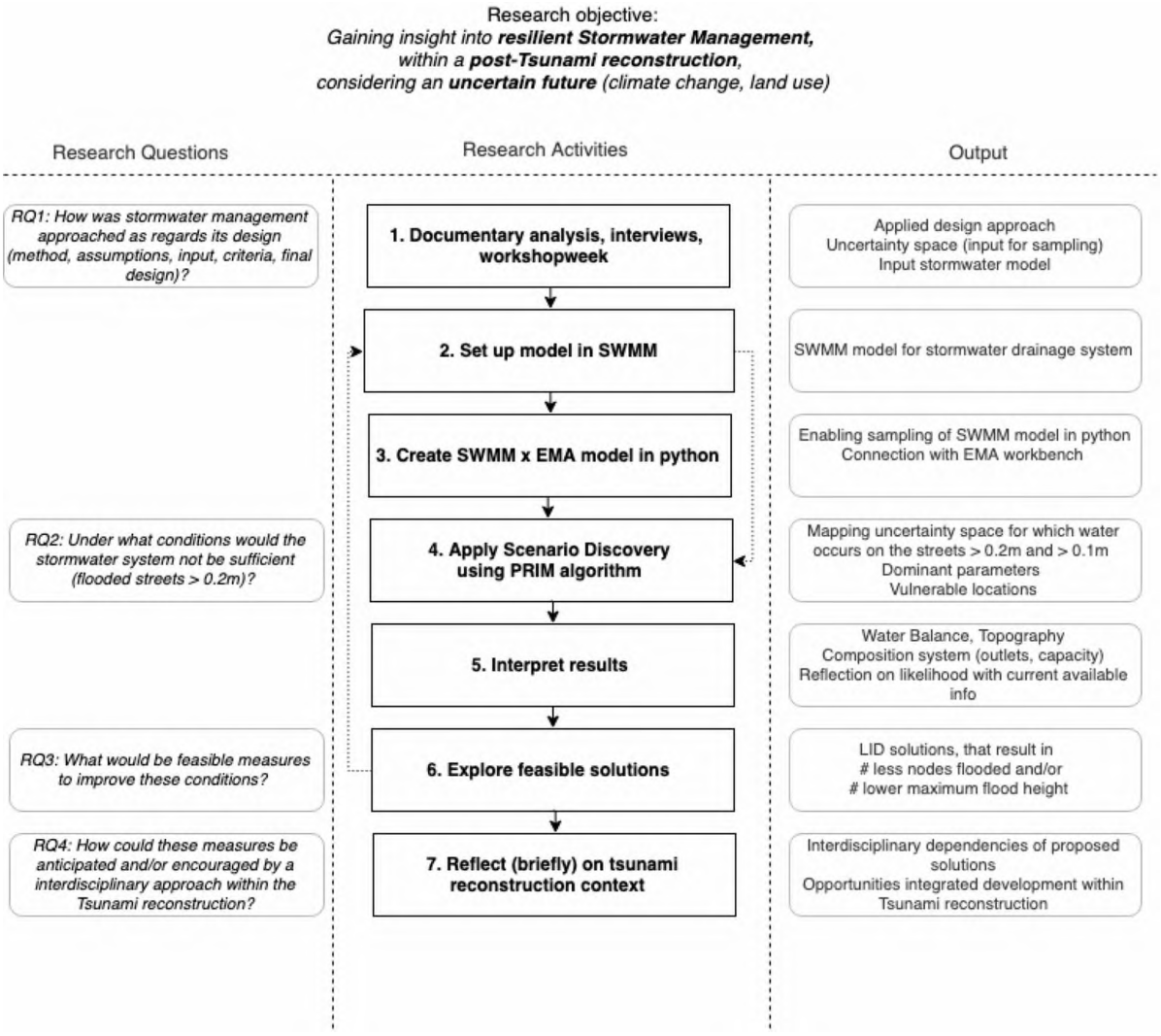

Figure 3.1: Conceptual framework of this study

3.2. Case study

First a case was selected: an urban area that has recently been subject to a tsunami, where after a comprehensive reconstruction was necessary: Ötsuchi Town, in Iwate Prefecture, Japan. Background information on

Ötsuchi Town is described in chapter 4.

To gain insights into the role of stormwater management within the reconstruction context, a workshop week was attended on learning lessons from the reconstruction of Ötsuchi Town. The workshop week included site-field excursions in Ötsuchi, 7 years after the tsunami had occurred. Both new urban development, part of the reconstruction measures, and, still existent damage caused by the tsunami were to be seen. Moreover, lecture were given by Ötsuchi Town officials concerning the reconstruction process, and reconstruction measures that were implemented. In addition, interviews were conducted with key figures of the reconstruction project, which are mentioned by Nakai (2013). Here, the data collection was focused on what design approach had been applied, what assumptions and design criteria were considered when establishing the stormwater system, and the characteristics of the stormwater drainage system that has been implemented. The collected data serves to obtain more background information on the role of stormwater management within the reconstruction, and as input for the experimental design set up for the Scenario Discovery.

The interviews were conducted with the project manager of the reconstruction project, the urban designers of the central district of Ötsuchi Town and the corresponding department of the government that concerns stormwater management. In comparison to structured interviews, semi-structured interviews allow to some extent more for asking supplementary questions to elaborate on relevant topics. However, in Japan, structured questionnaires are generally the way of asking questions approach officials in Japan. Also, for particular data collection like stormwater layout dimensions, structured questionnaires are sufficient. Therefore, both structured and semi-structured interviews are conducted. An overview of the addressed topics and interviewees can be found in table 3.1. Interview guides are provided in appendix A.1.

Table 3.1: Overview of conducted interviews and topics addressed

interviewee	**type interview**	**follow-up interview**	**design approach**	**interdisciplinary approach**	**characteristics Ötsuchi (e.g. soil, fresh water wells)**
project manager	semi-structured	questionnaire	x		x
urban planner	semi-structured	questionnaire		x	
technical advisor	semi-structured	-		x	x
governmental officials	semi-structured	questionnaire	x		x
researcher on fresh water wells	questionnaire				x

Also, documentary analysis and rainfall analysis were done to get information on both the system layout, and design inputs. The following topics were considered for the documentary analysis data collection:

- design criteria
- design assumptions
- decision-making choices
- soil characteristics
- land use / urban development
- topology
- rainfall
- system dimensions and layout
- dem

Rainfall analysis includes examining the IDF-curve and, extreme value analysis by fitting the annual extremes to a Log-Gumbel distribution. Long-term time series (30 years) of rainfall data with a resolution of at least 1 hour, is used for rainfall analysis. Rainfall data from the closest representative area available is used as proxy for the considered case study.

The information that has been retrieved is the input for both the SWMM model set up, and, the set of uncertainty parameters that are assessed by exploratory modelling.

3.3. SWMM model set up and settings

SWMM is used for simulating the stormwater flow for the current stormwater management system. Here, the steps of the model set up are explained, as well as the general settings. In chapter 5 the specific layout and uncertainty parameter ranges are given.

Model layout
The system dimensions of the established stormwater infrastructure is translated into a SWMM model layout. Common subcatchments with homogeneous characteristics like flow direction, slope and surface type, are aggregated, while ensuring a rectangular shape. This is according the assumptions how catchment overland flow is approached as described in Rossman (2006). The width of the catchment is determined by taking the average width perpendicular to the adjacent longitudinal channel flow. The slope of the subcatchment is assumed to be equal to the slope of the conduits, as it concerns open channel flow.

Flow routing
Flow is modelled by a kinematic wave approximation for shallow water (see also section 2.1.2).

Determining model parameters
The ranges of model constants and variables are derived from theoretical values suggested by Rossman (2006) (like ASCE (1992); McCuen (1996)) corresponding to the system characteristics of the considered study area. These include, the depression storage and Manning's roughness coefficient of both pervious and impervious areas. The soil parameters are derived from theoretical values as well (derived from the standard Astm and International (2006)), based on a sample size distribution of the study area. Imperviousness ranges are estimated based on the current land use layout and considered urban development plans.

Rainfall
The system's performance is assessed for single rainfall events, assuming a block rainfall profile. In this way no pre-assumptions are made on relations between rainfall intensity and duration. The ranges are derived from the corresponding IDF-curve of the area, taking a robust range.

Infiltration
Green-Ampt modified infiltration model is applied, which gives more representative values when the rainfall intensity is below the soil's saturated hydraulic conductivity, in comparison to the original Green-Ampt infiltration model (Rossman, 2006).

External inflow
Any external inflow is first directed towards an outfall node. This allows for that it is rerouted to the concerned subcatchment before it enters the stormwater infrastructure. This means it is equally distributed over the subcatchment first, in the same way rainfall is represented.

Flood height
SWMM provides flood volume timeseries for each node, which is a junction between two or more conduits. The flood volumes of the nodes are used as proxy for flooding occurrence. As we are interested in the flood height, the flood volumes are divided by the corresponding ponded area for each node. The area ponded of each node is assumed to be 0.5 times the area of the downstream subcatchment(s). As it concerns open channel flow, it is assumed that when the junction is flooded the surrounding area in the longitudinal conduit direction will be flooded as well. This is a simplification and therefore thresholds above 0.0 m and above 0.1 m are also considered within this study by comparing the different thresholds. However, the focus lies on the assumed flooding level of 0.2m.

Flow routing quality
Continuity errors of flow routing are considered to be adequate when they are below <10 % (Rossman, 2006).

3.4. Scenario Discovery

3.4.1. Steps towards an understanding of flooding occurrence

The steps to conduct Scenario Discovery according Bryant and Lempert (2010), and which are explained in section 2.2.2, are followed in this study. Aim here is to map a subspace $\boldsymbol{B}$ of input domain $\boldsymbol{H}$ to the cases of

interest as shown in figure 2.5. Input domain $\boldsymbol{H}$ is defined by $\boldsymbol{X}$, a set of i uncertainty parameters, x_i. The specific uncertainty parameters and their bounds are emerged from the documentary analysis, interviews and the set up of the SWMM model. Thus the ranges of the uncertainty parameters $\boldsymbol{X}$, represent plausible states of influential factors on flooding occurrence. To gain more insight in the range of conditions the system's capacity would be insufficient, the cases of interest (coi) are analyzed with PRIM. In this research the cases of interest are defined as: cases for which water occurs on the streets of 0.2m above groundlevel (= tatamilevel). The followed procedure is specified in a flow chart provided in figure 3.2 and is elaborated below.

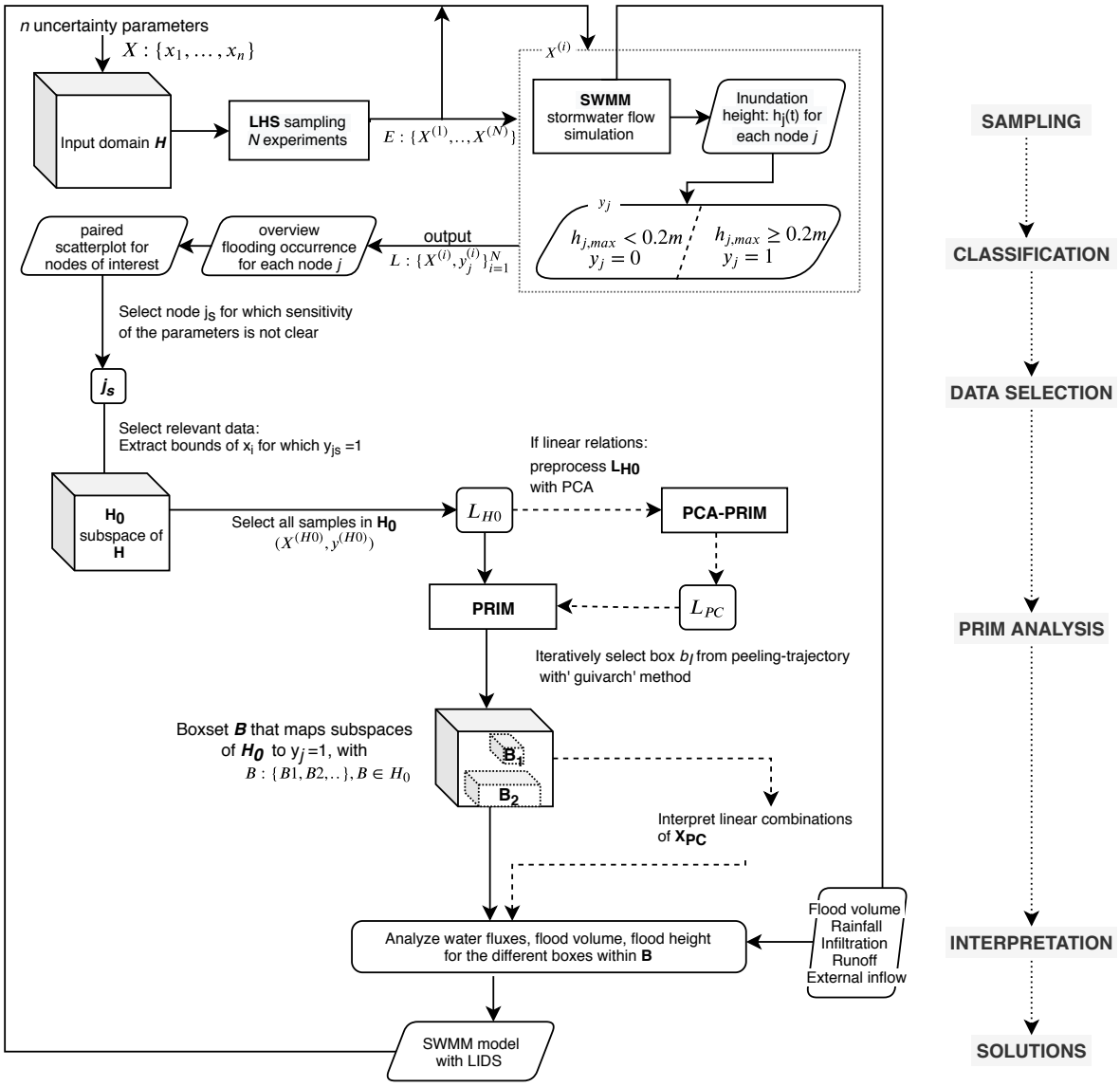

Figure 3.2: Scenario Discovery flow for this research

3.4.2. Sampling and classification

Sampling

The uncertainty parameters are sampled over uncertainty space $\boldsymbol{H}$ with a Latin Hyper Cube (LHS) sampling technique. LHS assumes a uniform statistical distribution. This allows for examining all plausible states, even the very extreme conditions. It is the latter we are aiming at when we consider a resilient stormwater management system. The outcome of the sampling is a set of experiments $\boldsymbol{E}$, consisting of N experiments $\boldsymbol{X^{(i)}}$ with i=1 to N. Each experiment corresponds to a unique combination of uncertainty parameter values, and represents a system state (1 scenario). Thus, an experiment is referred to as one sample of SWMM conducted with the EMA workbench. How sampling is enabled with the combination of SWMM and EMA-workbench

will be specified in section 3.5.

Enough samples should be taken to cover the entire input space. Therefore, iterative runs are done to ensure this for the desires interval resolutions. The experimental design is started with N = 1500 scenarios, until sufficient samples are taken to cover the whole uncertainty space. In addition, the upper and lower boundaries for the runoff volume are sampled, to set the runoff boundaries. A supportive tool provided by the EMA-workbench, called Dimensional stacking, is used to examine whether enough samples are taken: a pivot table in which each cell the ratio cases of interest to total samples represents for the dominant factors. The dominant factors, which form the columns of the pivot table, are feature scoring based and obtained using a CART technique (Kwakkel, 2017, see also).

Classification
The output metrics of the SWMM simulation, is non-binary: for each node j in the stormwater drainage system, a flood height (h) timeseries is given. Therefore a classification is required to specify the cases of interest (coi) for PRIM analysis. The classification is done by mapping whether or not h_{max} within the timeseries does exceed the threshold of 0.2m. This is done for each timeseries for l nodes j. Thus we obtain l binary outputs y_j: $y_j = 1$ for flooding occurrence (coi), and $y_j = 0$ for no flooding occurrence (cases not of interest, $cnoi$). The Scenario Discovery aims to map the dominant factors which explain coi, which represents thus the sensitive factors for flooding occurrence above a threshold of 0.2m.

3.4.3. Data selection

The output of the sampling and the classification is a learning set: $\boldsymbol{L}: \{\boldsymbol{X^{(i)}}, \boldsymbol{y_j^{(i)}}\}_{\boldsymbol{i=1}}^{\boldsymbol{N}}$, in which $\boldsymbol{X^{(i)}} \rightarrow y_j^{(i)}$. Prior to the PRIM analysis, a preliminary visualisation is done to examine the data and select the relevant data for further PRIM analysis. The relevant data, is defined by the boundaries of the cases of interest for each node j. The cases of interest lie in a subspace of the input domain, $\boldsymbol{H_o} \subset \boldsymbol{H}$. All samples within subspace $\boldsymbol{H_0}$ are selected and form the specified learning set $\boldsymbol{L_{H0}}$ which is analyzed with PRIM.

3.4.4. PRIM analysis

PRIM
The next step is the PRIM analysis, for which the EMA-workbench provides the tools. As can be seen in the flow chart, figure 3.2, the PRIM results into a boxset $\boldsymbol{B}$ with one or more sub boxes, each mapping a subspace of $\boldsymbol{H_0}$ to the cases of interest. The peeling-trajectory tradeoff curve provided by the EMA-workbench is used to select the sub boxes from the peeling-trajectory of PRIM, as mentioned in 2, according the three criteria density, coverage and interpretability.

The PRIM tool in the EMA-workbench enables to specify settings for the PRIM analysis procedure. In this research the 'guivarch' method is used as update function for selecting the sub boxes of $\boldsymbol{B}$. In each iteration of finding a new box $\boldsymbol{B_i}$ the samples already covered by the set boxes, are masked as not case of interest, rather than removing them entirely from the data set to avoid false positive errors.

PCA-PRIM
The EMA-workbench also enables pre-processing the sampling data ($\boldsymbol{L_{H0}}$) with the principal component methodology, which is referred to as PCA-PRIM (Kwakkel, 2017). Accordingly, if linear relations are suggested in the data, PCA-PRIM is applied. This can be summarized as the transformation of: $\boldsymbol{L_{H0}} \rightarrow \boldsymbol{L_U} \rightarrow \boldsymbol{L_{PC}}$, and will be explained here. The corresponding experiments of the data set that suggests linear relations, ($\boldsymbol{X^{H0}}$) within $\boldsymbol{L_{H0}}$, are first normalized and scaled to $\boldsymbol{X_u}$. This is done by subtracting the mean ($\boldsymbol{\mu}$) of $\boldsymbol{X^{H0}}$, followed by dividing the standard deviation ($\boldsymbol{\sigma}$) of $\boldsymbol{X^{H0}}$. See also equation 3.1:

$$\boldsymbol{X_u} = \frac{\boldsymbol{X^{H0}} - \boldsymbol{\mu}}{\boldsymbol{\sigma}} \tag{3.1}$$

where:

$\boldsymbol{X_u}$ = experiments expressed in scaled and normalized uncertainty parameters
$\boldsymbol{X^{H0}}$ = experiments $\in \boldsymbol{H_0}$ expressed in original uncertainty parameters
$\boldsymbol{\mu}$ = the mean of each uncertainty parameter over experiments $\boldsymbol{X^{H0}}$
$\boldsymbol{\sigma}$ = the standard deviation of each uncertainty parameter over experiments $\boldsymbol{X^{H0}}$

This result into a normalized and scaled experiments set $\boldsymbol{L_U}$, with ($\boldsymbol{X_u}$, y_j^{H0}). Hereafter, the principal components are found for the normalized and scaled experiments $\boldsymbol{X_u}$, which are the eigenvectors. The principal components form the synthetic parameters $\boldsymbol{X_{pc}}$. Each principal component is a linear combination of $\boldsymbol{X}$. The principal components form the columns for the orthogonal rotation matrix that is used to rotate $\boldsymbol{X_U}$. The experiments are now expressed in synthetic parameters, $\boldsymbol{X^{pc}}$, for which each component is a linear combination of the original scaled and normalized uncertainty parameters $\boldsymbol{X_u}$. This in turn, results into $\boldsymbol{L_{PC}}$: $\{\boldsymbol{X^{pc,(i)}}, y_j^{(i)}\}_{i=1}^{M}$, with M amount of experiments that were selected for the PRIM analysis ($\boldsymbol{X^{H0}}$).

As the experiments are now expressed in the synthetic parameters $\boldsymbol{X_{pc}}$, rather than the original parameters $\boldsymbol{X}$, the PRIM outcomes results into boxes described by the synthetic parameters $\boldsymbol{X_{pc}}$. Backwards interpretation is thus needed to interpret the outcomes of PRIM. This is done by analyzing the statistical moments, mean and standard deviation, and the boundaries of $\boldsymbol{H_0}$.

3.4.5. Interpretation and proposing solutions

Finally, all outcomes of the PRIM analyses, which consist of the dominant parameters explaining the cases of interest, are interpreted by analyzing the hyetographs and the hydrographs for the corresponding samples. What do the results mean for decision-making on resilient stormwater management? What are the reasons that for these conditions this particular area would flood? is aimed to answer.

The output for all experiments are aggregated, such as the hyetographs and the hydrographs, and classified for the corresponding sub boxes in $\boldsymbol{B}$. This allows for interpreting the outcomes of each sub box and comparison of the outcomes between PRIM and PCA-PRIM.

Conclusions drawn from the interpretation are used to propose solutions to reduce the vulnerability. If applicable, a preliminary feasability study is done on the proposed solutions by establishing a new SWMM model for the specific solutions.

3.5. SWMM x EMA

To enable the exploratory modelling with SWMM, SWMM needs to be operable in python to enable exploratory modelling by use of the EMA-workbench. Although some python library packages have already been released to enable the connection between SWMM and python (swmmio, swmmtoolbox), these are merely on reading the input and output files. The original SWMM code is written in another programming code (C+), and output data is stored in multiple and complex output files. Its attempts and developments enabling running SWMM fully from the python engine is still ongoing (see for example pyswmm).

A customized model, referred to as SWMM x EMA, is established. The model flow for a set of N experiments can be found in figure 3.3. Performing the sampling with EMA in combination with the SWMM x EMA model involves the following steps:

1. Settings the experimental design set up, which include i) the uncertainty parameter bounds, ii) the SWMM model template of the stormwater system that is examined, iii) and the sampling method and amount of scenarios should be specified for which the uncertainty parameters are permuted over the uncertainty space
2. The experimental design settings of 1) are specified in the EMA-workbench and the simulation starts iteratively for each experiment
3. The SWMM model template is modified according the parameter values within the experiment.
4. A new SWMM model follows from step 3) and a batch file is written with use of python, to enable starting running the SWMM model from python
5. The SWMM output which is specified as the output metrics y, is transformed into binary output. Which is in this study an acceptable flood level of 0.2m. Flood volumes timeseries are transformed into flood heights by dividing the flood volumes for each node. Accordingly, the maximum flood height of each timeseries for each location, are compared with the threshold of 0.2m and stored into a binary output y_j for each node j.
6. The sampling output of step 5) and additional swmm output variables used for supportive analysis, are stored in various outputfiles. These outputfiles are read with use of the swmmtoolbox python module,

and stored with use of the EMA-workbench and the swmm. All swmm outputs used in this study are provided in table 3.2.

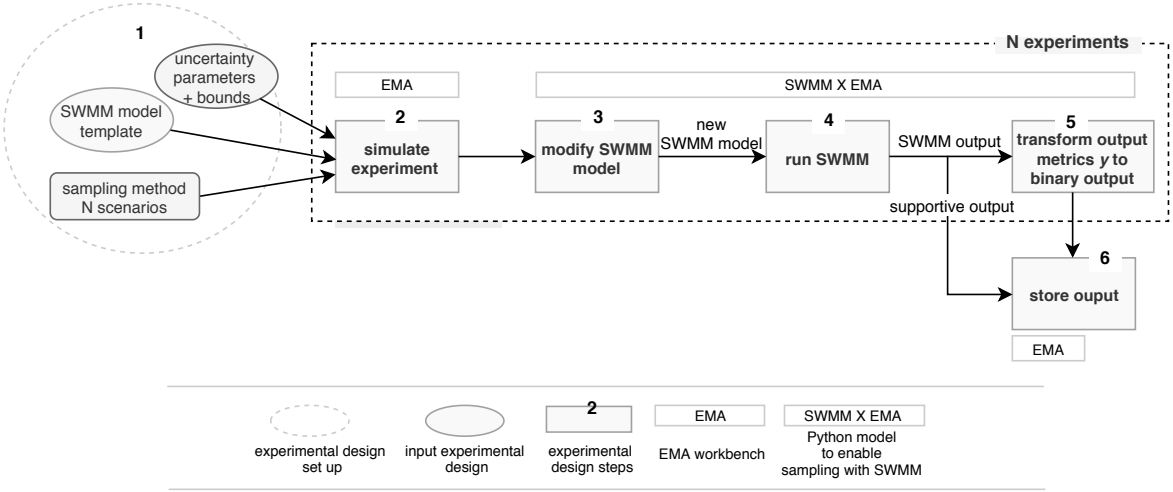

Figure 3.3: SWMM combined with the EMA-workbench with a customised model SWMM x EMA

Table 3.2: SWMM x EMA output files

SwmmxEma output	Used for	System	Data type	Units	Modifications of original swmm output
Volume stored ponded	Output metrics	Node	Timeseries	cms	
Height stored ponded	Output metrics	Node	Timeseries	hmm	Volume stored divided by area ponded (specific for each node)
Rainfall	Supportive analysis	Subcatchment	Timeseries	mm/h	
Infiltration	Supportive analysis	Subcatchment	Timeseries	mm/h	
Runoff	Supportive analysis	Subcatchment	Timeseries	cms	
Runoff rate - mm/hr	Supportive analysis	Subcatchment	Timeseries	mm/h	Runoff cms –>runoff mm/h
External inflow	Supportive analysis	External inflow	Timeseries	cms	
External inflow - mm/hr	Supportive analysis	External inflow	Timeseries	mm/h	External inflow cms –>External inflow mm/hr
Lateral inflow	Supportive analysis	Conduit	Timeseries	cms	
Total inflow	Supportive analysis	Conduit	Timeseries	cms	
Summary	Supportive analysis	System	Array	-	

3.6. Integrated approach within tsunami reconstruction

When all steps are succeeded, the questions posed in section 1.3 on how was water management approached, and under what conditions would the stormwater system not be sufficient can be answered. This, together with the outcomes on the examination on feasible strategies to reduce possible vulnerabilities allow for answering sub question 4 on what the the considered policy measures and/or conditions would mean for other disciplines in terms of measures in a reconstruction process or future adaptive planning. The opportunities and challenges with respect to an integrated reconstruction planning are discussed from a stormwater management point of view.

4

Study area: Ötsuchi Town

In this chapter the selected study area is introduced. The first section includes background information on Ötsuchi Town, such as the geographic location and climate characteristics. In the second paragraph an overview of the Tsunami reconstruction is given, where the focus lies on its final design. In the last section the design approach concerning stormwater management is discussed.

4.1. Characteristics of Ötsuchi Town

The selected study area is the central district of a town called Ötsuchi Town, which is located in Northern Japan, Iwate Prefecture (39°2129.7N, 141°5358E). See figure 4.1.

Figure 4.1: Location of Ötsuchi Town, Iwate Prefecture, Japan (39°2129.7N, 141°5358E)

Ötsuchi Town is a small coastal village (+- 10.000 inhabitants) with typical characteristics of a Ria coast: It is located in a valley between steep mountains, and the central district of the town is surrounded by two rivers that drain into sea.

The climate of the region is characterized as humid, with average temperature of 0.5 C during the winter months, and 24 C during the summer months (JMA, 2018). The average yearly precipitation value approximates 1330 mm (1988-2018) (JMA, 2018). In this area, precipitation rates can reach high values; maximum daily precipitation varies from 67 mm - 319 mm, during the period of 1988-2018. The average yearly precipitation and temperature pattern of Ötsuchi's neighbouring city Miyako, is shown in Figure 4.2. It is estimated that climate change will have impact on this region. The current trend of global warming in Japan, considering the next 100 years, is 1 degree higher than the global average (of the Environment; Ministry of Education Culture Sports Science, of Agriculture; Forestry, of Land, Transport, & Meteorological, 2018). In the northern region of Japan, Tohoku, it is estimated that more extreme (+0.1) rainfall patterns will occur, and overall it will

become dryer, with more frequent and longer periods of drought (of the Environment; Ministry of Education Culture Sports Science et al., 2018).

Figure 4.2: Average precipitation and temperature, Miyako 1988-2018 - Source data: JMA (2018)

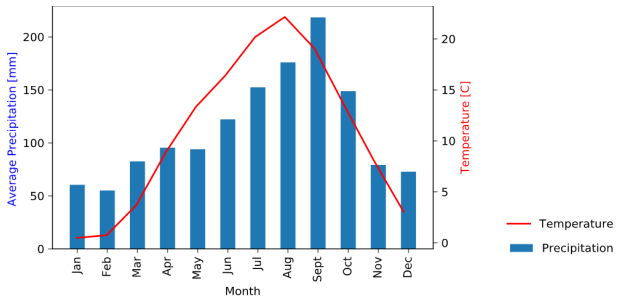

Figure 4.3: Study area: downtown of Ötsuchi Town (Machikata district)

Due to its geographic location, Ötsuchi is characterised by its rich aquaculture, and, the forestry in adjacent mountains. However, this geographic location makes the place also vulnerable to multiple natural hazards. It is a highly seismic active region, making it prone to destructive earthquakes and tsunamis. The region is subject to a Tsunami return period of 40 years (Esteban, Takagi, & Shibayama, 2015). Recently, in 2011, a 9 Magnitude earthquake hit Japan, inducing a disastrous Tsunami that washed away entire communities. Ötsuchi Town was one of the many villages that was severely hit (see also Figure 4.4).

The disaster took the lives of 1281 people in Ötsuchi Town, almost 10 percent of the total population before the disaster (Nakai, 2013). An area of 216,4 ha was totally destroyed. Particularly, the central district of the town (Machikata District) was severely damaged. Figures 4.5a and 4.5b show aerial photos of Machikata district before and after the tsunami. It can be seen that the town was completely destroyed. Machikata District used to be a dense residential and commercial area. After the disaster, a comprehensive reconstruction was required (Nakai, 2013).

4.2. Tsunami reconstruction design

4.2.1. Planning process

During the reconstruction planning of Ötsuchi Town, a combined bottom-up and top-down approach was applied (Nakai, 2013). The city was left behind without their governors, as the toplayer of the government had sadly lost their lives during the disaster. This induced the residents themselves to take responsibility for initialising the planning process and were closely involved ever since (Takezawa & Barton, 2016). The reconstruction was established by guidance of multiple parties provided by the national, or prefectural government: technical consultants, constructors and academics (see also Fukushima, 2017). Each district got their own technical advisor, to coordinate advice between the many stakeholders involved, such as the residents

Figure 4.4: Destructive site in Ötsuchi Town, just after the 2011 Tsunami. Source: A. Shimbun, 2011

and the consultants. The technical advisors of Machikata district were professional academics in the field of spatial planning. However, they were also managing other matters within the civil engineering domain, even it was not their expertise. This was necessitated due to limited available professional expertise during that time: many areas throughout Japan had to be rebuilt, which all needed a comprehensive planning team. In addition, a fast-paced development was necessary as many people had to be relocated.

4.2.2. Reconstruction measures

The overall reconstruction design is thus the outcome of a comprehensive planning process between consultants, residents and academical advisers. The design is characterised by a multi-preventive community planning: three types of tsunami disaster prevention are combined, as proposed by the prefectural government (Iwate Prefecture, 2011). That is, retreating from the tsunami danger by relocation to higher grounds, retreating from the tsunami by reclamation of residential area, and suppressing the tsunami energy.

The reconstruction of Machikata district includes the following key measures:

- the construction of a 14m height seawall
- the construction of 14m height floodgates in both rivers
- the raising of 31.1ha residential area by 2.2m (‘reclamation area’)
- assigning a retention area (‘lowland area’ adjacent to the sea)
- separate sewage system: stormwater network with semi-open conduits

The reconstruction measures are shown in figure 4.6. Also a cross-section of Machikata district is provided corresponding to the reconstruction design 4.7. T.P. is referred to as Tokyo Peil, the average sea level of Tokyo Bay, and is used as the standard height for national elevation.

To date, the reconstruction is still ongoing. The first houses have been built on the reclamation area and the sea preventive measures are (almost) finished (see figures 4.8).

(a) Before

(b) After

Figure 4.5: Machikata district before and after the 2011 Tsunami, Source: Ötsuchi Town, 2014

Whereas the previous seawall was only 6 meters height, now the city is enclosed by a massive concrete seawall and floodgates. The residential area is now concentrated, further away from the sea as the initial spatial plan of Ötsuchi, and closer to the foot of the steep mountains. The slopes can reach up to 20-50 % (Google Earth). The soil for filling the reclamation area was obtained from the mountains. And is referred to as decomposed granite. No precise properties of the soils are known and therefore estimated based on a soil sample.

The residential area will be a dense urban area, according the urban development plans (Otsuchi Town, 2014). Both the reclamation area and the lowland area were dense residential areas, before the disaster as seen in figure 4.5a. Now, these people should all be relocated, of which mainly in the much smaller reclamation area. However, it is expected that population numbers will decline, due to ageing population and people leaving after the disaster. The land use type of the residential area will thus probably be a mixture of 'green' and 'grey', rather than mainly concealed with pavement.

In addition to the infrastructural measures, the reconstruction plan is also very focused on non-infrastructural measures regarding disaster prevention. These include for example evacuation routes, locations. Also, a community center has been established as a meeting point, and education is considered important to pass on the awareness of tsunami danger towards future generations. Whereas the latter is aimed at retaining the retention area being an retention area, to prevent this tsunami hazardous zone from slowly being transformed into a residential area again.

4.3. Stormwater Management

4.3.1. Striving for resilience on all fronts?

As mentioned, Ötsuchi Town and most of the towns along the Sanriku-coast are subject to multiple hazards. Not only to tsunamis, also landslides and flooding could occur (see for illustration the hazard map in A.2). However, the only disasters explicitly addressed in the principles of the reconstruction guidance of Iwate Prefecture, are earthquakes and tsunamis (Iwate Prefecture, 2011). This may seem reasonable, as it concerns the reconstruction regards the aftermath of a tsunami. However, other long-term goals not specifically related to a tsunami disaster, are addressed too. Examples of such objectives are aiming for maximising the use of renewable energy, or enhancing tourism and industries. It seems that other disasters, are assumed to be managed according the national guidelines and not explicitly addressed within the general reconstruction strategy. Next to the tsunami-related measures taken in Ötsuchi, also landslide preventive measures have been taken. Also, in Ötsuchi, the stormwater drainage system was designed according the principles of the national technical standards.

4.3.2. System characteristics

The stormwater drainage system in Machikata district, consists of a separate urban drainage system, with semi-open conduits. The drainage system includes two subsystems, for which a schematization is shown in figure 4.10. The original design layout of the urban drainage can be found in appendix A.4. The conduits are only implemented in the residential area, which is +2.2m higher than the retention area adjacent to it.

Figure 4.6: Reconstruction design of Machikata district

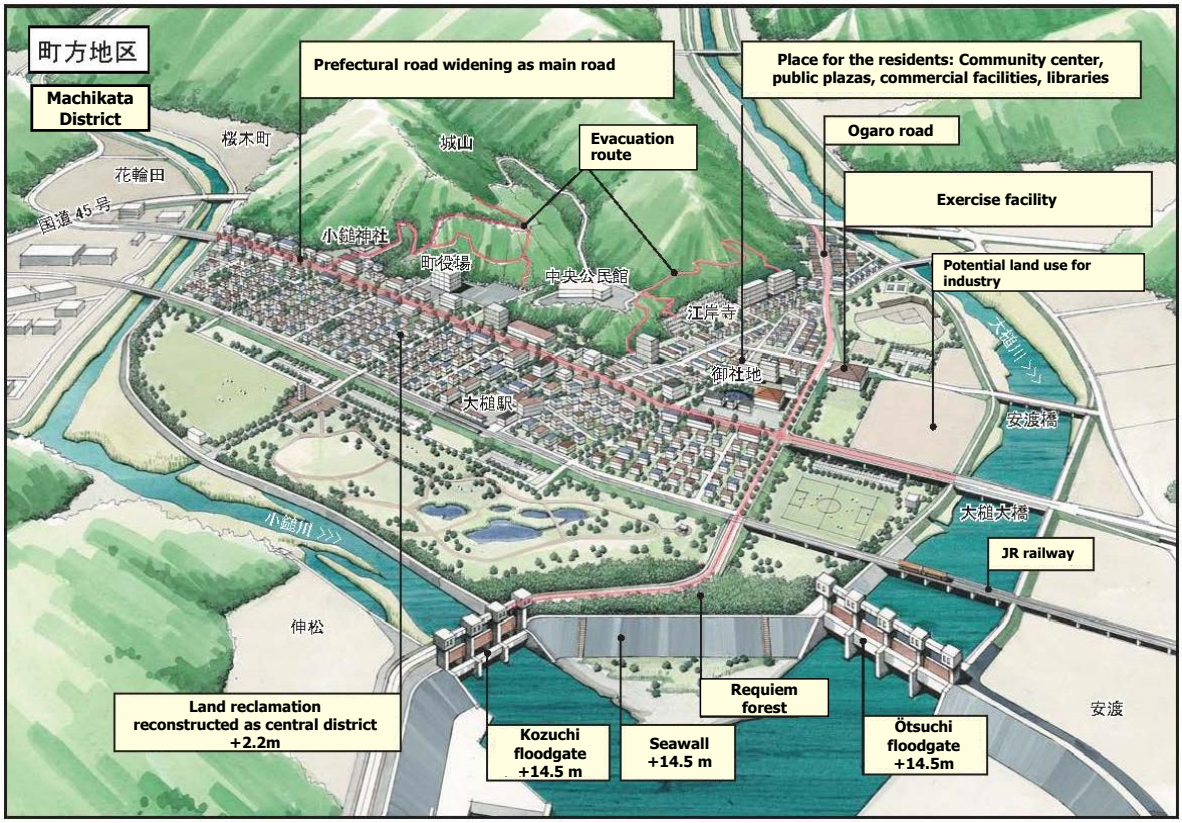

Source: modified from Urban Renaissance Agency (2013)

Figure 4.7: Cross-section of reconstruction of Machikata district

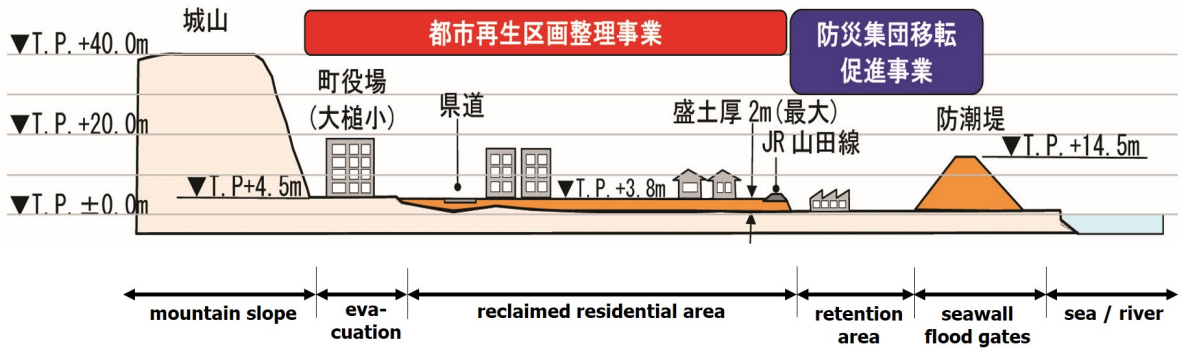

Source: modified from Maeda Corporation (2016)

Figure 4.8: Reconstruction of Machikata District, 2018. Source: F. Van de Ven, 2018

Figure 4.9: Schematized zone map of Machikata District

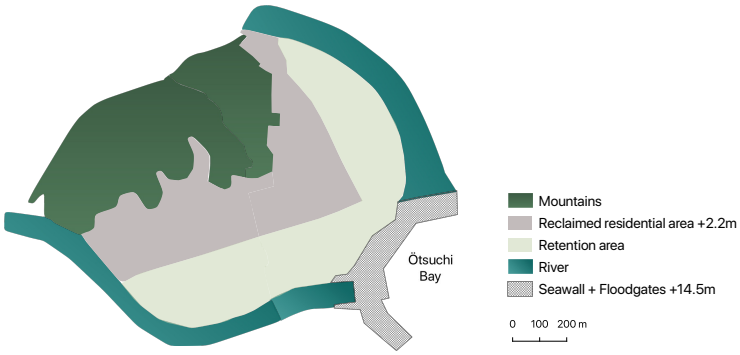

Figure 4.10: Reclamation area

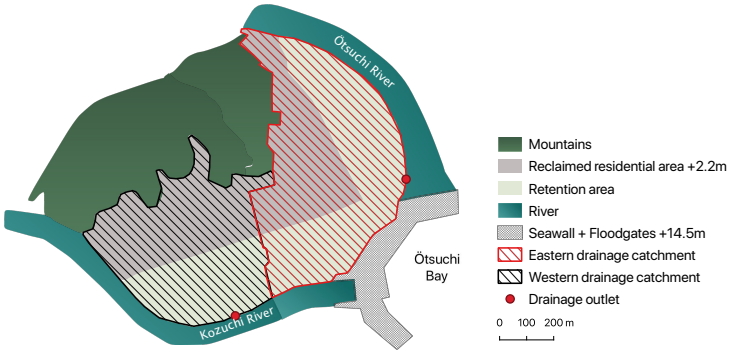

Stormwater is drained towards the low-lying area under gravity flow, where it is discharged onto the adjacent river mouths. The eastern part drains onto the Ötsuchi river, and the western part onto the Kozuchi river. Downstream each subcatchment is a pump, this allows for continuing water discharge, in case of high water levels in the rivers. In previous years, extreme river water levels in Ötsuchi occurred rarely ((River Port Section river sabo team, 2019)). The dimensions of the U-shaped channels vary between 300×300 to 1500×2000 mm.

There were no natural-based solutions or Blue-Green infrastructure solutions included in the design of the new drainage system. Only grey stormwater drainage infrastructure was applied. For small towns like Ötsuchi, no budget is made available for realizing measures to anticipate uncertain extreme conditions, in contrast to larger cities like Tokyo. Accordingly, the urban drainage system was implemented by following the design criteria posed by the national technical standards. These will be elaborated upon in the design approach later in this chapter.

In case a storm event would exceed the system's design capacity, the low-lying retention area was assigned to serve as buffer zone. However, if runoff flows are high, it has to pass the residential area first, before it reaches the buffer zone. In addition, no particular storage facilities were taken in the buffer zone itself. The buffer zone is partly assigned to recreational purposes like a sport court, other parts are assigned to industrial purposes. Managing excessive stormwater runoff seems thus feasible.

Moreover, there was an additional urban water related issue that emerge during the reconstruction. Ötsuchi was known for its natural artesian springs within the zone of the residential area (see also Mori, 2018). Due to the mountains, there is a confined aquifer present 30 meter below surface level. These springs provide very clean water and were commonly used in households and communal squares. The springs were extremely appreciated by the local population. However, due to the reclamation of the area >100 wells had to be closed, and cannot be used anymore. The pressure head of the water only reaches approximately 0.5 meter above sea level. By raising the residential area with 2.2 meter, the pressure head is not sufficient to rise above the elevated area. To compromise, one low-lying pond has been restored where the function of one artesian well is recovered. The layout can be seen in figure 4.11. Although they did not intentionally create additional water storage for stormwater purposes, in Dutch terms, this would be perceived as a potential water square.

4.3.3. Design approach

As mentioned, the stormwater system is designed on the basis of the national design standards. That is, applying a Rational Method approach, using the Talbot intensity duration curve as design criteria for a return period of 10 years. For a duration of 60 min, the rainfall intensity criteria is 48 [mm/hour].

The boundaries of the control system are the red lines on map A.4. Inflow from the mountains is thus considered as external inflow. According the Japanese guidelines, a runoff coefficient of C=0.2 was taken for the runoff from the mountain slopes, covered by forest.

Finally, the urban planners did not have any design criteria from the stormwater management side regarding rainfall runoff

(a) (b)

Figure 4.11: 'Water square' in Oshacchi Park, Ötsuchi Town. Source: [a] I. Nederlof, 2018 [b] A. Askarinejad, 2018

4.3.4. Closer look at input data: rainfall

To specify the bounds of extreme rainfall events for the experimental designs, a closer look is taken at the Talbot curve, and historical rainfall data for the area of Ötsuchi Town.

The Talbot curve has been aimed to analyse and to compare with historical rainfall data. No information could be found on the Talbot equation considering alternate return periods than 10 years. The available statistical information on rainfall frequencies include the IDF-curve for Miyako, a town just north from Ötsuchi Town. Figure 4.12a shows the IDF-curve for Miyako, which is based on the Cleveland equation (Iwate Prefecture sectie van de onderhoudsafdeling van het Prefectuur, 2015). As can be seen, for a return period of 100 years, the rainfall intensity ranges from 120 mm/hr to about 60 mm/hr for a rainfall duration of 15 minutes, and 120 minutes respectively. In order to get an understanding what kind of design criteria was used in Ötsuchi Town, the Talbot equation was compared with the Cleveland equation to see whether these are approximately the same. However, the Cleveland IDF-curve is only based on 7 years. Statements about return periods of for example 50 years based on a 7 year dataset is therefore quite inaccurate. Therefore additional analysis was done by plotting the annual extreme rainfall for a duration of 1 hour, based on recent rainfall data over a larger data range, namely 30 years, see figure 4.13a. Weibull plotting position was done, and plotted on a log-Gumbel distribution. It can be seen that the return periods of the Gumbel analysis give a higher value than for the Talbot design criteria. This could be caused by difference in the used dataset time range. Figure 4.13b shows that the threshold value, for T=10, I=60min, has occurred already 4 times in the past 10yrs. This could have occurred by chance, but, it could also be assigned to changing rainfall patterns, which suspects non-stationarity.

Figure 4.12: Intensity duration frequency curves, Miyako

(a) Intensity duration frequency curve - Cleveland, Miyako 2007 - 2013

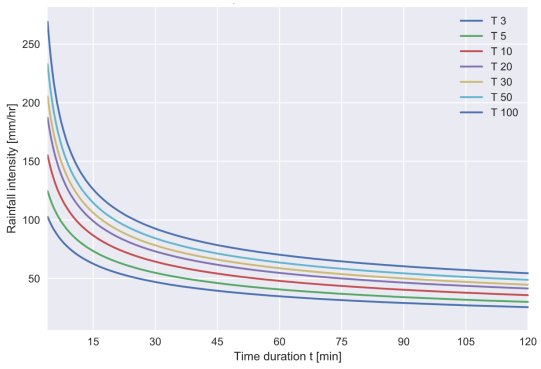

(b) Intensity duration curve - Cleveland and Talbot, T=10yr

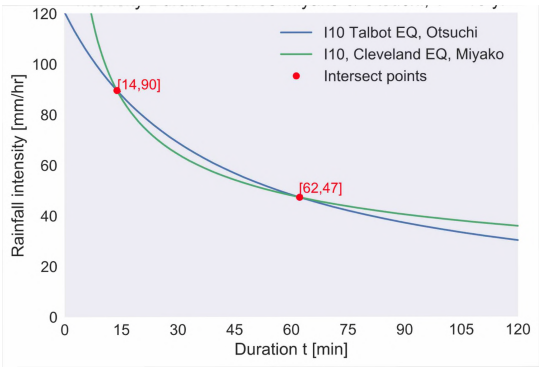

Figure 4.13: Extreme rainfall analysis, Miyako 1988-2017. Source data: JMA (2018)

(a) Gumbel of hourly precipitation

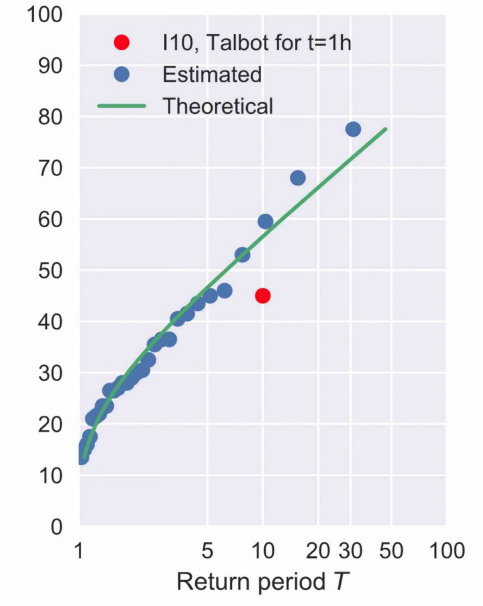

(b) Precipitation values above 48mm, t=1h

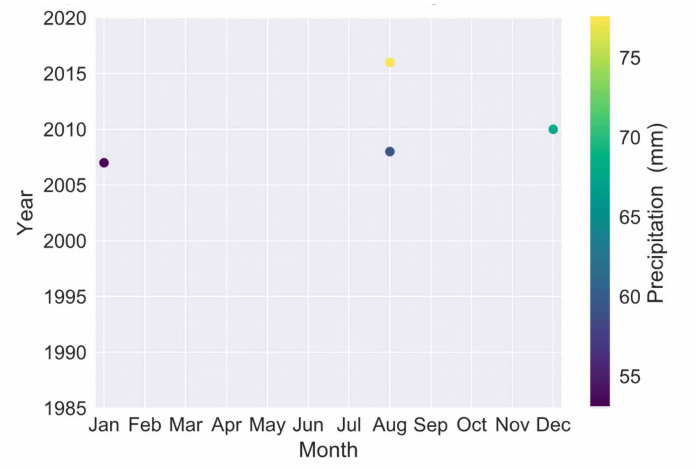

5

Model conceptualisation

The urban drainage system that is examined in this study, is transformed into a simplified SWMM model, based on the information on the case study data collection. The SWMM model and choices are explained below, where after the selected uncertainty parameters that influence the stormwater runoff are explained. In addition, the uncertainty parameter bounds are given in between is sampled in the experimental designs.

5.1. SWMM model layout and assumptions

Scenario Discovery is applied on one part of the urban drainage system in the reclaimed area: the eastern subcatchment that drains stormwater onto Ötsuchi River. The selected study area is shown in figure 5.1. A schematized representation of the corresponding SWMM model is given in figure 5.2. The model is a simplification based on the original stormwater drainage layout map, which is provided in the appendix A.4.

Figure 5.3 provides the labels of 4 important system elements. these are: the conduits, which represent the semi-open channels through which the stormwater is conveyed, the nodes, which are the junctions of two or more conduits, the subcatchments of the residential area, and the outfalls, of which Outfall 0 is the outfall that discharges the stormwater onto Ötsuchi River, and the remaining outfalls are the elements receiving the external inflow from the hill slopes. The direction of flow is towards outfall labelled Out0, which is the most downstream node, and the most upstream node is labelled J28. The dimensions of the conduits, and number of barrels, are provided in appendix B. As can be seen, the subcatchments are aggregated in a way such they have a rectangular shape, while ensuring that areas with the same direction of flow are in the same subcatchment. Some more assumptions are done to come to the final model:

(a) *Slope*: The slope of the subcatchments in the reclaimed area are assumed to be equal to slope of the

Figure 5.1: Selected study area

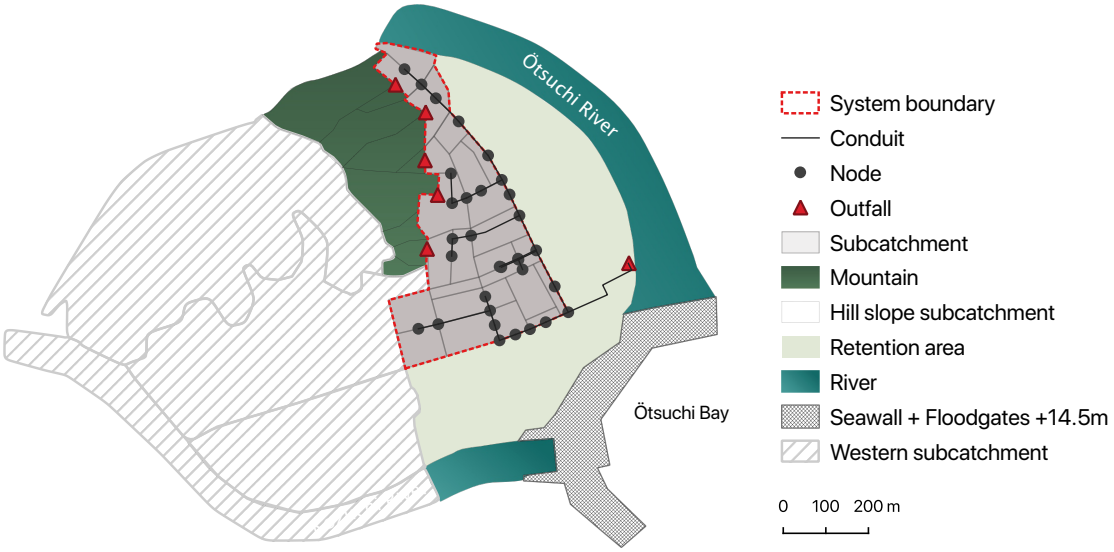

Figure 5.2: Schematized representation of the selected study area and SWMM model

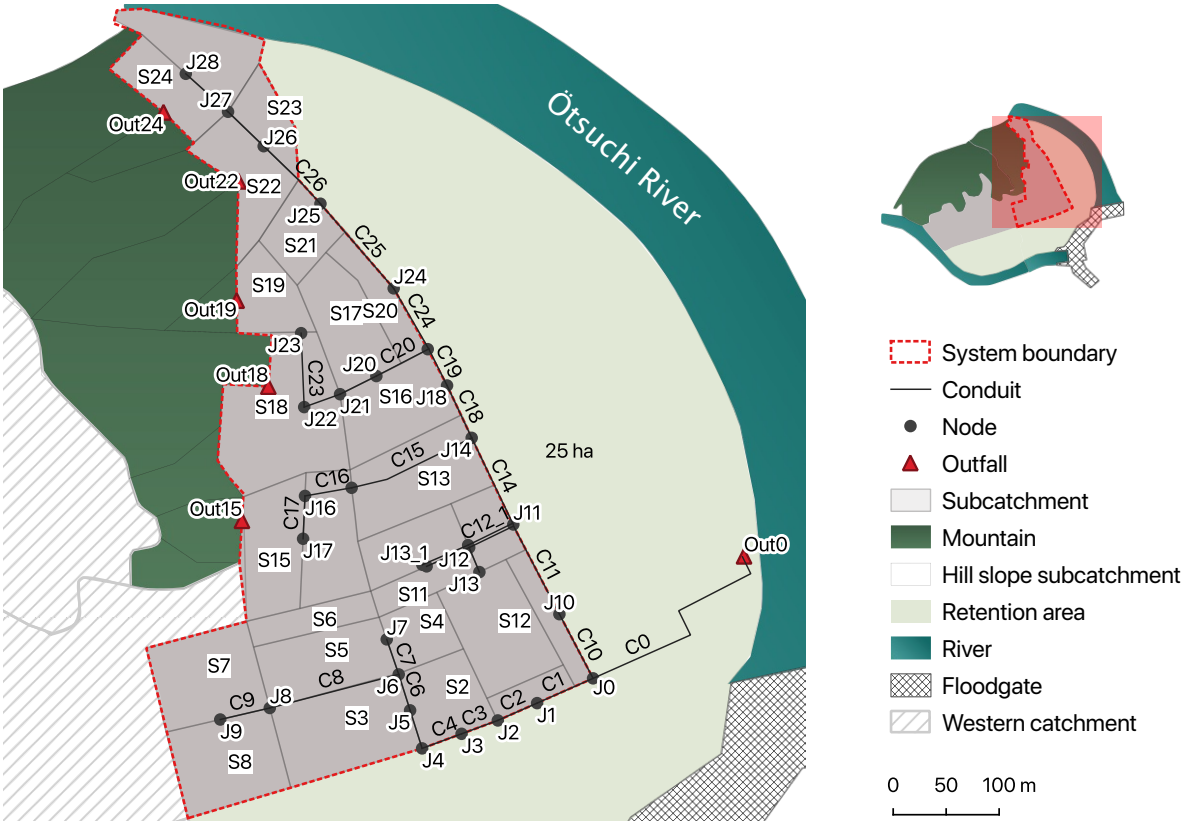

Figure 5.3: SWMM model of current stormwater system of Ötsuchi Town

open conduits.

(b) *Invert levels*: Invert levels of conduits and junctions are determined based on the conduits slope, starting from the lowest point in the catchment at the outfall, with a groundlevel surface of 1.2m +TP.

(c) *System boundaries*: The system boundaries are chosen to be the area covered in grey, by the subcatchments, plus the conduit C0 in the low-lying area. Apart from c0, no stormwater drainage has been established in the low-lying area, according this information. The water is discharged via Outfall 0, under the assumption this can be done under free gravity flow. Runoff from the mountains is calculated according the Rational Method equation, enabling to compare it with the original runoff coefficient, more on that in the next paragraph. The runoff is assigned to the receiving outflows (Out24, Out22, Out19, Out19 and Out15), where after it is re-routed onto the adjacent subcatchment before it enters the drainage system.

(d) *Runoff coefficient cemetery area*: The runoff coefficient of the more concrete area, as can be seen in 5.4, is assumed to be 0.7 according the Japanese standards for rocky surface under a slope > 6%(MLIT, 2015a). The corresponding subcatchment within the model is given in appendix B.

(e) *Flooding area*: The area ponded of each node is assumed to be 0.5 times the area of the downstream subcatchment(s). As it concerns open channel flow, it is assumed that when the junction is flooded the surrounding area in the longitudinal conduit direction will be flooded as well.

(a) Concrete slopes

(b) Cemetry hill slope

Figure 5.4: Steep hill slopes with higher runoff than forest covered hill slope. Source: I. Nederlof, 2018

5.2. Uncertainty parameters

The uncertainty parameters $\boldsymbol{X}$ that will be permuted in the sampling are given in figure 5.5. The uncertainty parameters form together collection $\boldsymbol{X}$: $\{Ri, Rd, C, Imp, k, n_p, s_p\}$. Input domain $\boldsymbol{H}$ is defined by the bounds of each uncertainty parameter, shown as the experiment range in figure 5.5.

(i) *Rainfall Intensity (Ri) and Rainfall Duration (Rd)*
Rainfall Intensity (Ri) and Rainfall Duration (Rd) are chosen based on the IDF of Miyako. Given that the experiments are permuted over the whole range of both parameters, and the fact that rainfall intensity is inversely proportionally related with rainfall duration, the ranges are somewhat robust. However, this can be reflected on when the scenarios are generated.

(ii) *External inflow coefficient (C)*
The external inflow coefficient (C) belongs to the external inflow from the mountains. This was assumed to be 0.2 in the original design, since the infiltration capacity of the mountains seems large. However, if the infiltration capacity becomes lower, due to long-term antecedent rainfall, when after initial losses runoff is created, C=0.2 could be on the lower side given the steep slope (>20%) of the adjacent mountains (see also Masatugu, n.d.). Therefore, the external runoff coefficient is permuted. The external inflow is estimated with use of the well-known runoff equation $Q = CiA$ in which Q is the runoff discharge, C the runoff coefficient, i the rainfall intensity and A the area of the subcatchment. Thus, hill slope subcatchments characteristics are implicitly taken into account by the runoff

Figure 5.5: Uncertainty parameter ranges of initial experiments run, defining input domain $\boldsymbol{H}$

coefficient.

(iii) *Imperviousness rate (Imp)*
The imperviousness rate (Imp) is estimated to be between 10 and 50% given the urban development and demographic developments of Ötsuchi-town.

(iv) *Hydraulic Conductivity (k)*
The advised classification of the soil, based on the soil sample, is the soil classification silty gravel - silty sand according the USCS soil classification ASTM D 2487 (Astm & International, 2006). The corresponding ranges for hydraulic conductivity derived from (Fitts, 2013) are: 10^{-5} - 10^{-2} cm/s. Which comes down to 0-300 mm/hr.

(v) *Manning's roughness coefficient (n)*
The empirical ranges for the Manning's roughness coefficient of impervious area is very small (McCuen, 1996). To limit the amount of dimensions in the experimental design, therefore a reasonable constant is chosen of 0.011. Manning's n for pervious area (Bermuda grass) ranges from 0.15 to 0.41 (McCuen, 1996).

(vi) *Depression storage pervious surface(s_p)*
Depression storage of impervious surfaces ranges from 1-2 mm according (ASCE, 1992). To be on the safe side a constant of 1 mm is chosen. For pervious surfaces a range of 2-5 mm is chosen which is the empirical value for lawns (ASCE, 1992).

For each simulation the uncertainty parameters are permuted, and a new SWMM model is as mentioned in 3.5. Given that the maximum rainfall duration is 120 minutes, each simulation, simulates the flow of stormwater behaviour for 5 hours. At t=0 the storm event is initiated, and represented by a single block rainfall event with the permuted rainfall duration and rainfall intensity. The characteristics of the subcatchments that are permuted (hydraulic conductivity, imperviousness) are assumed to be constant over space, within each simulation. A routing step of 30 seconds have been chosen.

6

Modelling results

6.1. Overview of conducted experimental designs

The modelling results include the output of multiple experimental designs. An overview of the conducted experimental designs can be found in table 6.1. Each experimental design is denoted by 'Run X'. After iterative runs, the amount of 4502 permuted experiments has been chosen to be sufficient to span the whole uncertainty space in each experimental design. The corresponding dimensional stacking tables show that for this amount of experiments enough simulations are conducted: no blank cells are present for an appropriate resolution of the uncertainty parameter intervals (see for example figure 6.1).

Table 6.1: Overview experimental designs

Run		**Run I**	**Run II**	**Run III**	**Run IV**
Objective		identify uncertainty space of flooded cases	examine uncertainty space of flooded cases	examine solution	examine solution
SWMM model	*Type*	base model	base model	modified model	modified model
	Description	current system	current system	vegetative swales storage unit	infiltration trenches storage unit
Uncertainty space	*Description*	initial uncertainty space $\boldsymbol{H}$	subspace of $\boldsymbol{H}$	subspace of $\boldsymbol{H}$	subspace of $\boldsymbol{H}$
	ID	$\boldsymbol{H}$	$\boldsymbol{H}^*$	$\boldsymbol{H}^*$	$\boldsymbol{H}^*$
Experiments	*LHS sampling*	4500	4500	/	/
	Boundary scenarios	2	2	/	/
	Total experiments	4502	4502	4502	4502
	ID	E_I	E_{II}	E_{II}	E_{II}

In the initial experiment round (Run I), the current stormwater system in Ötsuchi Town has been simulated 4502 times. The uncertainty parameters are permuted within the initial uncertainty space $\boldsymbol{H}$, for each experiment $\boldsymbol{X}^{(i)}$. Preliminary analysis of the output of Run I allowed for narrowing down the uncertainty space into $\boldsymbol{H}^*$, with $\boldsymbol{H}^* \in \boldsymbol{H}$ (see also table 6.2), in order to examine the uncertainty space of the flooded cases more closely. Accordingly, in Run II, a new set of experiments (E_{II}) were generated, by permuting the uncertainty parameters within the ranges of $\boldsymbol{H}^*$. Note that for Run II the input domain $\boldsymbol{H}^*$, corresponds to the input domain in figure 3.2 denoted with $\boldsymbol{H}$. The specific ranges and analysis of the output of Run I and II are elaborated in paragraph 6.2 and 6.3. The interpretation of the PRIM analysis is discussed in 6.4, and is the basis for the choice of solutions that are examined by means of Run III and Run IV. For these experimental designs a modified SWMM model, specific for its solution, has been runned for exact the same experiments as in Run II (denoted by E_{II}), allowing for accurate comparison of the solutions with the current system. The assessed solutions and analysis are discussed in paragraph 6.5.

6.2. Preliminary analysis

6.2.1. Run 1: Identify uncertainty space of flooded cases

Figure 6.2 is a preliminary visualisation of the first simulation results. Each graph shows for which parameter values flooding might be (or not be) expected. As can be seen this varies over space. Only a few nodes are

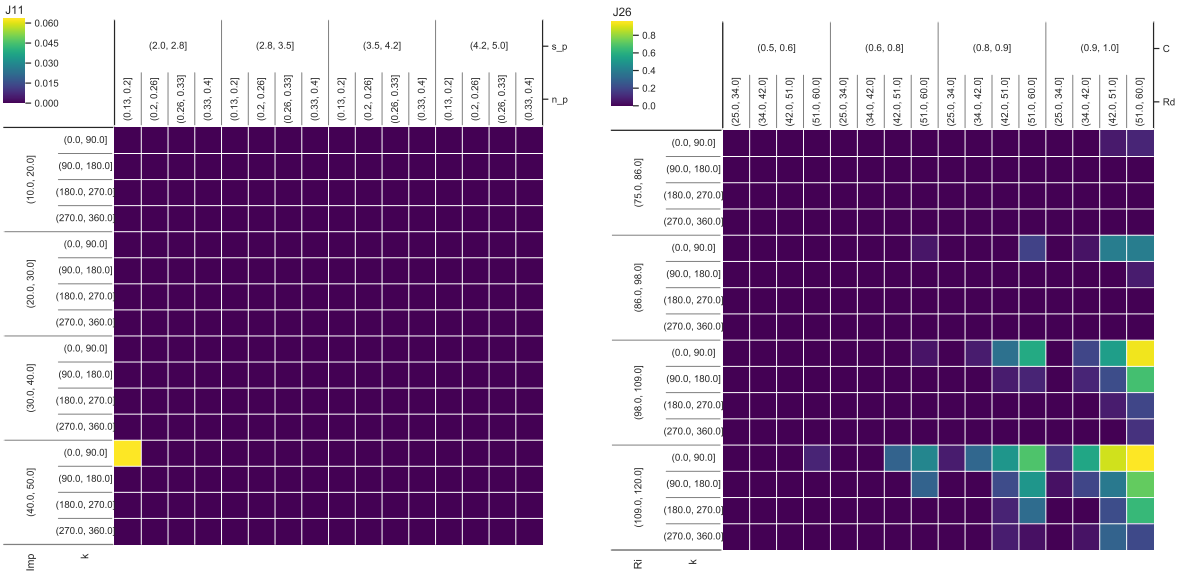

(a) Node J11

(b) Node J26

Figure 6.1: Dimensional stacking pivot table for flood height threshold 0.2m. Each cell represents the ratio flooded cases to not-flooded cases. A blank cell means no experiments are simulated for the corresponding parameter intervals. No blank cells are present here.

subject to flooding regarding the experiment range. Only five nodes appear to experience damageable flooding (>20 cm) under certain conditions within the experiment range: J11, J14, J19, J25 and J26. These nodes are close located to the mountains, connected to relative small sub-catchments which can be seen in the SWMM model layout in the right corner (or see figure 5.3). Also, these nodes are along the same direction of flow to downstream. The ranges for each parameters are significant wider for J25 and J26 in comparison to the other nodes. Along these lines, also the amount of cases for which the system's capacity is exceeded is for these nodes significant higher than for the other nodes as can be seen in figure 6.3. Regarding flood height (>10 cm), only a few more locations are flooded for specific rainfall intensities and rainfall duration. The locations that may experience flooded streets (>0 cm) are more distributed over the study area (appendix C.1). For J7,J5, J4, J3 the threshold is flooded for certain combinations of parameter states, where rainfall intensity is at least 120 mm/hr.

Please note that the unique parameter values for which flooding might occur, must be considered in isolation. To illustrate: flooding might be expected at node J26, at a Rainfall Intensity of 100 mm/hr, but we cannot tell yet under what specific conditions this might occur (i.e. for what specific parameter set this applies). A follow-up approach is needed to take the interaction of the parameters into account and to provide a statistical estimation: the scenario discovery analysis. The overview figures, like figure 6.2 are however, useful to visualise the input for the scenario discovery. It gives significant insight into both the parameter ranges and locations where there is no flooding expected. For example, if and only if the Runoff Coefficient of the external inflow would be lower than 0.4, there is no flooding expected in any of the scenarios considered within this experimental design. The if and only if conditions on no flooding occurrence for a specific parameter, such as $C < 0.4$, expose the experiments for which the system performs as desired in any case regardless the parameter states of the remaining parameters. These in turn, are excluded from the cases of interest being assessed in the scenario discovery. Here the aim is to analyse the conditions for which the system does fail. Accordingly, the cases of interest in the next analysis are the locations J26, J25, J19, J14, J11 for flood height >0.2m. The corresponding subspace ($\boldsymbol{H}^*$) for the next analysis is based on the most vulnerable node, J26, and can be found in table 6.2. The intervals of three variables have been adjusted: Rainfall intensity, Rainfall duration and the Runoff coefficient. The adjusted values are shown in orange.

6.2.2. Run II: a closer look at the flooded cases

To examine the flooded cases in more detail, run II has been done for a smaller experiment range ($\boldsymbol{H}^*$) with more samples (see also table 6.1). A preliminary overview of the output is shown in figure 6.4. Within this experiment range, node J26 is flooded for nearly the entire range of each parameter. However, the interaction

Figure 6.2: Preliminary visualisation of flooding occurrence - Run I for flood height thresholds 0.1 m and 0.2 m

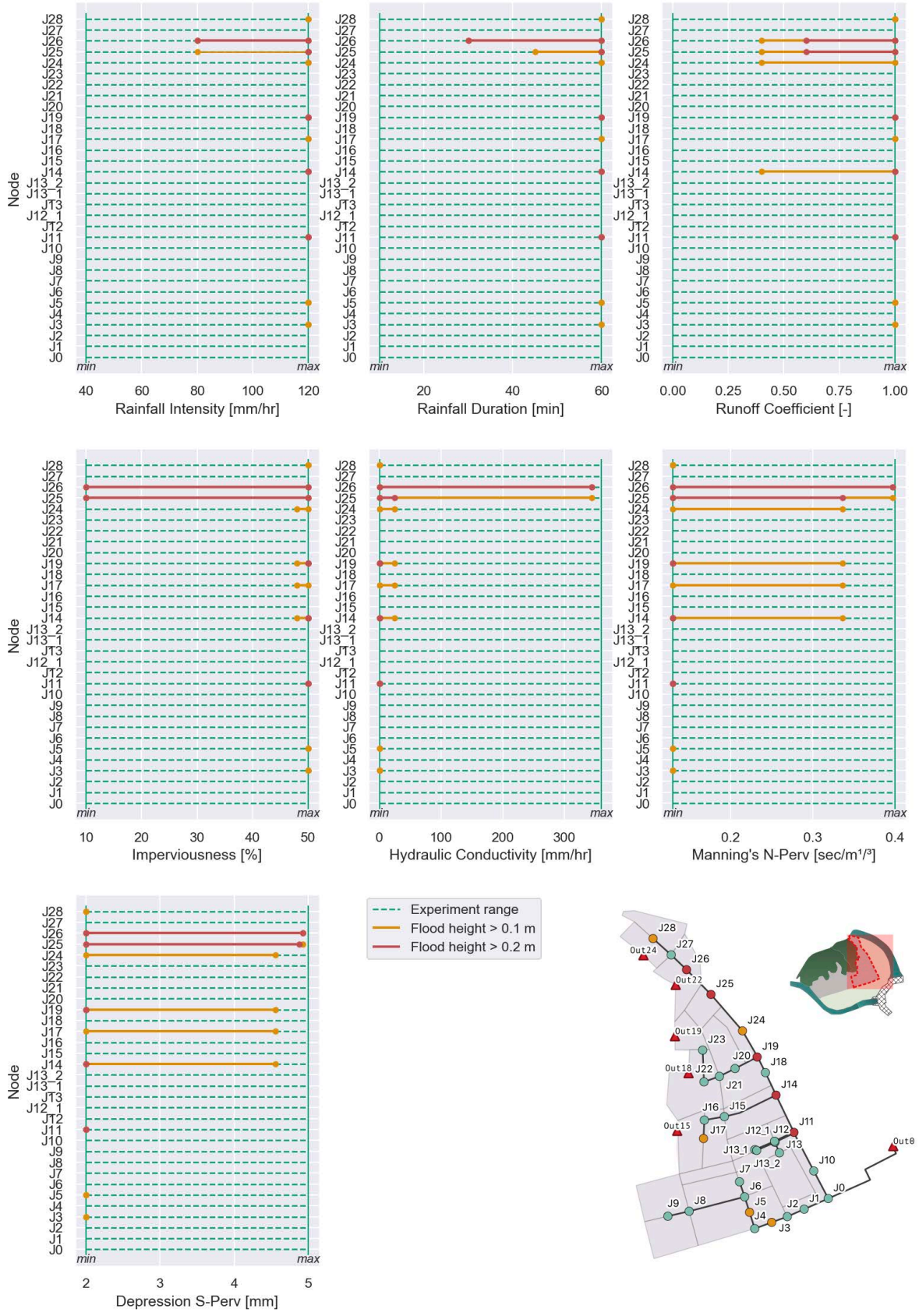

Figure 6.3: Number of flooded cases per node, for different threshold levels

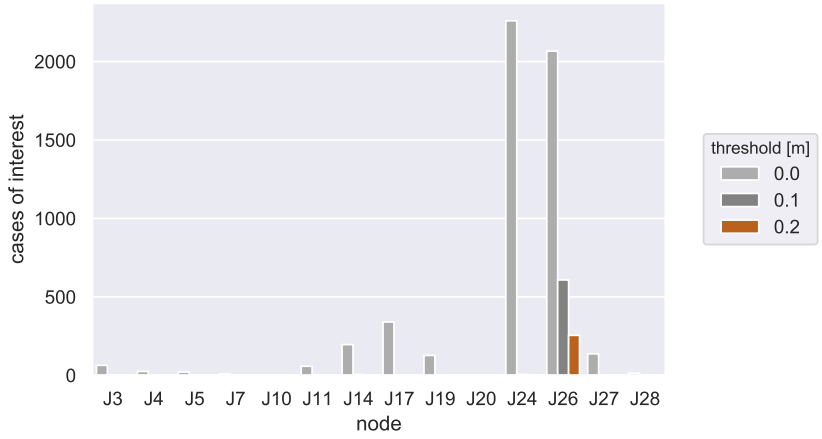

Table 6.2: Uncertainty parameter space $\boldsymbol{H}^*$

Uncertainty parameter space $\boldsymbol{H}^*$				
Uncertainty parameter	**Acronym**	**Unit**	**Low**	**Up**
Rainfall intensity	Ri	mm/hr	75	120
Rainfall duration	Rd	min	25	60
Runoff coefficient external inflow	C	-	0.5	1
Imperviousness rate	Imp	%	10	50
Hydraulic conductivity	k	mm/hr	0.36	360
Manning's roughness coefficient - pervious surface	n_p	$\text{sec/m}^{\frac{1}{3}}$	0.13	0.4
Depression storage - pervious surface	s_p	mm	2	5

between the parameters is for node J26 not revealed in this graph. Whereas from this graph we can retrieve, that node J25 only floods for the higher rainfall intensities (>115mm/hr) and rainfall duration (>55 min). These kind of downpours are very extreme. The other nodes are only flooded above 0.1m, for a very low hydraulic conductivity. For flood height >0.2m, the nodes are only flooded for the worst case scenario, that is if all parameters would be on the outer ranges of the experiment range (this can clearly be seen from both figure 6.4 and the paired scatter plot of each parameter, where all sample points are plotted, which can be found in figure C.3).

The relations are less clear for node J26, which is located upstream along the same longitudinal direction of the other nodes that are vulnerable for only a narrow range, as can be seen in the figure in the right corner of the overview map 6.4. In the corresponding scatter plot (figure 6.5), we see a more rectangular pattern for the Manning roughness coefficient, and the depression storage value. Whereas the remaining factors seem to be centred in a triangular shape. Each sample point represents a 7-dimensional input, however, therefore PRIM is applied to take a closer look at node J26.

Figure 6.4: Preliminary visualisation of flooding occurrence Run II

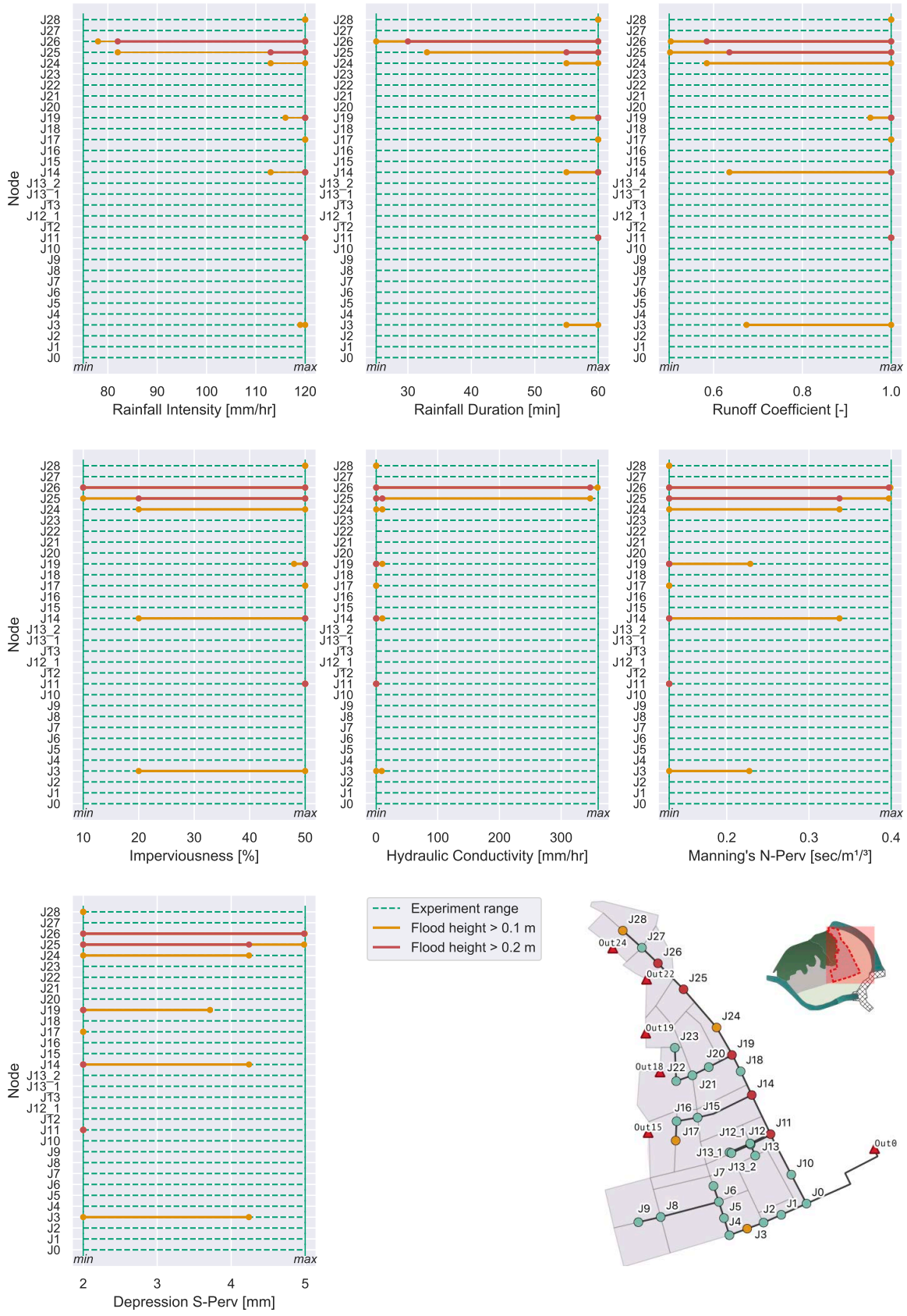

Figure 6.5: Scatterplot node J26 - Run II - flood height threshold = 0.2m

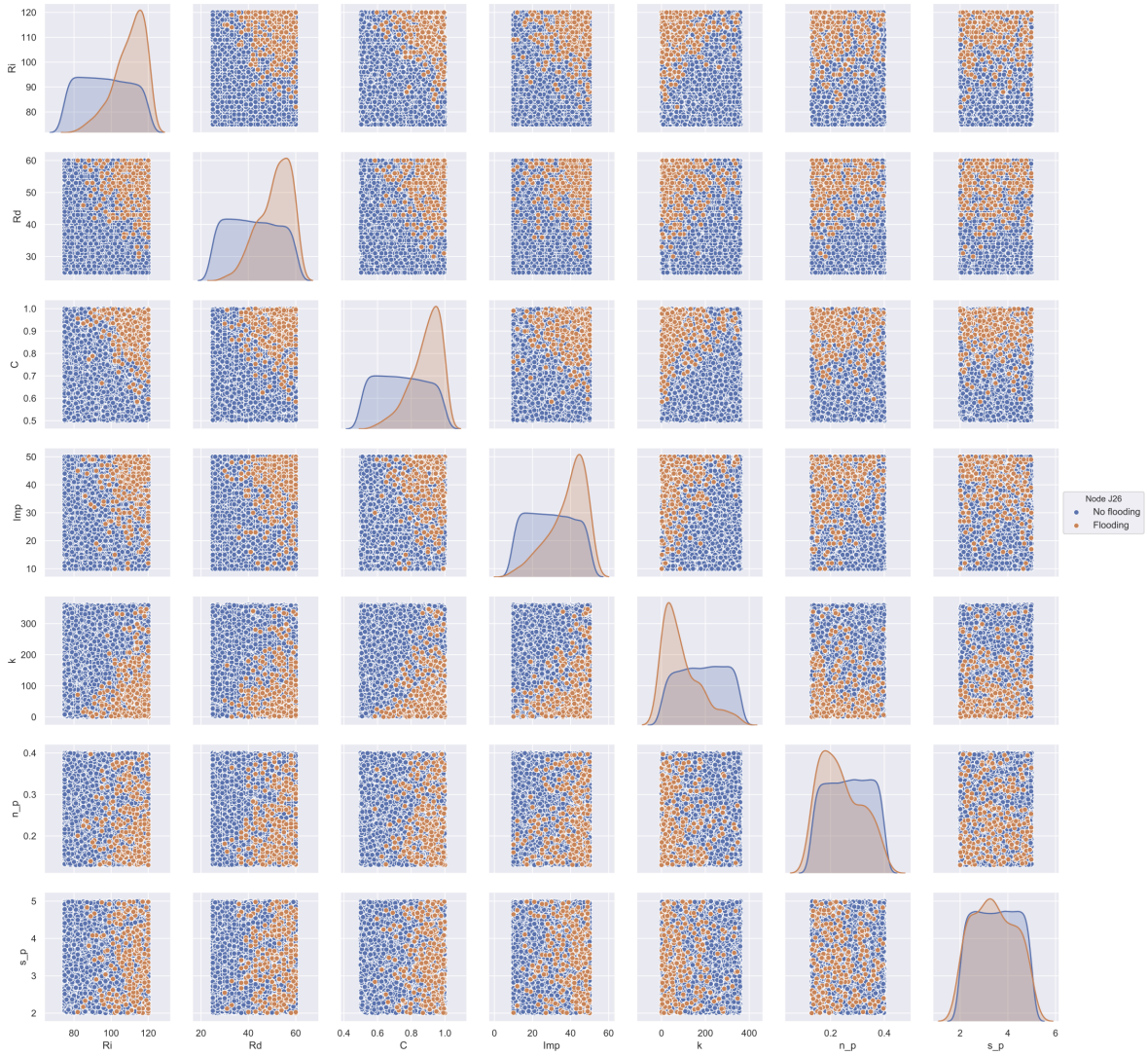

6.3. PRIM analysis of node J26

6.3.1. PRIM

Node J26 is flooded above 0.2 m for 255 cases out of the 4502 experiments that are simulated in Run II. The 255 flooded cases are denoted as the cases of interest of Run II (coi_{RII}). To narrow down the amount of experiments to analyse in PRIM, the PRIM analysis is conducted on a selection of the simulated experiments corresponding to the experiment ranges of coi_{RII}. The selected experiments are denoted as $\boldsymbol{X^{H0}}$ and count 2571 cases. A description of this set of experiments is given in the appendix (table C.1).

Accordingly, two PRIM boxes are found which suggests the sensitive key factors in explaining the failure of node J26. The boxes are summarized in figures 6.6, and 6.7, 6.8. In figure 6.6 the constrained ranges of the dominant parameters are given with the corresponding quasi-p value. In figures 6.7 and 6.8 the PRIM boxes are visualized for each paired scatter plots of the dominant parameters.

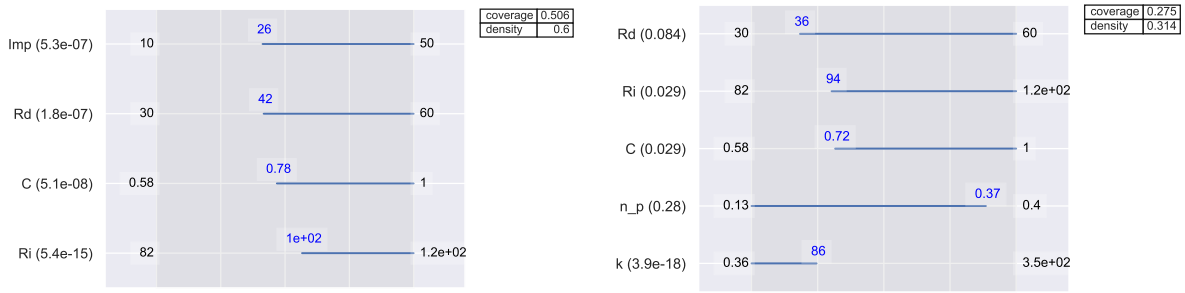

(a) Box 1

(b) Box 2

Figure 6.6: Prim boxset, node J26

Figure 6.7: Prim box 1: J26

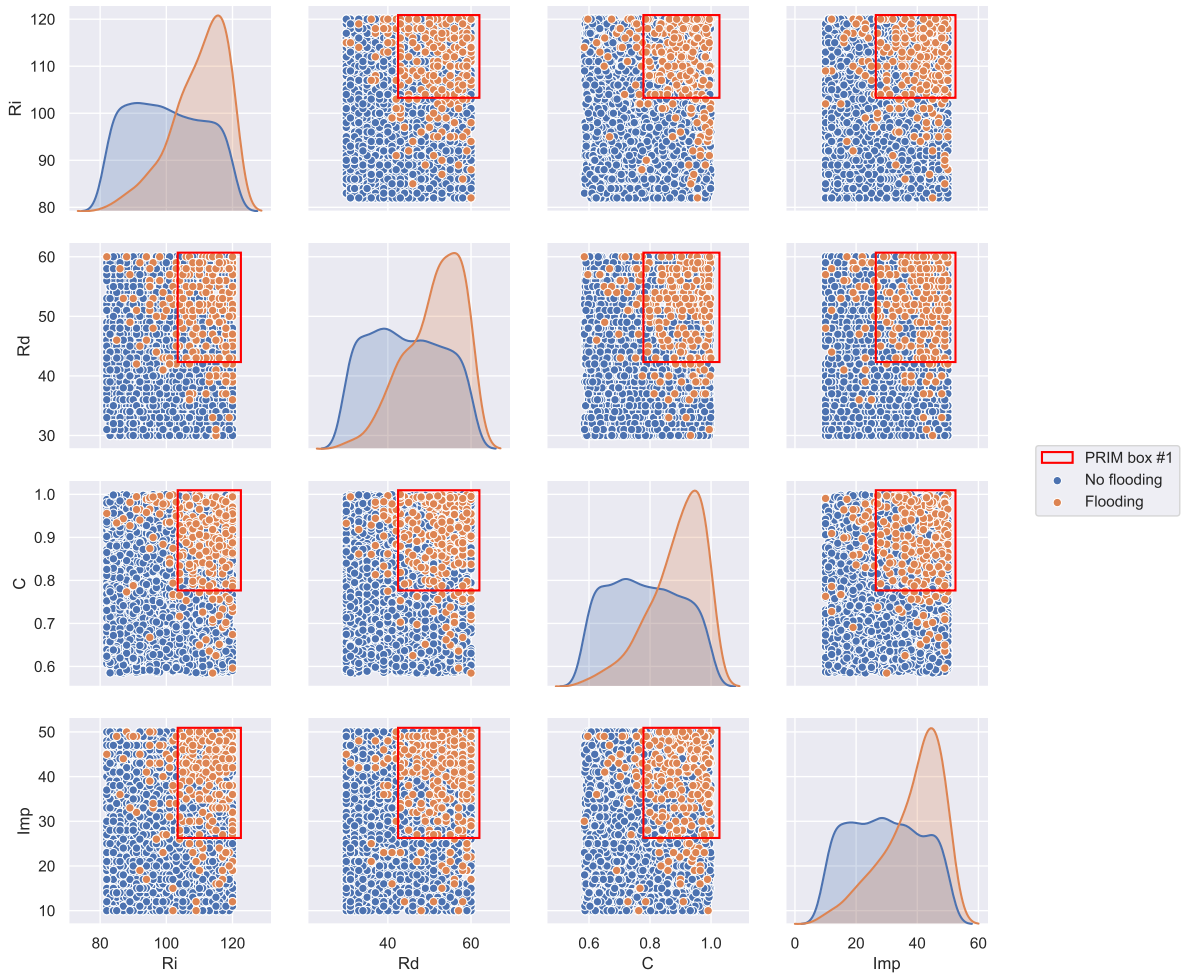

The first PRIM box has a coverage of 50% and density 60% and is mainly constraint by Rainfall Intensity, Rainfall duration, External runoff and Imperviousness. This means that the majority of the cases for which flooding occurs is caused by the higher values of these 4 parameters. The quasi-p value, shown between brackets of figure 6.6, indicates the relative sensitivity, given the relative lower value for Rainfall intensity, it seems that for these cases the Rainfall intensity is more sensitive then the other three parameters. Approximately 30 % of the cases can be explained by the parameter space represented by box 2, figure 6.6b. Here, the hydraulic conductivity seems more dominant than all other parameters. Again the value range for C is rather

Figure 6.8: Prim box 2: J26

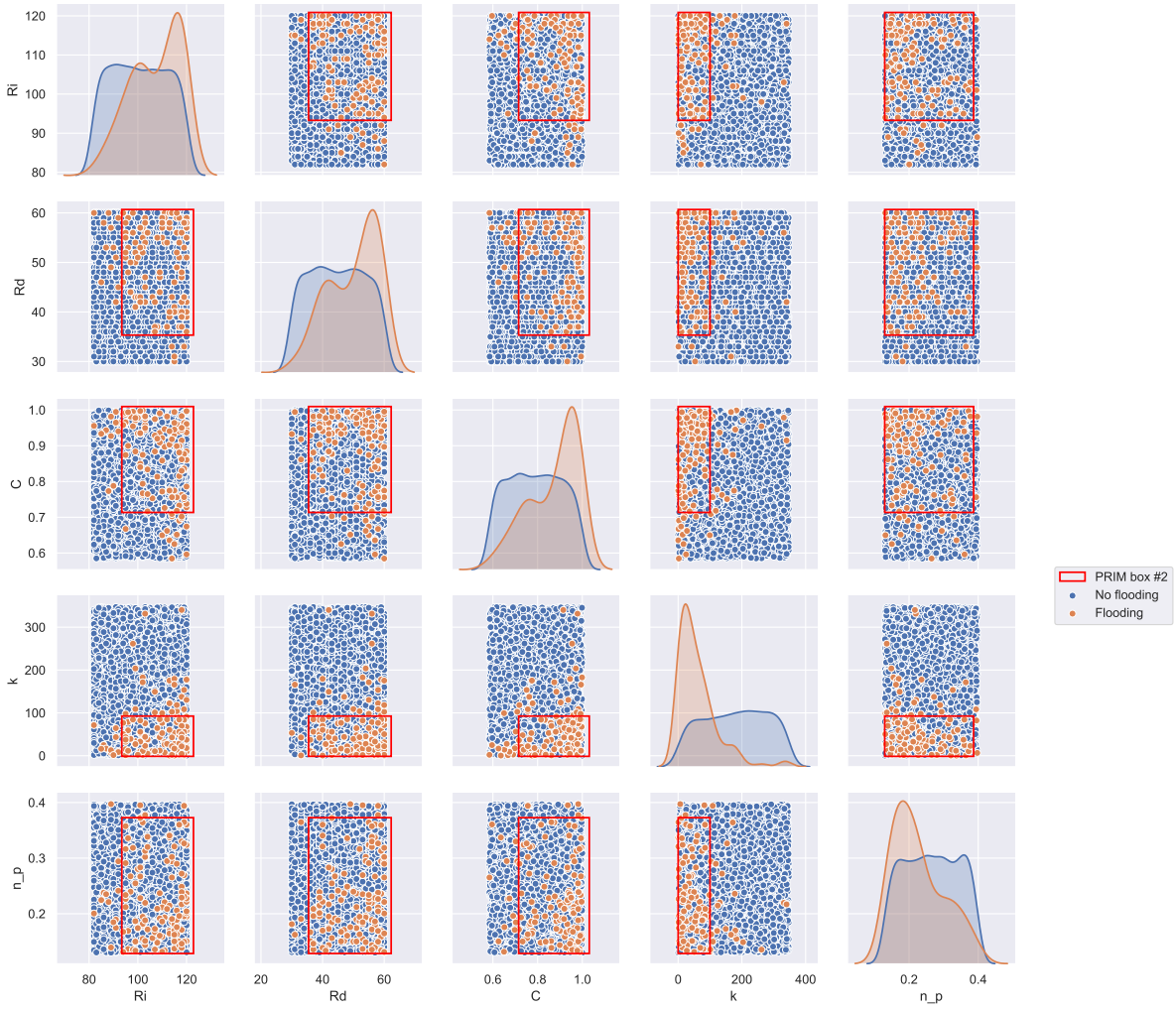

large, and Rainfall duration spans almost its entire range between 30 minutes and 60 minutes. The density is much lower, however.

A tabular overview of the PRIM results is given in the appendix (tables C.2 and C.3).

6.3.2. PCA-PRIM

Both the triangular spaces of cases of interest for node J26 (see scatter plot 6.5) and the rather low density of the PRIM boxes, suggest that the quality of the PRIM scenarios could be improved with PCA-PRIM.

PCA-PRIM is conducted on the simulated experiments with input data $\boldsymbol{X^{H0}}$. The principal components are derived from the cases of interest coi_{RII}. Given the 7 dimensional input space ($\boldsymbol{X}$), 7 principal components were obtained, forming the synthetic parameters: $\boldsymbol{X_{pc}} = \{PC1, PC2, PC3, PC4, PC5, PC6, PC7\}$. Each parameter is a linear combination of the scaled and normalized original uncertainty parameters: $\boldsymbol{X_u} = \{Ri_u, Rd_u, C_u, Imp_u, k_u, np_u, sp_u\}$. The principal components $\boldsymbol{X_{pc}}$ form the columns of the rotation matrix for rotating the original input data $\boldsymbol{X^{H0}}$. The rotation is done following the steps mentioned in the methodology chapter, paragraph 3.4.4. The transformation of the experiments and corresponding outputs is clarified in table 6.3. Now $\boldsymbol{X^{H0}}$ has been rotated into $\boldsymbol{X^{PC}}$, each experiment is translated and expressed into a unique combination of synthetic parameter values, rather than the original uncertainty parameters. Both the rotation matrix consisting of $\boldsymbol{X_{pc}}$, and the moments of the original parameter ranges of $\boldsymbol{X^{H0}}$ used for the normalization and later for the interpretation, can be found in the appendix (C.4, C.1).

When PRIM is conducted on the rotated experiments with corresponding outputs, there is one difference: the resulting PRIM boxes are now expressed in terms of ranges of the synthetic parameters $\boldsymbol{X_{pc}}$, rather than the original parameters $\boldsymbol{X}$ like the results discussed in section 6.3. To put it differently: explaining the conditions for which flooding occur is expressed in restricting the range of the synthetic parameters $\boldsymbol{X_{pc}}$. For example, imagine a PRIM box with coverage 50 % a density of 80 %, and 2 restricted dimensions, PC1 > 3, and PC2 < 1. This would imply that 50 percent of the flooded cases would be explained by the experiments for which both PC1 has a value above 3, and PC2 has a value below 1, with a precision of 80%. The constraints on the synthetic parameters thus expose the conditions for which the system would be flooded, expressed in linear combinations of the normalized and scaled uncertainty parameters. This requires backwards interpretation towards the original uncertainty parameters $\boldsymbol{X}$. This is more elaborated in section 6.4. First the PCA-PRIM outcomes are explained below.

Table 6.3: Transformation of selected experiments ($\boldsymbol{X^{H0}}$) into normalized experiments ($\boldsymbol{X^{U}}$), into rotated experiments ($\boldsymbol{X^{PC}}$) expressed in synthetic parameters $\boldsymbol{X_{pc}}$. Corresponding output y_{j26} remains the same during the transformation.

Input: selected experiments run II (X^{H0})									**Output: flooding occurrence** (y_{j26})
		Uncertainty parameters ($\boldsymbol{X}$)							
Index	**Experiment ID (from run II)**	**Ri**	**Rd**	**C**	**Imp**	**k**	**sp**	**np**	y_{j26}
0	Experiment 3	106	56	0.75	15	324.22	0.32	3.22	0
1	Experiment 6	100	60	0.94	19	324.47	0.30	4.55	0
..	Experiment ..	..	..	..	..	..	..	..	..
2569	Experiment 4499	112	56	0.87	41	112.25	0.26	4.72	1
2570	Experiment 4501	106	42	0.62	45	315.87	0.23	4.65	0

Input: normalized experiments (X^{U})									**Output: flooding occurrence** (y_{j26})
		Scaled and normalized uncertainty parameters ($\boldsymbol{X_u}$)							
Index	**Experiment ID (from run II)**	**Ri_u**	**Rd_u**	**C_u**	**Imp_u**	**k_u**	**sp_u**	**np_u**	y_{j26}
0	Experiment 3	0.440	1.236	-0.374	-1.308	1.494	0.670	-0.310	0
1	Experiment 6	-0.092	1.687	1.226	-0.968	1.497	0.457	1.241	0
..	Experiment ..	..	..	..	..	..	..	..	..
2569	Experiment 4499	0.973	1.236	0.629	0.897	-0.620	0.004	1.438	1
2570	Experiment 4501	0.440	-0.339	-1.461	1.236	1.411	-0.435	1.359	0

Input: rotated experiments (X^{PC})									**Output: flooding occurrence** (y_{j26})
		Synthetic parameters ($\boldsymbol{X_{pc}}$)							
Index	**Experiment ID (from run II)**	**PC1**	**PC2**	**PC3**	**PC4**	**PC5**	**PC6**	**PC7**	y_{j26}
0	Experiment 3	0.417	0.499	-0.437	-1.057	1.943	-0.365	0.843	0
1	Experiment 6	-0.676	1.269	-1.234	0.476	2.267	-0.571	0.011	0
..	Experiment ..	..	..	..	..	..	..	..	..
2569	Experiment 4499	-0.699	1.247	-0.561	-0.111	0.100	0.249	-1.920	1
2570	Experiment 4501	-0.754	0.501	-1.855	-1.129	-1.025	1.014	0.620	0

When PRIM is conducted on the rotated data a high qualitative PRIM box can be found in which only 1 synthetic parameter is restricted: $PC7$. PRIM's peeling process of finding an appropriate PRIM box clearly shows that constraining only one synthetic parameter gives the best scenario set for explaining the flooded cases. This peeling process is captured in the trade-off curve in figure 6.9. This Pareto-optimum curve, represents the steps in the peeling process of PRIM. Each dot corresponds to a PRIM box with a certain density, coverage and interpretability. The latter is expressed in the number of synthetic parameters that is constrained in the corresponding PRIM box, and is visualized by different colours. From this graph it can be clearly seen that constraining just one synthetic parameter results into a better PRIM 'box' than when two parameters are constrained - given the one dimension that is restricted the PRIM box can be visualized as a line in this case rather than a box. As constraining 2 synthetic parameters might enhance the density (see the green dots in the trade-off curve), it would be way more complex to interpret, given that each synthetic parameter consists of a linear combination of multiple parameters. Moreover, the paired scatter plot of $PC5$ and $PC7$ for the rotated sample points, shown in figure 6.10, illustrates that constraining only $PC7$ would give a high quality PRIM outcome with high density, whereas if only $PC5$ would be constrained also a lot of non-flooded cases would be captured, which in turn would result into a low density PRIM box.

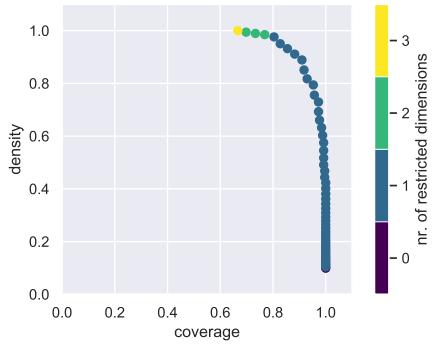

Figure 6.9: PCA-PRIM tradeoff curve - peeling process of PRIM

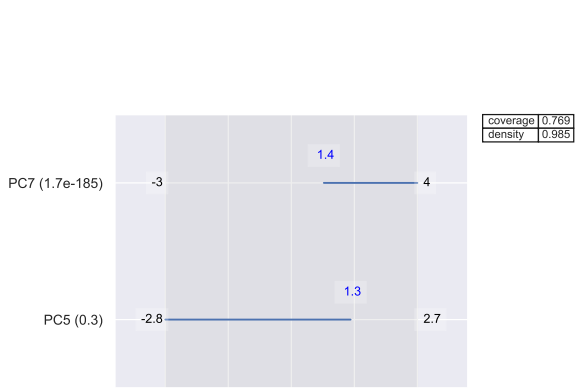

(a) PC5 and PC7 constraints

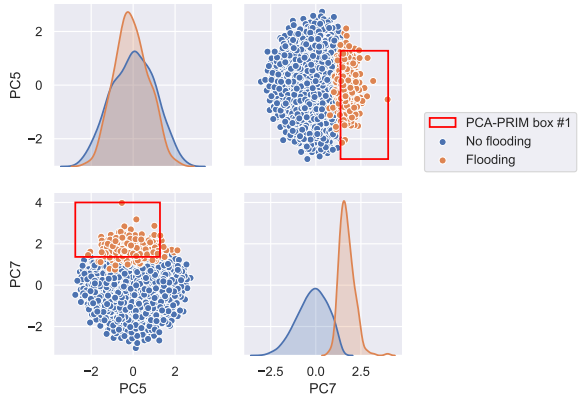

(b) Paired scatterplot of rotated data

Figure 6.10: PCA-PRIM outcome - 2 dimensions

Therefore, in the analysis is chosen for the PRIM box in which only 1 dimension is restricted ($PC7$), with density and coverage of 90 percent. This means that 90 percent of the flooded cases can be explained within the range of the constrained parameter $PC7$ with a precision of 90%. The resulted PRIM outcome is demonstrated in figure 6.11. Thus, 90 percent of the experiments for which PC7 is equal or above 1.3, in which each experiment is a proxy for a system state described by PC7, node J26 would be flooded above 0.2 m. The PCA-PRIM outcome can be expressed mathematically, with density and coverage of 90% for:

$$PC7 = 0.49Ri_u + 0.38Rd_u + 0.44C_u + 0.40Imp_u - 0.48k_u - 0.17np_u + 0.03sp_u \tag{6.1}$$

and

$$y_{j26} = \begin{cases} 1, & \text{if } PC7 \geq 1.3 \\ 0, & \text{otherwise} \end{cases} \tag{6.2}$$

where:

y_{j26} = system performance outcome of node J26 (flooding: $y_{j26} = 1$, no flooding $y_{j26} = 0$)

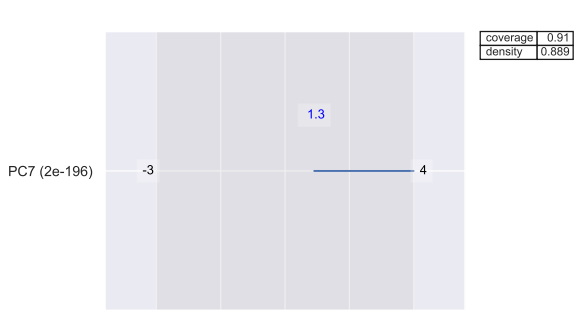

(a) PC7 constraint

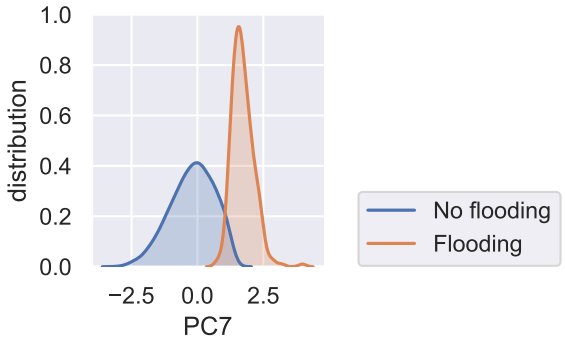

(b) PC7 density plot

Figure 6.11: PCA-PRIM outcome

The coefficients of $PC7$ represent the relative weights of the parameters for explaining whether or not node J26 would be flooded or not. As can be seen the relative weights are almost equal for rainfall intensity, rainfall duration, runoff coefficient, imperviousness and the inverse of hydraulic conductivity. Whereas the Manning's roughness coefficient for pervious surface has a much smaller weight, and depression storage is almost negligible compared to the other parameters.

Since $PC7$ is a linear combination of multiple uncertainty parameters, the PRIM box can be considered of very high quality, that is being applicable in practice, if the corresponding linear combination can be interpreted well: could the relative dependencies of the uncertainty parameters represented by $PC7$ be explained? This will be more elaborated in the next paragraph in which the interpretation of the entire scenario discovery analysis is discussed.

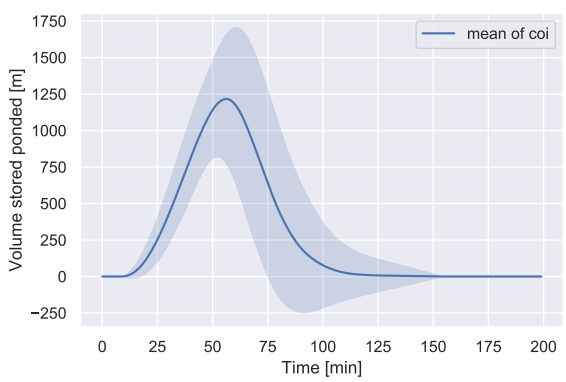

(a) Flood volume

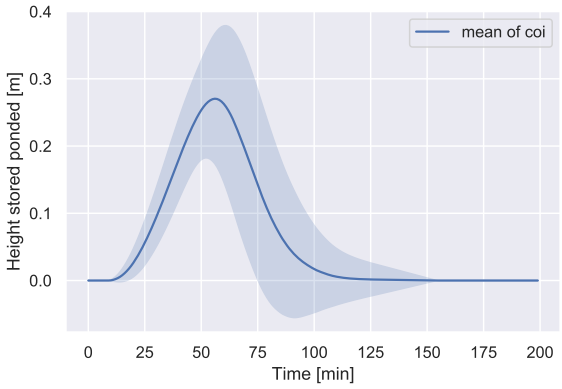

(b) Flood height

Figure 6.12: Flood volume and flood height for node J26. The curves show the mean for all cases of interest (flooding > 0.2m) with one standard deviation above and below the mean

6.4. Interpretation

6.4.1. A robust system if...

What becomes clear from the scenario discovery analysis, is that the overall system is robust for the wide-ranging plausible states. The large size of the semi-open channels that are implemented in the relative small subcatchments seems to be sufficient for managing very extreme conditions. The different flood height levels have been assessed as well, as more nodes appear to be flooded for the lower thresholds [0,0.1). However, for the threshold of flood height [0,0.1), in most cases the flood heights are only a few mm above ground surface level. A few mm of water on the streets, is no need to react.

For the applied design criteria of T=10 years, rainfall intensity of 48mm, and rainfall duration of 1h, the system would be ok for all plausible states. Even for extreme conditions, for which the design criteria is exceeded,

there would be no flooding. However, if there would be much runoff from the mountains (C>0.58), node J26 is possibly flooded. The results show that the corresponding flood volumes are large (+- 1200 m3), as can be seen in figure 6.12, hence water depth can reach far above tatami-level. The conduits upstream of node J26 are getting full for these conditions, and this suggests that the northern region adjacent to node J26 is vulnerable.

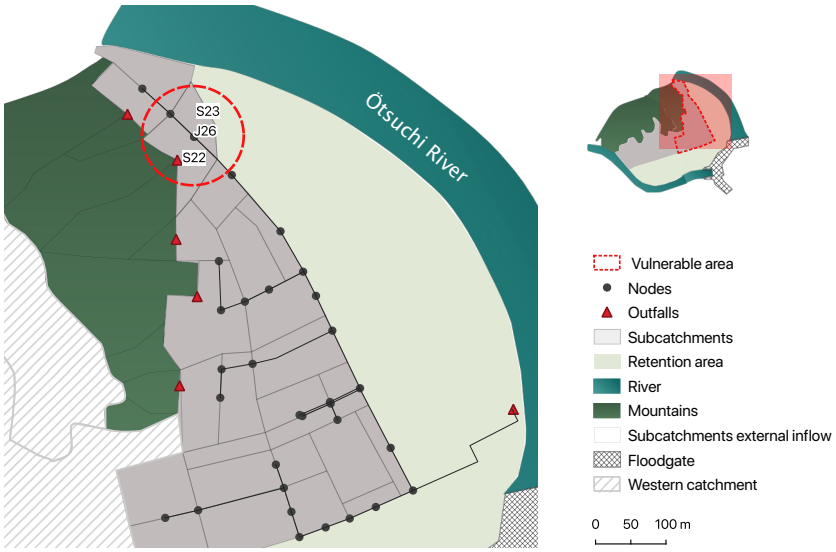

Figure 6.13: Vulnerable area

The PRIM results discussed in section 6.3, illuminate that node J26 is flooded for most situations if the runoff coefficient is above 0.7. However, only 50 percent of the cases, the remaining 30% are explained by a lower hydraulic conductivity, but again with not a very high precision. As almost 90 percent of all experiments for which node J26 is flooded can be described with $PC7 \geq 1.3$ it is first elaborated on how this can be interpreted. Whereafter, the differences between the PRIM and PCA-PRIM outcomes are further examined.

6.4.2. Interpretation of PCA-PRIM outcome PC7

If we turn to the PCA-PRIM results, we can use equation 6.1 to 'play around' with the variable states, given that 90 percent of the cases for which the system would flood in the area of node J26, can be explained by $PC7 \geq 1.3$ (equations 6.1 and 6.2). At first, it is obvious that the direction of the contributing parameters are intuitive for influencing flooding occurrence. A positive contribution to the value of $PC7$, implies that it positively contributes to flooding occurrence. For example higher rainfall intensity will make the occurrence of flooding more likely. In line with this, a higher rainfall intensity will result into a higher value for $PC7$, given the positive sign for rainfall intensity in the linear combination of $PC7$ (eq 6.1). In contrast, increasing hydraulic conductivity of the soil would make flooding occurrence less likely. Likewise, a negative sign for hydraulic conductivity in equation 6.1 implies that the value of $PC7$ decreases with increasing hydraulic conductivity. For the remaining synthetic parameters within $\boldsymbol{X_{pc}}$ the directions are much harder to interpret, as becomes clear from the linear combinations of $\boldsymbol{X_{pc}}$, which can be found in rotation matrix C.4). In addition, it should be noted that the equation of $PC7$ is only valid for the ranges of the original parameter ranges for which node J26 is flooded. These ranges are denoted by the corresponding uncertainty space of the selected experiments $\boldsymbol{X^{H0}}$ (see also table C.1). For example a runoff coefficient of C=0.58 would be the minimum value for which $PC7$ is valid. To illustrate, the outcomes suggest that for a runoff coefficient of 0.58, the $PC7$ equation becomes:

for

$$C_u = \frac{C - \mu_c}{\sigma_c} = \frac{0.58 - 0.79}{0.12} = -1.75 \tag{6.3}$$

$$PC7 = 0.49Ri_u + 0.38Rd_u + 0.44 * 1.75 + 0.40Imp_u - 0.48k_u - 0.17np_u + 0.03sp_u \tag{6.4}$$

where:

C_u = scaled and normalized runoff coefficient external inflow
C = runoff coefficient external inflow
μ_c = the mean of C over experiments of $\boldsymbol{X^{H0}}$
σ_c = the standard deviation of C over experiments of $\boldsymbol{X^{H0}}$

Accordingly, a variable state, that is ≥ 1 standard deviation under its mean, would suggest a negative influence on the $PC7$ value; a variable state ≥ 1 standard deviation above its mean, would suggest a positive influence on the value of $PC7$ (and the latter would thus contribute to more flood risk). An example scenario is provided in table 6.4.

Table 6.4: Example scenario: plausible states of the uncertainty parameters and corresponding values for X_u

Uncertainty parameter X_i	**Ri**	**Rd**	**C**	**Imp**	**k**	**n_p**	**s_p**
Value X_i	112.27	53.90	0.58	42.21	74.13	0.26	3.48
Deviation from the mean of experiments $\boldsymbol{X^{H0}}$	+ 1 std	+ 1 std	- 1.8 std	+ 1 std	- 1 std	0.00	0.00
Scaled and normalized uncertainty parameter $\boldsymbol{X_u}$	**Ri_u**	**Rd_u**	**C_u**	**Imp_u**	**k_u**	**np_u**	**sp_u**
Value X_u	1.00	1.00	-1.79	1.00	-1.00	0.00	0.00

If we would fill the obtained scaled and normalized parameters for this example into the linear combination of $PC7$, the following equation is obtained:

$$PC7 = 0.49 * 1 + 0.38 * 1 + 0.44 * -1.75 + 0.40 * 1 - 0.48 * -1 - 0.17 * 0 + 0.03 * 0 = 0.98 \tag{6.5}$$

This would suggest that node J26 would not be flooded for this scenario, as the corresponding value for $PC7$ is 1 and thus stays below the threshold value of 1.3. In this case, the above average rainfall intensity and rainfall duration is outweighed by the relative low runoff coefficient of the external inflow with regard to the experiment range. This addresses the significance of the amount of runoff from the mountains on whether or not flooding can be expected. The provided example shows how the PCA-PRIM outcomes could provide more insights on a wide range of scenarios. The explanation of the relative contributions of the uncertainty factors, represented by the coefficients of $PC7$, is aimed to be clarified in the next paragraph.

To explain the relative contribution of the uncertainty factors on flooding occurrence, we take a closer look at the water flows of adjacent subcatchments of node J26. The hyetograph and hydrographs are demonstrated in figure 6.14. The graphs are aggregations of all samples of run II. Each curve represents the mean of all scenarios and the corresponding shaded area represents one standard deviation above the mean and one standard deviation below the mean. The fluxes are flow rates per unit of area. At first glance, it is obvious that the runoff from the mountains is much higher than the precipitation flux. The resulting runoff is much higher in subcatchment 22 due to the external inflow flux, as subcatchment S22 is adjacent to the foot of the mountain and subcatchment S23 is not, as can be seen in figure /reffig:subcatchments-S22S23. Given the relative large size of the external inflow flux with a quite large standard deviation, it is reasonable that the runoff coefficient is sensitive with respect to flooding occurrence.

In addition to the runoff coefficient that is sensitive, more uncertainty factors appear to be almost equally important in explaining flooding occurrence. As the linear combination of $PC7$ discloses, the factors rainfall intensity, rainfall duration, the proportion of impervious area and the hydraulic conductivity of the soil of the subcatchments are almost equally weighted with respect to flooding occurrence. With both higher rainfall intensity and higher rainfall duration the pervious soil gets more saturated. In addition, higher rainfall intensity, gives higher peak flow in a shorter time, and stresses the drainage system. Whereas with higher rainfall duration the total water volume is more important. It is thus disputable what the more sensitive factor would be causing the system to flood. However, here we see that rainfall intensity is a bit more dominant than rainfall duration. So a higher peak flow in a shorter time does stress the system.

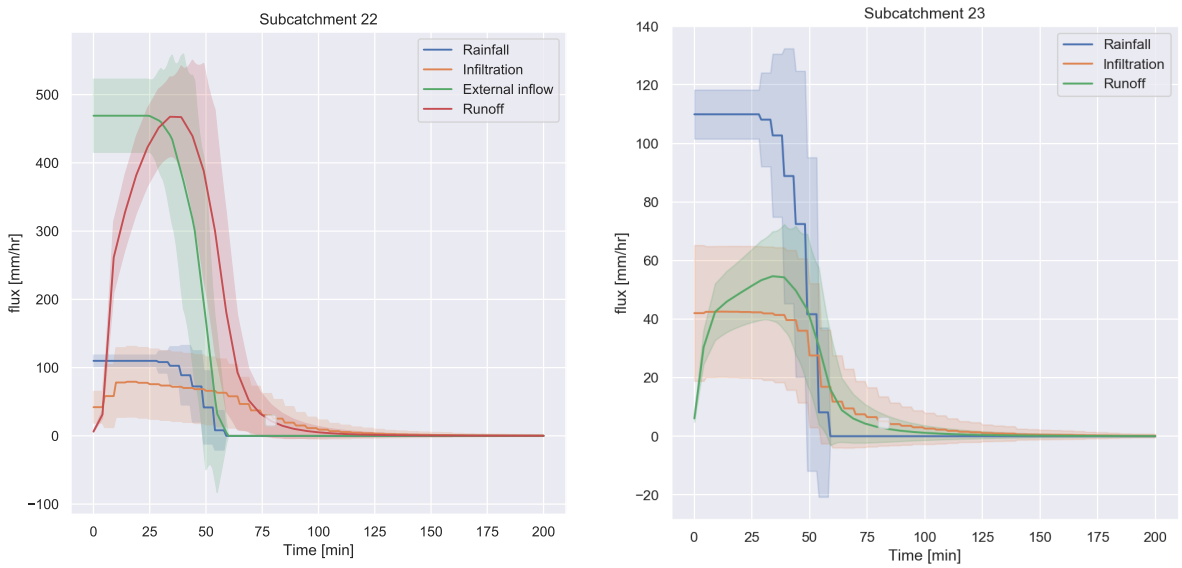

(a) (b)

Figure 6.14: Water flows (hyetograph + hydrographs) of adjacents subcatchments of node J26

It should be emphasized, however, that the factors in which $PC7$ is expressed, are the scaled and normalized variables. Interpretation should therefore always be considered with respect to the corresponding experiment domain of the variable states. Hence, it is reasonable the five dominant factors - rainfall intensity, rainfall duration, runoff coefficient, imperviousness and hydraulic conductivity - are almost equally weighted for the considered variable states. To illustrate: both ranges for rainfall intensity and rainfall duration are starting from high values. Raising rainfall intensity or duration would cause more runoff. The total runoff volume from the mountains depends on the rainfall intensity and the rainfall duration, thus C is related to these two parameters as well. Also, given the wide range of hydraulic conductivity, a very low hydraulic conductivity of the soil would make the rate of imperviousness even more important, and the other way around. This wide range of hydraulic conductivity also implies that if the soil would be really permeable (e.g. 250 mm/hr) it can outweigh the higher rainfall intensity and duration.

For these extreme rainfall events; long duration and high rainfall intensity, the depression storage is relative so small, a varying state of this variable is negligible, as confirmed by the model. The same holds for the roughness coefficient, when the runoff volumes are that high, the sensitivity of Manning's roughness coefficient are very small. It can be questioned whether depression storage and Manning's roughness coefficient should be included in the equation. Only if their strength is significantly different from zero.

6.4.3. PRIM vs PCA-PRIM outcomes

Now $PC7$ is better understood, the outcomes of both PRIM and PCA-PRIM analysis are compared for the runoff fluxes, flood volume and flood height of node J26. The graphs in figure 6.15, show the water fluxes of subcatchment S22 for three different classifications: all cases of interest (TOTAL COI) demonstrated in the top row, the cases of interest within the obtained boxes of PRIM (PRIM) in the second row, and in the third row the cases of interest in the obtained PCA-PRIM boxes (PCA-PRIM). Again, each curve represent the mean of the grouped samples, and one standard deviation is represented by the shaded area around the mean. The main characteristics of each classification can be found in table 6.5 below.

The grouped scenarios derived from the PRIM analysis (box 1 and box 2, row 2 figure 6.15), disclose that the runoff peak of the cases explained by box 2 is slightly earlier than the runoff peak of box 1. This behaviour seems to be in accordance with the corresponding dominant uncertainty domain PRIM has provided: most cases could be explained by a very high rainfall intensity, rainfall duration, runoff coefficient and imperviousness (box 1), whereas box 2 was mainly explained by very low hydraulic conductivity. It is clearly seen that a lower hydraulic conductivity cause less infiltration (row 2, infiltration) resulting in earlier runoff peak compared to the other scenarios.

Table 6.5: Brief summary of the scenario sets captured by PRIM and PCA-PRIM. * for these cases of interest no specific subset of input domain $\boldsymbol{H}^*$ could be found by the PRIM analysis

category	% coverage	% density	dominant factors
TOTAL COI			
total coi	100	9.9	
PRIM			
coi box 1	50	60	Mainly dominated by high Ri, Rd, C, Imp
coi box 2	30	30	Mainly dominated by low k
coi box 3 *	10	0.1	Distributed over entire input domain $\boldsymbol{H}^*$
PCA-PRIM			
coi box 1	90	89	Mainly dominated by Ri, Rd, C, Imp, k, described by $PC7$
coi box 2 *	10	0.1	Distributed over entire input domain $\boldsymbol{H}^*$

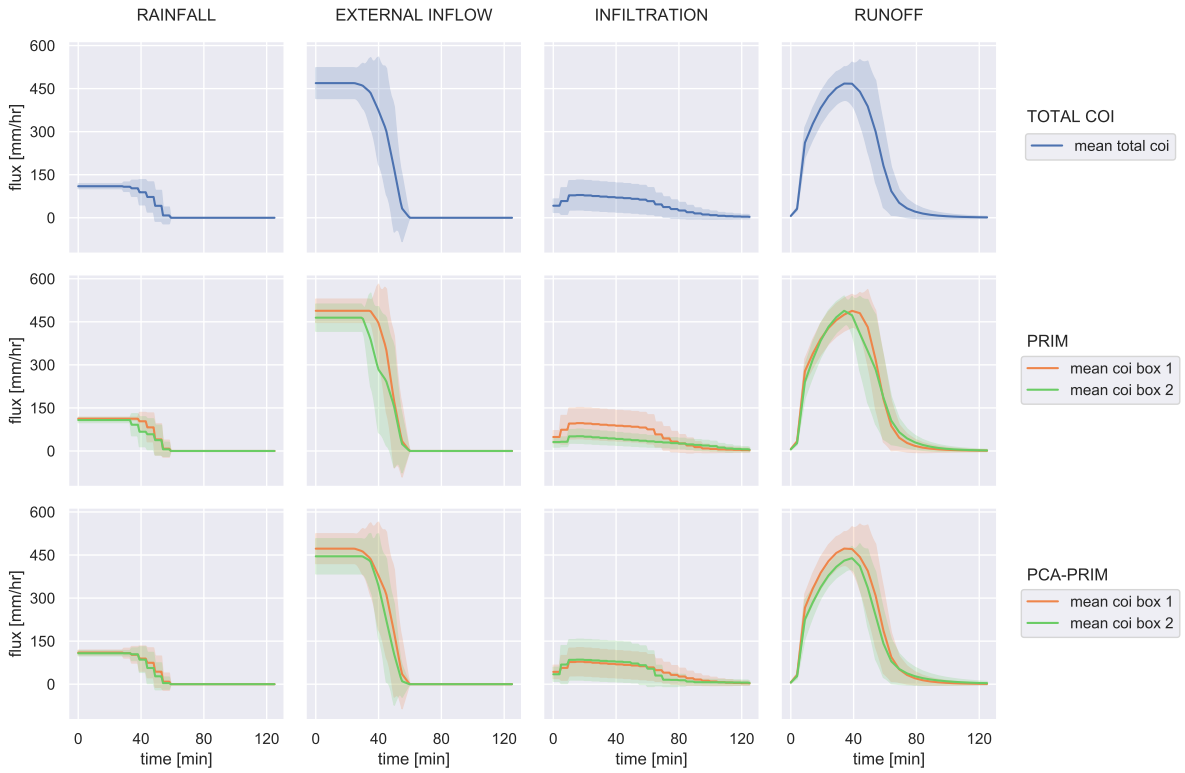

Figure 6.15: Subcatchment S22 for PRIM and PCA-PRIM results

In addition, the runoff peak of box 1 is wider than the runoff of scenarios represented by box 2. Given the dominant uncertainty space belonging to box 1 this seems reasonable too. The larger runoff for the scenarios within box 1 imply larger flood volume and flood height as can be seen in the second row of figure 6.16, where flood volumes and flood heights are provided for the three classifications. It is reasonable that hydraulic conductivity is less dominant for the more extreme rainfall events, given that the longer and more intense the rainfall event is, the range of hydraulic conductivity becomes relative less important. Accordingly, figures 6.16 for the PRIM analysis, show clearly that the volume of the scenarios captured with PRIM by box 2 result in lower flood volumes than the scenarios captured by box 1. This emphasizes that the scenarios represented by box 2 are the events for lower rainfall duration and intensity.

When we look at the PCA-PRIM graphs, seen in the third row of 6.16, it can be seen that the cases of interest that are not captured by the first box of PCA-PRIM, only 10 percent, the corresponding flood volumes are captured within the range of box 1. It seems thus sufficiently to only focus on box 1 with equation 6.1. We see

that the runoff peak of box 1 of PCA-PRIM is slightly earlier than the peak of represented by box 1 of PRIM. PCA-PRIM's runoff peak equals more or less the runoff of the TOTAL COI. Which is understandable, as PCA-PRIM box 1 is the aggregation of almost all cases of interest. The runoff fluxes of boxes 1 from both PCA-PRIM and PRIM lie in the same range.

PCA-PRIM gave a more precise outcome in comparison to PRIM, for which multiple plausible states can be assessed by the user using the equation of $PC7$. However, the PRIM graphs show us quickly the difference between the more extreme events and the less extreme events dominated by the lower hydraulic conductivity. The linear equation of $PC7$ confirms this relation. For higher rainfall intensity, and rainfall duration, changing the hydraulic conductivity would become less sensitive in explaining flooding occurrence.

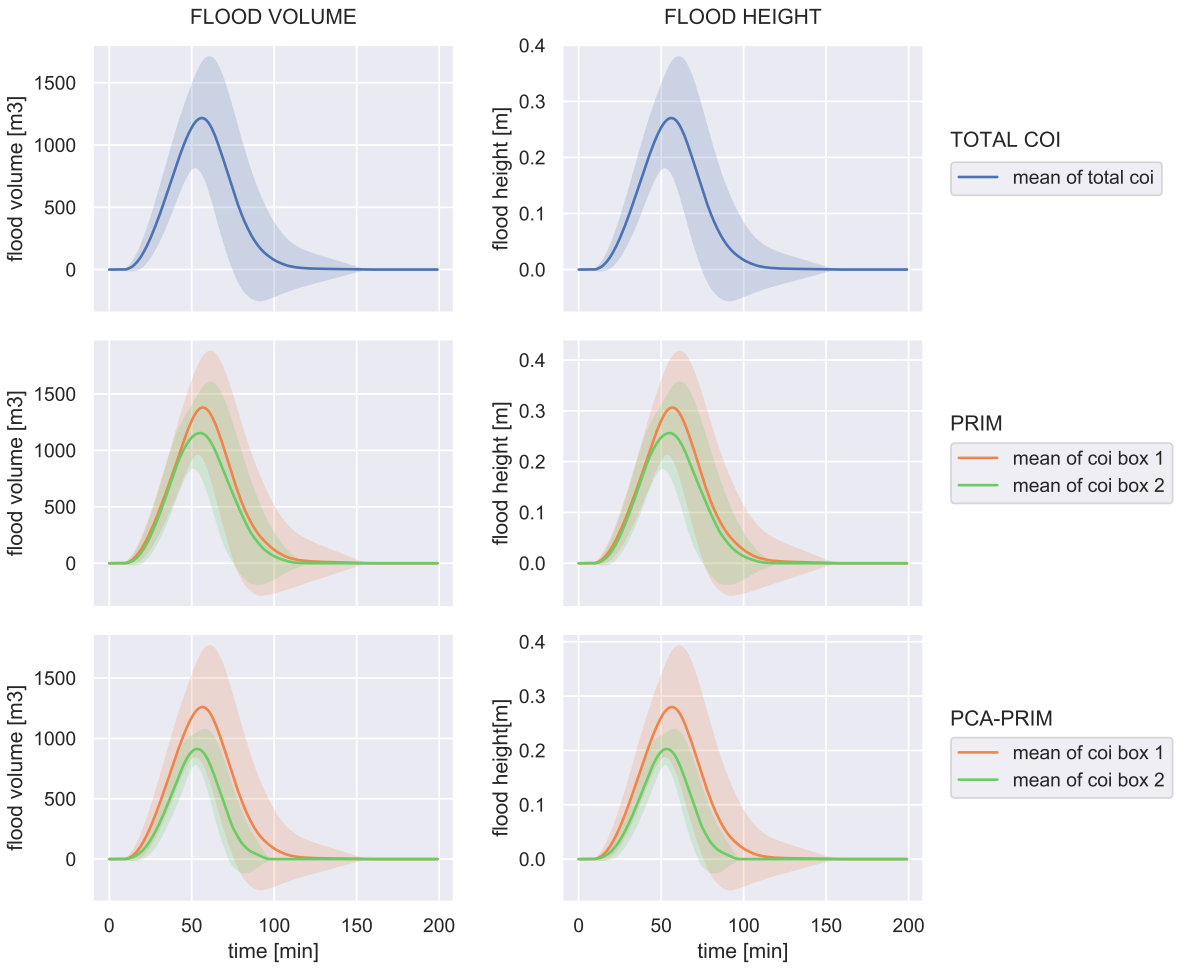

Figure 6.16: Flood height and volume of node J26 for PRIM and PCA-PRIm results

6.4.4. Analysis outcomes put into practice

The model outcomes are based on the assumptions that the external inflow is directly routed onto the sub-catchment. This implies that there is no delay taken into account for the raindrop that falls at the furthest point from the mountain foot. Would assuming rainfall runoff without delay be wrong? As can be seen from the graph (figure 6.14) the external inflow is almost ten times higher than compared to the runoff that is generated from the catchment only. Therefore we see that, not taking into account the delay might somewhat overestimate the peak flow a little, however, given the extent of the volume, and the long duration of the rainfall event, the peak flow will probably be more or less the same.

Given the area includes new housing as well as a temple, flood height > 0.2m would cause damage. For the estimated ranges based on the current information available, it would thus imply that for even really extreme rainfall it would be effective to pay attention to the proportion of impervious surface as well as the drainage

capacity of the pervious areas.

Why would node J26 flood, and J27 and J28 do not? The runoff from both the mountains adjacent to subcatchment 24 and subcatchment 22 should be conveyed through node J26. Also, both conduits C27 and C28 consist of 2 parallel conduits. Whereas C26 only consists of 1 conduit. C27 and C28 have higher volume capacity than C26 alone.

Table 6.6: Limits of uncertainty parameters for which flooding of node J26 occurs, corresponding to $\boldsymbol{X^{H0}}$

	Ri	**Rd**	**C**	**Imp**	**k**	**n_p**	**s_p**
min	82	30	0.585	10	0.36	0.13	2
max	120	60	1	50	347.125	0.397	4.985

The conditions for which the system capacity would be exceeded are the intervals for the parameters given in table 6.6. In which 90 percent can be explained by the linear combination of $PC7$ (eq 6.1). So the higher rainfall intensities and rainfall duration only cause flooding when the hydraulic conductivity of the soil would be really low, and the antecedent rain conditions would be extreme such that there is significant runoff from the mountains. In addition, if a few parameters of the five dominant parameters would be much lower than its mean, the system would only be flooded if the other parameters are much higher than its mean. When we look at the rainfall intensity and rainfall duration, (figure 4.12a) minimum rainfall intensity 75 mm/hr and from duration of 30 min onwards, the T=20 yrs return period according the IDF curve is exceeded. If that duration is increased towards 60 minutes, the return period becomes T=100 yrs. A rainfall intensity of 100 mm/hr for a duration of 45 minutes is not captured on the IDF curve, as that would be a really high return period. However, as mentioned this curve was only based on data from 7 years. Where the latest years have not been taken into account. The considered rainfall events for which the northern area would be vulnerable are thus very extreme, however, not impossible.

Given the fact that these events would only occur for very high runoff loads from the mountains, there is a small chance that both the infiltration capacity of the forest soil becomes so low and there will be such a heavy rainfall. Therefore it is not suggested to increase the capacity of the 'grey infrastructure'. To avoid flooding in this northern area more natural based solutions are suggested.

Table 6.7: Overview of the examined stormwater management policies. *Settings of model modifications can be found in appendix C.1

policy	**A0: reference situation**	**A1: drainage capacity soil**	**A2: vegetative swales + storage**	**A3: infiltration trenches + storage**
description	current situation grey infrastructure no natural-based solutions or Blue-Green infrastructure	hydraulic conductivity >200 mm/hr	natural channels to convey water towards lower area	infiltration trenches in subcatchment adjacent to mountains
		limit paved area: imperviousness <40%	storage facility in retention area	storage facility in retention area
analysis settings	experiments run 2	selection experiments run 2 for which k >200 and imperviousness <40	new experimental design (run 3)	new experimental design (run 4)
	base SWMM model		same experiments run 2 modified SWMM model	same experiments as run 2 modified swmm model
			Modified SWMM model: additional conduit barrel C28,27,26 storage unit in retention area	Modified SWMM model*: infiltration trenches* in catchment S22, S24 storage unit in retention area
output				
counts cases flooded	x	x	x	x
paired scatterplots	x	x	x	x
dimensional stacking	x			x
emperical CDF	x	x	x	x
PRIM	x			x
PCA -PRIM	x			x

6.5. Potential solutions

6.5.1. Overview of examined solutions A1, A2, A3

Based on the Scenario Discovery outcomes, three vulnerability reducing strategies are proposed that anticipate the high runoff volumes by either 1) managing the sensitive parameters related to infiltration: imperviousness and hydraulic conductivity, 2) adding natural-based solutions like a vegetated swale and a storage

retention area in the lower lying area or 3) adding infiltration trench in combination with the storage retention in the lower lying area. The policies are referred to as A1, A2, and A3, respectively. Table 6.7 gives an overview. The current system of Ötsuchi is denoted as the reference situation A0. A1 is analysed by selecting the samples corresponding to a subspace of $\boldsymbol{H}$. To analyse A2 and A3 additional experimental designs are done, with the same experiments of Run II, denoted by $\boldsymbol{E_{II}}$ In this paragraph an overview summary of the results is given. In the paragraphs below each strategy is elaborated in further detail.

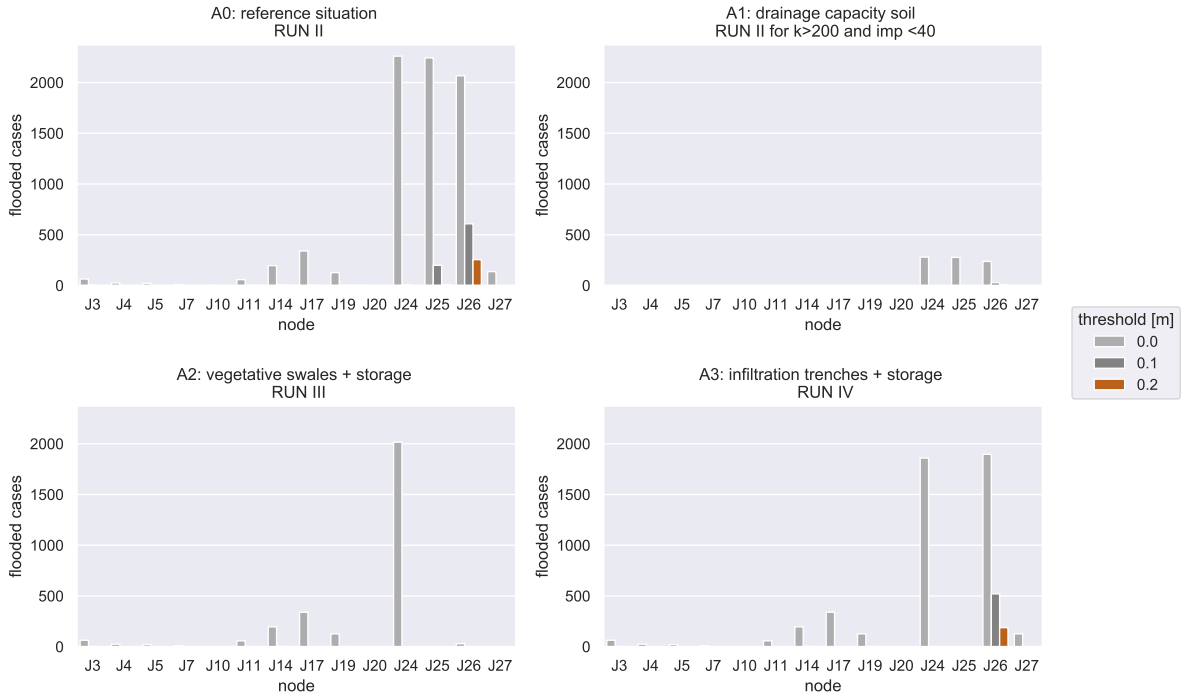

Figure 6.17: Samples count for which flooding occur for each node, for all examined policies

Figure 6.17 shows the amount of samples for which a node is flooded for all examined policies. As can be seen for policy A1 and A2 no flooding occurrence above 0.1 m would emerge. Whereas with policy A3 node J26 remains vulnerable. For policies A2 and A3, no data is available for node J25, therefore the counts are here zero. This is because node J25 is a divider node to reroute flow to the retention area, for these node types no ponded volume time series are recorded.

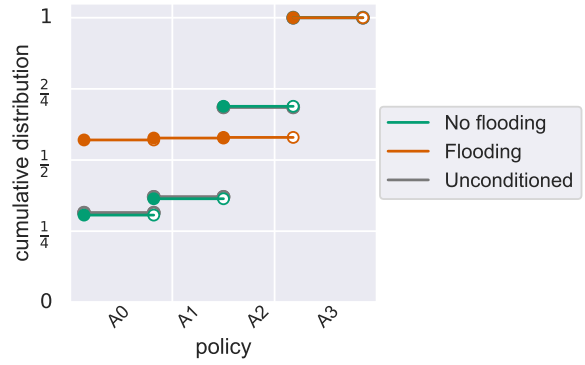

Figure 6.18: Empirical cumulative density function of the examined policies

When applying scenario discovery using the EMA-workbench, a supportive tool to visualize the regional sensitivity of the policies is to graph the empirical cumulative distribution. The relative sensitivity of the policies

on flooding occurrence is shown in the cumulative distribution curves of figure 6.18. All samples of all policies are aggregated and accordingly classified into either flooded samples or no flooding samples, after which the cumulative distribution can be demonstrated. The grey line, shows the aggregation of all samples without classification. What can be seen is that the proportion of samples considered for A1 is much lower than for the remaining samples. Also, it emphasizes the same conclusions as shown in the count plot above: policies A1 and A2 are most insensitive to flooding occurrence, and in terms of reducing the vulnerability the most feasible policies to imply.

6.5.2. A1: Low impervious surface area and high hydraulic conductivity

The easiest way to increase the resilience would be to manage the proportion impervious area. If the composed granite soil, has such a high permeability, it would be suggested that this would be a good initiative to reduce the flood risk, as the scenario discovery outcomes also confirms. If the soil appears to have lower hydraulic conductivity, drainage pipes could be installed. If drainage could be installed such that the permeability of the soil would be above 200 mm/hr, and the surface area would be paved below 40 percent, nearly no flooding occurrence are expected. The scatterplot for the samples of Run II, corresponding to the restrictions of $k > 200$ and $Imp < 40$ can be found in appendix C.1.

6.5.3. A2+A3: LIDS

Vegetative Swale & Infiltration trench

Given the high water volumes the system would possibly need to convey, much storage capacity would be needed. To avoid it being spread uncontrollably through both the residential area, and the low-lying area, the water should be managed through the subcatchment. This could be done by for example LIDS, for which a Vegative swale, or an Infiltration trench (figure 6.19) are mostly suggested: much storage capacity is needed, and high sediment concentration could accelerate clogging in alternative LIDS, such as a bio-retention cell, if not equipped with a sediment retention facility.

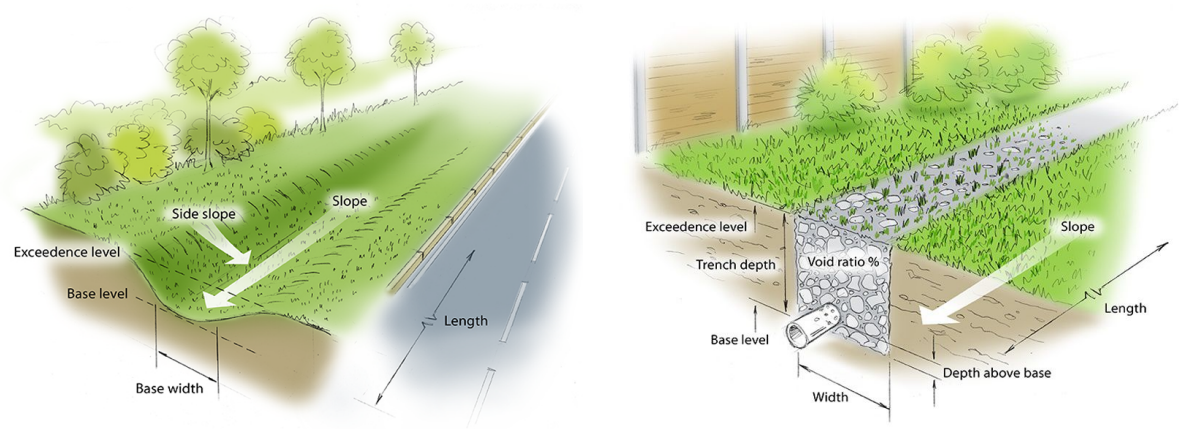

(a) Vegetative Swale

(b) Infiltration trench

Figure 6.19: Potential LIDS. Source: https://help.innovyze.com

Storage capacity in lower retention area

In addition, to release the stress of the whole urban system, the water could potentially be conveyed and stored in the lower lying retention area. According the urban development plans (Otsuchi Town, 2014), as can be seen in 4.6, there is parking place, and 'temporary ground' reserved for recreational purposes, like sports.

Moreover, although this is not the 'hot spot' area of the many artesian wells prior to the tsunami, there is exactly just one previous artesian well to be found in this specific spot. As can be seen in the figure attached to appendix A.5. This suggests there is access to this high water pressure aquifer in this spot too. Restoring a communal place for the beloved water wells, would add to the urban quality in favour of the local people of Ötsuchi Town (more ideas could be retrieved from (Mori, 2018)). A commutative opportunity emerges here: This place could be a communal place for access to the fresh water wells (just like there were a few before the

tsunami), and when in times it is needed, a storage basin for stormwater.

It is assumed that Ötsuchi Town has abundant fresh water availability, given the Shiroyama mountains and the water supply source at Mizukawa just a few kilometers north of Ötsuchi Town (Sumi, 2003). Therefore, reusing stormwater would maybe not be applicable here. However, in case water availability is a scarce, stormwater, from upstream could potentially be reused for household or industrial purposes. So the bypass towards the low lying area would come in handy not only during rare extreme events, but more on a regular basis. Driven by sustainability and the close relation with nature, Japan is very proficient in recycling water (see also van de Ven, Furumai, & Koga, 2008). Whereas Japan has been proficient in reusing 'grey water', stormwater has been somewhat lacked behind (MLIT, 2016). Due to pollution and sediments present in stormwater. However, it is aimed to increase the reuse of stormwater too. Given the prospects of more droughts, this holds the promise of accelerating innovative techniques that enables the ease of stormwater recycling.

SWMMxEMA results for A2

The solution including the vegetative swale is referred to as A2. The corresponding adjustments in the original SWMM model can be found in appendix C.1. The vegetative swale is represented by adding another barrel to the current conduits. This would overestimate the flow that can be conveyed through the vegetative swale, as the conduit has much lower roughness coefficient. However, just for exploring this would succeed. The schematized representation of the model is provided in figure 6.20. In this model only conduits are represented parallel to the current model, however, in reality the vegetative swales would be suggested to be adjacent to the mountains, and a few implemented perpendicular to the conduits. The flow is divided at node J25, when the conduits upstream J25 reach just below full flow capacity.

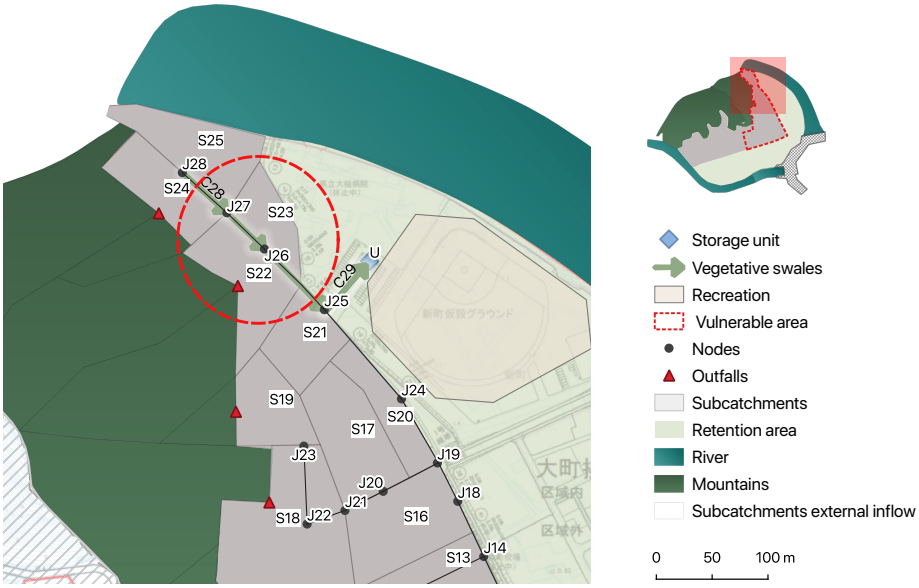

Figure 6.20: Vegetated Swale SWMM model

No flooding occurs for all experiment ranges, which can be seen in the overview map in the appendix C.1. Downstream node J25, it appears that due to the solution implemented in the area of J26, for some nodes downstream the vulnerability is reduced as well. For node J24, just downstream of node J25, the effect of rerouting the flow from node J25 towards the lower retention area has been analysed with the dimensional stacking graphs for A0 and A2, for a flooding threshold of 0.1 m. The difference of both dimensional stacking graphs (A0-A2) is provided in figure 6.21. Whereas in the original dimensional stacking tables for A0 and A2 each cell represents the ratio flooded samples over the total samples within the specific interval, here the point difference is taken of the two dimensional graphs. A positive difference thus means that for samples within that interval the amount of samples flooded have decreased for node J24. As can be seen this is partic-

ularly the case for the yellow cell, corresponding to conditions for very high rainfall intensity (>109), for very high runoff and the lower hydraulic conductivity values.

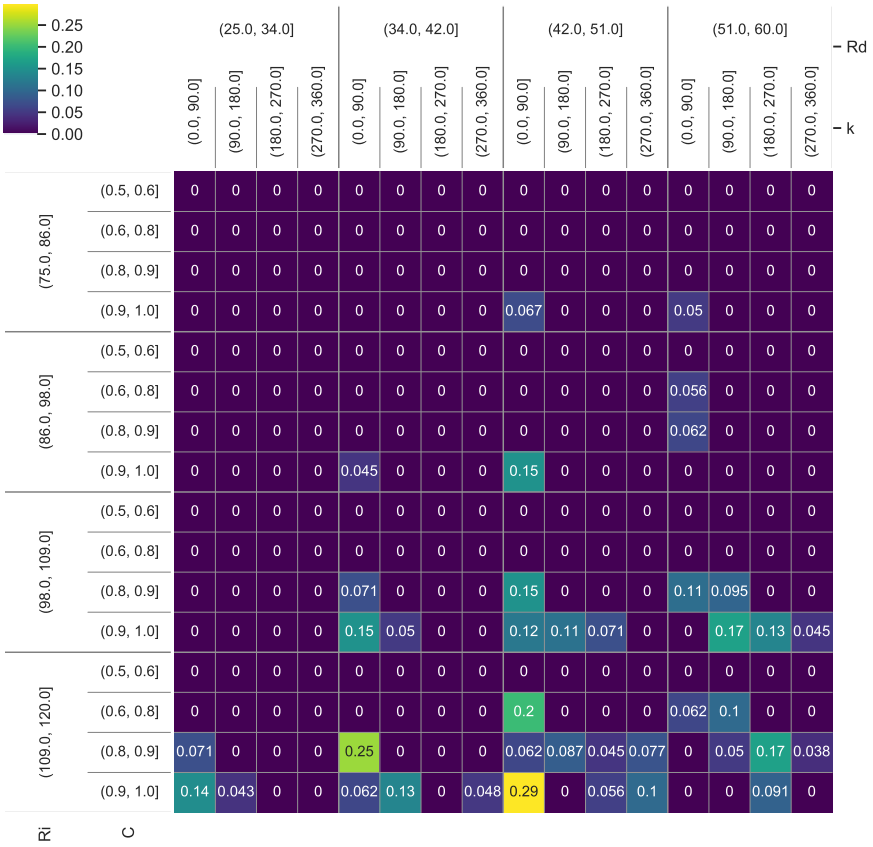

Figure 6.21: Improvement of node J24 by policy A2: dimensional stacking difference between policies A0 and A2. Each cell represents the point difference between the ratio flooded samples (>0.1m) over the total samples within that interval for A0 and A2.

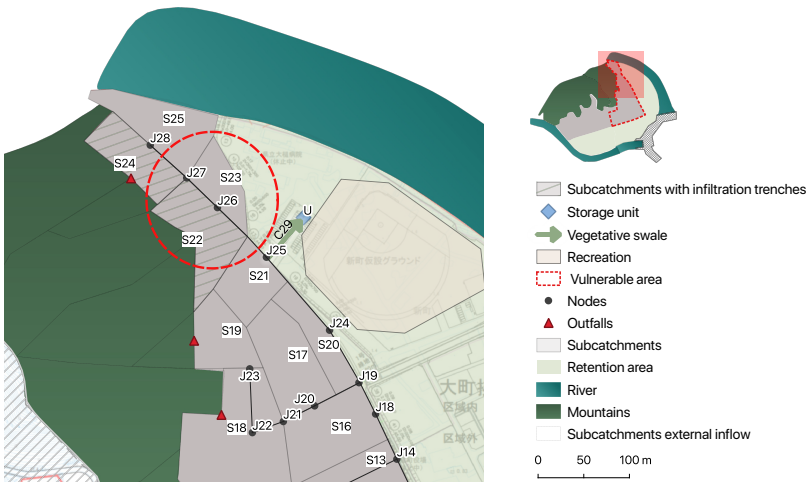

Figure 6.22: Infiltration trench SWMM model

SWMMxEMA results for A3

Moreover, another solution is explored and that is adding infiltration trenches for both subcatchments S22 and S24, in combination with rerouting high stormwater volumes to the low-lying retention area via node J25. Specific model settings can be found in appendix C.1. As seen in the count plot (figure 6.17), still a significant amount of samples show flooding occurrence for solution A3. The cases that are 'solved' and which ones are not, are therefore analysed. The scatter plot of all cases of interest from the reference situation are plotted in figure 6.23. The orange points are the cases that show no flooding occurrence for node J26 in A3, whereas it did in A0, the grey points show the points for which the cases both flooded in A0 and A3. At first glance, no distinctive patterns can be detected. However, for the upper range of rainfall duration there seem to be less solved cases than for the lower ranges.

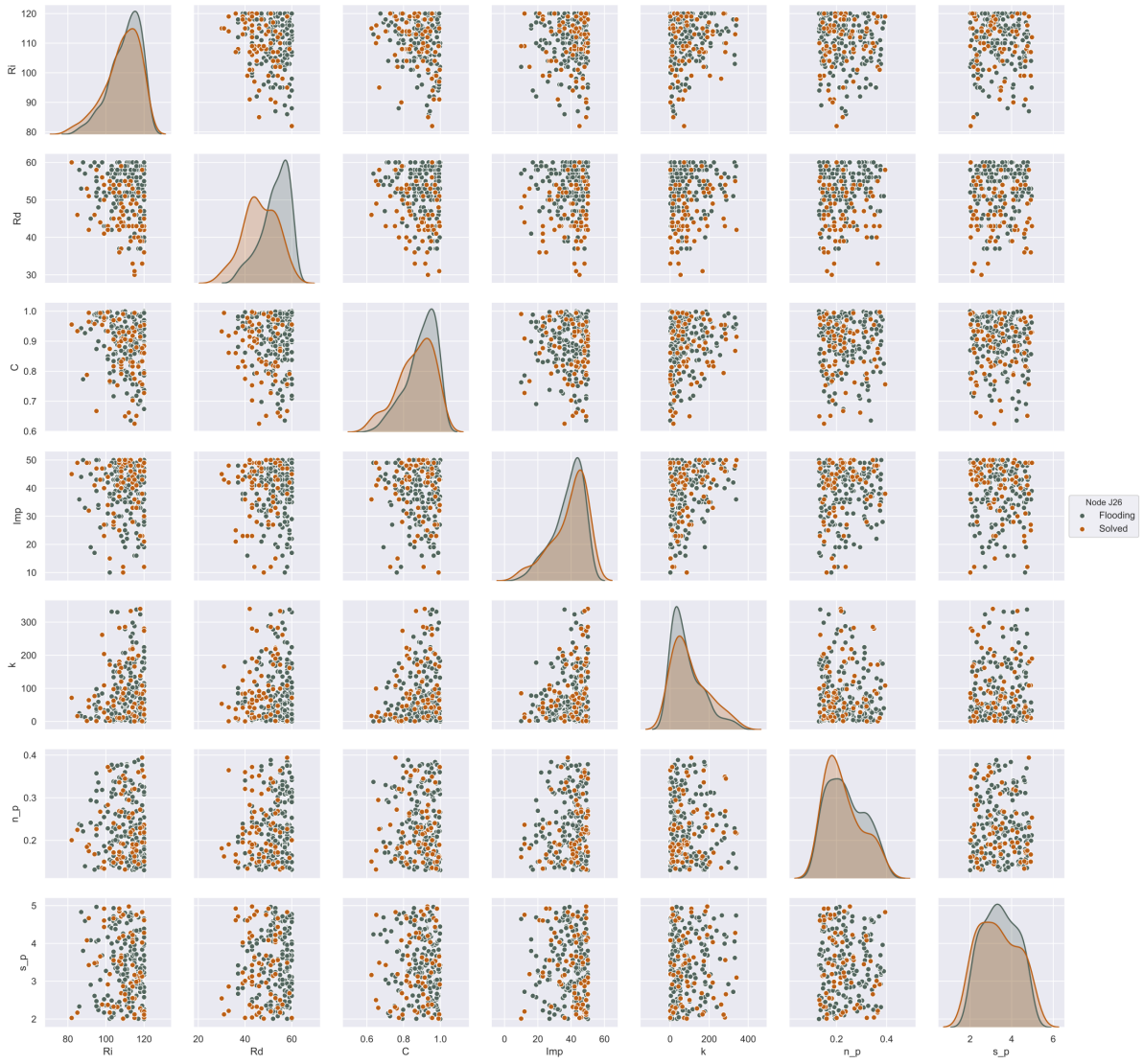

Figure 6.23: Scatterplot of cases of interest that are still flooded or solved with policy A4

To get a better understanding why some cases are solved, and some are not, PRIM is applied of all cases of interest of A0 that are shown in the scatter plot below. First, PRIM was used by considering the cases of interest to be the flooded cases just like the previous PRIM analysis. However, these results show almost the same results as the PRIM outcomes for A0, and do not provide particular insight for explaining why some cases are solved in this case, and which are not. The corresponding graphs can be found in appendix C.1.

Therefore, PRIM is applied on the samples, by considering the cases of interest to be the 'solved' cases. Note that for this particular case a new classification emerge: the cases of interest to be explained by PRIM are now

the 'solved' cases, and the flooded cases are considered as the cases not of interest within the PRIM analysis. Both PRIM and PCA-PRIM are applied. The results are summarized into table 6.8. PCA-PRIM outcome is given below in equation 6.6. Again, a PCA-PRIM box is found for nearly 100 % coverage, with a precision of almost 70%. Note that the signs in $PC7$ are inversed as it concerns the solved cases. When the value of $PC7_A3$ is above 0.22 it means that it is very likely the vulnerability of node J26 has been improved by implementing infiltration trenches. This applies thus for the lower values of Ri, Rd, Cu and Imp, or either higher values of k. Whereas from the scatter plot and the PRIM analysis, rainfall duration seems very sensitive, from the PCA-PRIM results both rainfall intensity and rainfall duration are sensitive. $PC7_{A3}$ show nicely the effect of the infiltration trench: when comparing $PC7_{A3}$ with $PC7$ from the analysis on A0, the Imperviousness is less important in scenario A3. This seems reasonable as part of the runoff from the impervious surface is treated by the infiltration trenches.

Table 6.8: brief summary of the scenario sets captured by PRIM and PCA-PRIM for A3

category	**% coverage**	**%density**	**dominant factors**
TOTAL COI			
total coi	100	7.27	
PRIM			
box 1	66	50	Mainly dominated by lower Rd
box 2	19	0.25	Mainly dominated by Ri, C
PCA-PRIM			
box 1	97	68	Mainly dominated by Ri, Rd, C, k, Imp described by $PC7_{A3}$

$$PC7_{A3} = -0.49Ri_u - 0.46Rd_u - 0.44C_u - 0.32Imp_u + 0.48k_u + 0.19np_u - 0.03sp_u \tag{6.6}$$

and

$$y_{j26_{A3}} = \begin{cases} 1, & \text{if } PC7 \geq 0.22 \\ 0, & \text{otherwise} \end{cases} \tag{6.7}$$

where:

$y_{j26_{a3}}$= system performance outcome of node J26 for policy A3 (solved: $y_{j26_{a3}} = 1$, still flooded $y_{j26_{a3}} = 0$)

7

Discussion

7.1. Design approach case study

The stormwater system in Ötsuchi Town seems robust. The outcomes of the exploratory modelling suggests that the majority of the system would be sufficient for the governments' design criteria and beyond. However, being designed according the Rational Method, it is not clear whether or not extreme conditions have been explored during the design phase. Whereas the Tsunami prevention measures are very resilient - a combination of retreat, attack and accommodate measures - there has no additional measures been taken for in case the urban drainage system would fail. That is, during a very extreme rainfall event, both in duration and intensity, on top of the premise that the threshold for initial precipitation losses are reached, such as infiltration, to cause any runoff generation. Then, much runoff could be created from the steep mountain slopes, as also have been found by Masatugu (n.d.). However, hill slope runoff processes are very complex, and is rather a non-linear process, as stated by McDonnell (2003). Subsurface flows and spatial heterogeneity of the soil plays a significant role and is very specific. It is therefore still unclear how the initial losses processes are, and should be further examined to put the PRIM outcomes into perspective. However, if runoff generation would be present, this would cause stress on the urban drainage system as shown by the results. In this sense the stormwater system would be not resilient.

Moreover, if the reconstruction would have taken place today, anno 2019, maybe it would have been different. During the time of the reconstruction of Ötsuchi-town (> 2011), maybe pluvial flooding was less 'on topic' than now. In the past few years, Japan has been suffering from large pluvial floods multiple times. Accordingly, in 2015, the Japanese government changed the sewer and drainage law, in which is posed that governments should not only design their drainage for the design criteria but also explore the ranges of exceedance (MLIT, 2015b), which underlines the perspective of this study. In addition, the change in regulation includes that not only peak volume should be examined, but also possible flood height occurrence by using flow routing models and effective approaches, by working together with academics and companies. This study proves exploring these ranges can help in disclosing the vulnerabilities. As a major disaster strikes, this disaster seems to be the central focus of the reconstruction design. However, maybe the change in regulation could provoke to consider resilient stormwater management solutions, even if at first it seems not a danger that needs to be managed.

7.2. Sensitivity SWMM model

Whereas in this research many parameters have been tested on sensitivity, the sensitivity of the model layout itself has not explicitly been quantified. However, this was not neglected. This can be verified by the following reasons;

Multiple model layouts
Many improvements have been made on the model layout starting from a more complex model, towards a really simple model, towards a more complex model again. Along the way also many experiments were runned. For every model layout the outcomes for flood height >0.2m suggested the same vulnerable spots in the system. So it is assumed that a small change in the number of conduits and nodes would not bring

very different outcomes. An example for the more simple model with the emerged vulnerable area is given in appendix C.11. In addition, changing the conduits and invert levels is not conducted quickly, when no DEM is available. This hampers the process of examining multiple model layouts.

Energy losses
Kinematic wave approximation assumes no pressure forces and inertial forces, therefore most energy losses at junctions and backwater curves could not be taken into account - but the friction losses are implicitly taken into account with the Manning roughness coefficient. However, in reality, at junctions the energy losses would occur. Also in manholes, however, these are also not taken into account. This implies that the flow rates might be somewhere overestimated, whereas in reality the flow would be hampered. Again, given the quite low values for all flood height thresholds, except for the northern area, the results do not suggest that this would make a difference in the conclusions drawn.

Calibration
As no discharge data is available, no calibration could be done. However for the exploratory phase, it assumed this model has been sufficient because the exact dimensions of the sewer system were present. Also, some simplifications were made on surface type, which would never give the exact runoff, however a good insight into the order of magnitude. For exact design purposes a more advanced model would be feasible, and thus discharge data, and more information on the soil types, DEM, and land use types should be obtained.

System exceedance
As surface exceedance routing can not be done with SWMM, the flood height should be considered as indication of severe flooding or not. As this is an estimation, multiple levels of exceedance were assessed. Where it appeared that for the lower flood volumes, the flood height would be minimum.

When more information on system characteristics would be known, such as more detailed land use maps, and heights, more advanced models could be established to examine whether for the given scenarios out of this research, they would give similar results by using the more complex models.

Mountain runoff
The cases of interest in this study, involve very high mountain runoff values. Given the steep slope, a runoff coefficient above 0.58 seems reasonable, as found by earlier researches on after initial losses for steep hill slopes in Japan (Masatugu, n.d.), which states that runoff coefficient is approximately 0.55, after initial losses for rain events with rainfall intensity above 100 mm/hr. Given the steep hill slopes of 20 to 50 %, of the concerned vulnerable area, however, this runoff coefficient is thus likely to be even higher when the initial losses threshold is reached.

Very high mountain runoff values implies that sediment transport may play a significant role. Energy of the flow should be dissipated to capture the sediments before it enters the urban drainage system. The very high runoff values could also imply that under these wet conditions, other water processes are going on than sheet flow, for which the assumptions of the current model not valid anymore. Mountain runoff for such high runoff values, would suggest higher velocities of the flow in big amounts, and would potentially lead to flash floods. This would cause another danger, and should be assessed with 2d hydrodynamic models (see for example Huang, Wu, and Zhao (2013)).

Cross-linguistics
As many documents and retrieved maps used were in Japanese, this might have caused any wrong interpretations on the concerned topics and input data. However, much have been discussed and verified with relevant stakeholders, to limit this issue.

7.3. Assumptions uncertainty parameters

Setting the bounds of the uncertainty parameters is critical when applying an exploratory modelling and analysis methodology. In particular, the relative weights of the uncertainty parameters, obtained with PCA-PRIM, must always be considered with respect to their input domain. This implicitly implies that the PCA-PRIM results could be different when a different input domain is chosen. This sensitivity is however yet to be investigated in a later phase.

Whereas most uncertainty parameters and ranges are derived from literature, the external inflow runoff has

been explored for a broader range, to include the extreme events. Where a runoff coefficient of 1 would be maybe too much, its impact of including this range within the scenario discovery analysis should be checked.

Considering the remaining uncertainty parameters, if would be expected that a slightly higher range would cause different system behaviour, it would do no harm to check these ranges as well.

Also, the applied block rainfall is very coarse. However, it is more easy to implement and permute in the experimental design, in case of this specific set up. Whereas each rainfall shape has it own peak and runoff volume, a wide range is covered when permuting over rainfall intensity and rainfall duration block-wise. For a less robust system, the design storm profile could be more important in being sensitive for the system behaviour.

7.4. Outcomes Scenario Discovery

7.4.1. Adaptive planning solutions

As stated by (Lempert et al., 2013), in most cases, the application of scenario discovery lead to adaptive planning approaches, in which there is room to evolve over time as more information becomes available. Likewise, the results obtained in this research suggests that no immediate measures should be taken at this state, however it is suggested to examine the runoff from the mountains more closely in relation to the hydraulic conductivity of the mountain slopes. When the hydraulic conductivity is likely to decrease that much - for example due to very wet antecedent conditions - such that it triggers runoff corresponding to a $C > 0.58$, the northern area would be vulnerable. Feasibility of implementations of the Green-Blue infrastructure proposed in this study, could be examined. Taking into account that measures may be needed in the future, this could be incorporated future urban development plans.

7.4.2. Interdisciplinary approach

Whereas during the reconstruction of Ötsuchi Town it seems that little interaction has taken place between the urban water management discipline and the urban planners, the outcomes of this research underlines the advantage of an integrated planning approach in the tsunami reconstruction. The vulnerability of the system could have been reduced by relative simple measures, related to the spatial planning. An example would be to create a lower-lying buffer zone between the mountains and the residential area. Also, the tsunami retention area emerged to be a potential commutative reconstruction measure. Multi-purpose stormwater storage facilities can be established here, which addresses again the benefits of collaboration between stormwater management discipline and spatial planning. In addition, potential interdisciplinary collaboration between geo-technical engineers and stormwater management emerge here as well. Whereas geo-technical matters that are taken into account within the reconstruction, such as that the reclaimed area is well drained to prevent liquefaction. The results show that the permeability of the soil seems to be decisive in the vulnerability of the northern area. When the residential area was raised, a gravel layer has been established for encouraging drainage. If it appears that the hydraulic conductivity of the soil is likely to be in the lower ranges that are examined in this research, additional drainage facilities could have been implemented during the reconstruction phase. In addition, geo-technical engineers, concern that mountain slopes remain stable to prevent landslides and debris flows, these matters relate to the vulnerability caused by pluvial flooding. More information on flash floods or debris flows occurrence may make other solutions more feasible to implement than the solutions considered in this research. Collaboration could enhance insights into the concerned physical processes, and serve as input for more resilient and effective measures.

7.5. SWMM x EMA: potential

7.5.1. Scenario Discovery applied on resilient stormwater management

Since an exploratory and modelling approach for urban drainage problems is promoted by Babovic et al. (2018), here will be reflected upon the usage of scenario discovery on resilient urban stormwater management problem. Main reason of applying scenario discovery on urban drainage problems is to gain more insight into the possible load conditions and related sensitive factors. In this research scenario discovery was applicable on an urban drainage problem in two different ways. This emerge from the fact that an urban drainage system includes multiple locations, with varying vulnerability over space. The difference of applicability will be explained with figure 7.1. The figure shows the steps in understanding the sensitive key factors on system performance. The top row, shows the process of understanding the sensitive parameters

on a rather vulnerable area such as the area of node J26. Graphs 1-4 show the sequential steps of how flood occurrence could be analysed and used as input for solutions. Each step knows its specific density (precision) and coverage (recall). For the area of node J26, all steps, up to the application of PCA-PRIM, were needed to get a full understanding of the sensitive parameters. For the remaining nodes, which appeared to be vulnerable for very limited amounts of cases, caused by one or two dominant parameters and states, this is different. Only the first steps of the scenario discovery were sufficient to get a full understanding of system behaviour in extreme conditions. Namely, the sampling and the preliminary visualisation (see row 2 of figure 7.1). No additional PRIM analyses were needed for these locations to examine flood volumes and its dominant factors. However, scenario discovery could in turn, be applied to assess multiple policies, and their effect on reducing the risk.

The PCA-PRIM outcomes for the vulnerable node J26 results in understanding whether or not either impervious rate, or hydraulic conductivity, is sensitive for causing failure of the system for wide-ranging plausible states. Both variables are related to the infiltration capacity. Based on these outcomes, it can be decided whether or not it is effective to take relative easy actions, such as adding drainage, or implementing more green surface, to reduce the vulnerability of the system at hand.

In addition, for modelling purposes, knowing the dominance of the parameters for a wide range makes the applied assumptions more robust when in the final design phase, where complex models, with high computational cost, could only be analyzed for a small range of states of the system. This research proves that using scenario discovery can aid in this, as the results for flooding occurrence at node J26 suggests that the depression storage and the manning roughness would be insensitive to explaining flooding for the very extreme rainfall events at J26. Whereas literature suggests this is likely to assume, the outcome of this research confirms that.

Finally, the complexity of the SWMM model in this research had been kept quite simple for computational running time purposes. For one experimental design of 4502 experiments, the run time could reach up to 8 hours, when using a 'regular' computer. As only single events were examined for a quite simple model, the runtime of one SWMM model was minimal. However, the long run times were mainly caused by the workarounds how SWMM outputs were read and imported into python. A complete transfer of the SWMM code, written in C+, to the python engine would enable would enable running SWMM and saving SWMM outputs within python itself. This would optimize reading and saving output files significantly, and decrease the computational cost. In addition, the concerned study area was relative small making it less computational intensive. However, when both the SWMM x EMA model would be optimized, and faster computers of parallel computing could be applied, also larger ares and more complex SWMM models are expected to be feasible for using the EMA-workbench in combination with SWMM modelling.

7.5.2. Tsunami reconstruction

Applying the exploratory modelling and analysis approach with SWMM during a tsunami reconstruction could aid in revealing both the vulnerabilities and robustness of the urban drainage system that is considered. As multiple stakeholders are involved, the results could take away doubts of whether or not a system would be expected to be robust in for a wide range of plausible states. The method provides a good tool to visualize vulnerabilities and illuminate potential solutions. For example, knowing that the hydraulic conductivity and imperviousness would be sensitive to flood occurrence would have been beneficial to know during the design phase, and would encourage an interdisciplinary approach. Using scenario discovery within a tsunami reconstruction design could thus enhance the integral approach between stormwater management, geo-technical engineering and spatial planning. This would make taking advantage of the disaster reconstruction to establish an integrated resilient reconstruction, more likely.

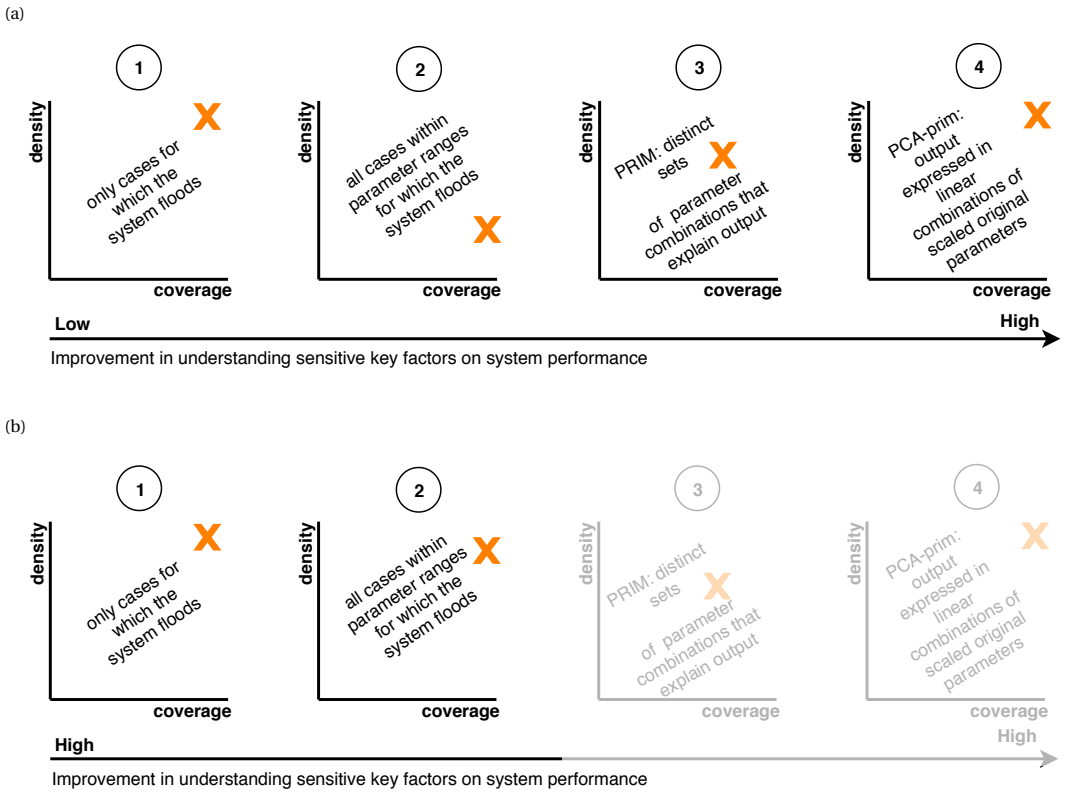

Figure 7.1: Application of Scenario Discovery in two ways: a) System performance is insufficient for a wide range of multiple variables. Dominant key factors cannot be retrieved from preliminary visualisation only (e.g. J26). Linear relations for certain range in system behaviour can be illuminated by using PCA-PRIM - b) System performance is robust for wide-ranging plausible states. If system failure is caused by one or two dominant factors, or scenarios, this can be retrieved from preliminary analysis only, for which no further PRIM analysis is needed.

8

Conclusion & Recommendations

8.1. Conclusion

In the case of Ötsuchi Town, a less resilient approach was applied for establishing stormwater management, in comparison to the other disaster preventive measures that were taken (earthquake, tsunami). No additional measures were done to increase the resilience of the stormwater system, while meeting the design criteria of the national government at that time. On the other hand, this research illuminates that the considered stormwater system in the tsunami reconstruction has been rebuilt very robust, for a wide range of plausible futures. A separate open storm sewer was established, which proves to be beneficial in managing a wide range of load conditions. The established combination between SWMM and EMA workbench, enabled to illuminate both the robustness and the vulnerabilities of the concerned stormwater system. For which the latter, it seems that have not been found by the original applied design approach.

Due to the preventive plans to protect from the tsunami, the residential area was forced to be built adjacent to steep mountains. Whereas in the applied design approach it was assumed the runoff coefficient was rather low, this research explored the broader ranges, and found that if and only if the runoff coefficient from the adjacent mountains would be above 0.6, a small area could be vulnerable to pluvial flooding that would cause disruption. The dominant factors found sensitive for these conditions, are the rainfall intensity > 75 mm/hr, rainfall duration > 30 min, hydraulic conductivity of the soil and the proportion of paved area. The interdependency between these parameters, for explaining whether or not flooding would occur, was found by a linear combination of the parameters using PCA-PRIM. A very high quality scenario description could be found, which explains the co-dependencies of the parameters. It suggests that all above mentioned parameters are more or less equally sensitive with respect to the extreme boundaries that are chosen. This tells us that deviating from the mean value would induce less or higher vulnerability to flooding, depending on the direction. Also, given these extreme conditions, the depression storage and the Manning's roughness coefficient of pervious area appear minimal sensitive. This implies that when easy-to-implement solutions are trying to be found managing the drainage capacity of the soil and the proportion of paved area would significantly aid in reducing vulnerability to flooding, and thus enhancing resilience.

It can be concluded that flooding occurrence is only likely to happen if the threshold for the initial precipitation losses of hill slope runoff is reached, as earlier researches on steep forestry hill slopes (>15%) in Japan, showed that a runoff coefficient around 0.5 is common after the initial precipitation losses. It is still unclear under what conditions these thresholds would be reached given the complexity of hill slope runoff processes. However, given the very steep hill slopes adjacent to the vulnerable area (>20-50%), it is not likely that soils are very deep, and could be saturated quickly in wet antecedent conditions. Anticipating the extreme conditions would therefore be recommended, as residential area is at stake.

The rainfall values of the concerned extreme conditions, are not outside the realm of possibility, as derived from the current Intensity-Duration-Curves. However, the concerning return period for the rainfall would be in the order of range 20 to >200 years based on the current available information. Rainfall analysis of the last past years suspect the trend of non-stationarity of weather patterns, however. When more information is known on the uncertainty parameters, a more narrow range of potential flood volumes could be obtained.

In addition, the solutions could be multi-functional, which makes them more feasible to implement. Additional solutions that are proposed to implement are natural-based solutions and Green-Blue infrastructure, which proves to reduce the vulnerability to flooding significantly. The stress on the urban water system could be reduced by storing the excessive stormwater in the lower-lying retention area, which was initially assigned as tsunami buffer zone. On top of that it is suggested to provide storage facilities for extreme rainfall events, which could at the same time, bring back the common artesian wells, the 'local treasures' that have been disappeared due to the tsunami. Thus, multiple opportunities could be found, to use the tsunami preventive measures, and anticipate the urban quality of life, while enhancing the resilience of stormwater management.

Concerning a broader context, this research indicates that 'Building Back Better' stormwater management can be achieved within a tsunami reconstruction. An exploratory approach would aid in this by seeking strategies to make the system less vulnerable and making multi-purpose strategies seem very logic. What these strategies are, remains however context-dependent.

For the vulnerable locations the application of (PCA)-PRIM provided more insight into the dominant factors, and could eliminate the range of two model uncertainties. Regarding more robust locations, PRIM analysis was not necessary to obtain the information needed for which potential solutions would be based on. Therefore preliminary analysis was sufficient to obtain the load conditions for extreme conditions. When choosing between multiple policies, applying PRIM could however be applicable in both cases.

It follows that combining both open source tools, SWMM and EMA workbench, could encourage further development in the field of scenario discovery and resilient stormwater management planning in not only a tsunami reconstruction, but for a wide-ranging stormwater management questions.

8.2. Recommendations

The results of this research entail multiple suggestions for further research. The suggestions are grouped into three categories: i) stormwater management in a disaster reconstruction ii) follow-up analysis for the case of Ötsuchi in particular and iii) various researches on applying scenario discovery on resilient urban stormwater management.

8.2.1. Disaster reconstruction in another context

Whereas from this research lessons can be learned from how the stormwater system has been established in the reconstruction of Ötsuchi Town, more insights could be gained when other contexts would be considered: either another geographic location, or another time horizon. It could give another perspective if a comparable case that was hit by the 2011 Tsunami, is examined in the same way. In addition, given that the Tsunami reconstruction took place during 2011-2017, at this time of writing 2019, climate change issues are much more acknowledged. If a Tsunami would happen in the near future, it would be really interesting to see how climate uncertainties are handled now in a reconstruction, and if the anticipation on rare extreme conditions would be the standard rather than an exception. Finally, also cases that are hit by a different disaster types could be examined and compared with this study. This could reveal new lessons from either studies.

8.2.2. Follow-up analysis for Ötsuchi Town

Concerning the case of Ötsuchi Town in particular, a follow-up probability analysis could be done on the results if more information would be known on the mountain runoff behaviour. A process that would be useful to examine would be the runoff behaviour in circumstances for which the hydraulic conductivity would be likely to decrease, such as in very wet conditions. To what extent the hydraulic conductivity would decrease, taking into account the spatial heterogeneity, and if and where it would trigger much runoff are interesting questions to be answered. It is not neglected that hill slope runoff processes are very complex and difficult to understand. However, the relation between stormwater runoff and antecedent rain conditions could for example be examined. If more information can be derived from the mountain runoff processes, a joint-probability analysis could then be done of the corresponding rainfall intensity and rainfall duration values for which the system would flood, related to antecedent rainfall and mountain runoff.

When the retrieved joint probability are combined with information on changing weather patterns, which is available over time, a better consideration could be made on whether or not additional solutions that are proposed in this thesis would be necessary in the near future. Moreover, the original models used for the design of the stormwater system could aid in verifying the model response of the model used in this research.

In addition, if the results on the mountain runoff behaviour reveal that deep water flows are expected, more destructive flooding behaviour is at stake, and it is suggested to further examine how to anticipate these processes.

8.2.3. Applying scenario discovery on resilient urban stormwater management

Whereas the scope of this study was not to optimize the application of scenario discovery methodology on a stormwater management problem, the research results stimulate to do so. Scenario discovery can be used for assessing systems that need rehabilitation to become more resilient, or when entirely new system designs are about to be established, a first simple model and scenario discovery can be used to explore vulnerabilities in the system. Therefore, various topics are interesting to explore with regard to the application of scenario discovery and a stormwater management problem.

Density model stormwater drainage system
Whereas now a rather simple SWMM model is used, a more complex SWMM model could refine the vulnerable locations subject to flooding. By applying exploratory modelling, it is however suggested to start with a rather simple model to disclose the vulnerable locations. Accordingly, a more complex model with higher density of nodes and junctions could be examined for a specific area of interest. When a more dense model is used, also, water flows near and in junctions could then be considered more accurately.

Different storm profiles
First, it would be interesting to assess the response of a stormwater drainage system for different design profiles of various storms using SWMM x EMA, as only block rainfall has been used in this research. Whereas the coarse block rainfall covers the whole input space of both rainfall duration and rainfall intensity, would triangular of (modified) historical storm profiles provide more accurate information for designing a resilient stormwater system, given the uncertain conditions? The possibility of permuting many different storms with SWMM should be assessed.

Varying input for experimental design
If the same research would be done with either a) a more complex model b) different uncertainty parameter ranges, or c) more advanced routing of the external inflow, it is yet unclear whether or not the results would provide the same relations for the uncertainty parameters as are derived in this research. Follow-up research on the sensitivity of complexity of a SWMM model would be recommended. Moreover, if scenario discovery would be used for optimizing LIDS solutions that are considered only, this could potentially become a very useful tool that would provide insights in how to reduce the vulnerability at what conditions.

Examining more vulnerable systems
Moreover, since the stormwater management system in the concerned case study appeared to be robust, it would be interesting to explore the outcomes of the applied research methodology on a less robust system. What would be the outcomes of the PRIM analysis? Would it still be interpretable? Or would too many vulnerable cases hamper the process? Whereas this research succeeded to do the PRIM analysis for one location that was vulnerable, with the applied methodology it is an exhausting task to do it for a great amount of locations. Some modifications of implementing more automatised selection procedures in each peeling-trajectory of PRIM could be thought of. However, this is not straightforward. Automatization of selecting the boxes that together form a box set would be at the expense of the ability for the user to consider the quality criteria of the outputs by one itself. However, if this PRIM analysis would be done for multiple stormwater management problems, and the selection process would be reported, another algorithm could be build on predicting the selection of the boxes in the peeling-process of PRIM. This would fasten the process of getting PRIM results quickly for a wide range of locations and various vulnerabilities.

Improving operationalization of SWMMxEMA
Finally, more practical recommendations are done concerning the operationalization of the experimental designs. For further expansion of the EMA-workbench with SWMM, it is recommended to transform the C+ code of SWMM in its entirely to the python engine. The workarounds for SWMM x EMA were sufficient to conduct this research. However, using SWMM from the python engine would be more efficient to modify model templates, and, to store outputs of all types of variables - e.g. time series, summaries - for each location. At present, more advanced modification in the original model template (e.g. LIDS, divider of flows) give variable output files. The current reading-files-modules in python are not build on that yet. In addition, if no DEM is available and invert levels can not be automated easily, it would be feasible to implement a feature

that automates the changing invert levels with changing conduit dimensions. Varying conduit dimensions could be incorporated in the experimental design, and examined for finding optimal solutions.

A

Data collection case study

A.1. Interview guide

In the table below (table A.1) the interview guide is provided, which was used as guidance for obtaining the relevant information from key figures of the reconstruction project.

Table A.1: Interview guide

Design approach	
	Ötsuchi government
	Project manager
1	What design method was used to design the stormwater management system of Ötsuchi?
2	What were the used design criteria for establishing the stormwater management system?
3	What type of stormwater system was implemented?
4	What are the system layout properties and characteristics?
5	Were measures taken outside the grey stormwater drainage infrastructure?
6	Were extreme conditions considered?
7	To what extent were uncertainties considering climate change involved?
8	Were commutative reconstruction measures considered?
Interdisciplinary approach	
	Urban planner
	Technical advisor
1	To what extent was stormwater management involved in the urban reconstruction design process, and its final design?
2	Were any stormwater management related design criteria given for the urban reconstruction design?
3	Were the urban designers aware of pluvial flooding occurrence and/or hillslope runoff?
	Otsuchi government
	Within the reconstruction a safety level of a 1/1000 yr tsunami was used.
1	What were the reasons for not implementing green-blue infrastructure or natural-based solutions outside the grey stormwater drainage infrastructure to anticipate very extreme conditions?
	Constructor company [1]
1	What are the design codes regarding liquefaction of the reclaimed area?
2	Why is chosen for the type of drainage facility that was implemented in the land reclamation?
3	Why were no additional drainage pipes implemented?
4	How are risks on landslides determined?
Characteristics Ötsuchi	
	Ötsuchi government
	Project manager
1	What filling material was used for the reclaimed land?
2	What are the characteristics of the fresh water wells: location, pressure head, usage

A.2. Theme maps of Ötsuchi Town

In this appendix a variety of maps are given on background information of Ötsuchi Town. These include, a hazard map, the stormwater drainage system layout, and information on the natural spring wells.

Figure A.1: Location of Ötsuchi Town and the epicentrum of the 2011 Tsunami. Tectonic faults are shown by the thick grey lines

[1] This interview could not be conducted

Figure A.3: Tsunami flood area (red) and Tsunami run-up heights

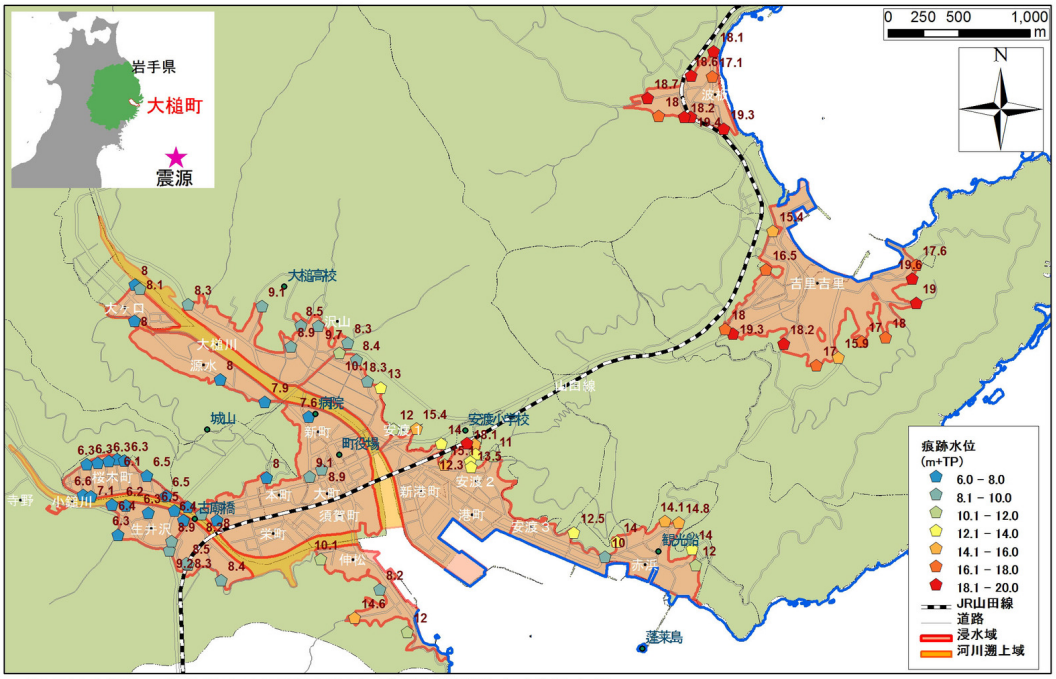

岩手県大槌町　東北地方太平洋沖地震　津波氾濫域および痕跡水位
（標高は，地震による地殻変動(30–60cm程度)を考慮していません．）
現地調査2回：2011年4月5～6日，4月29日～5月2日，（5月29日作成版，大同大学　鷲見哲也）

Source: Iwate Prefecture, `http://www.pref.iwate.jp/kasensabou/kasen/fukkyuu/tsunami/index.html`

Figure A.2: Hazard map of Ötsuchi Town

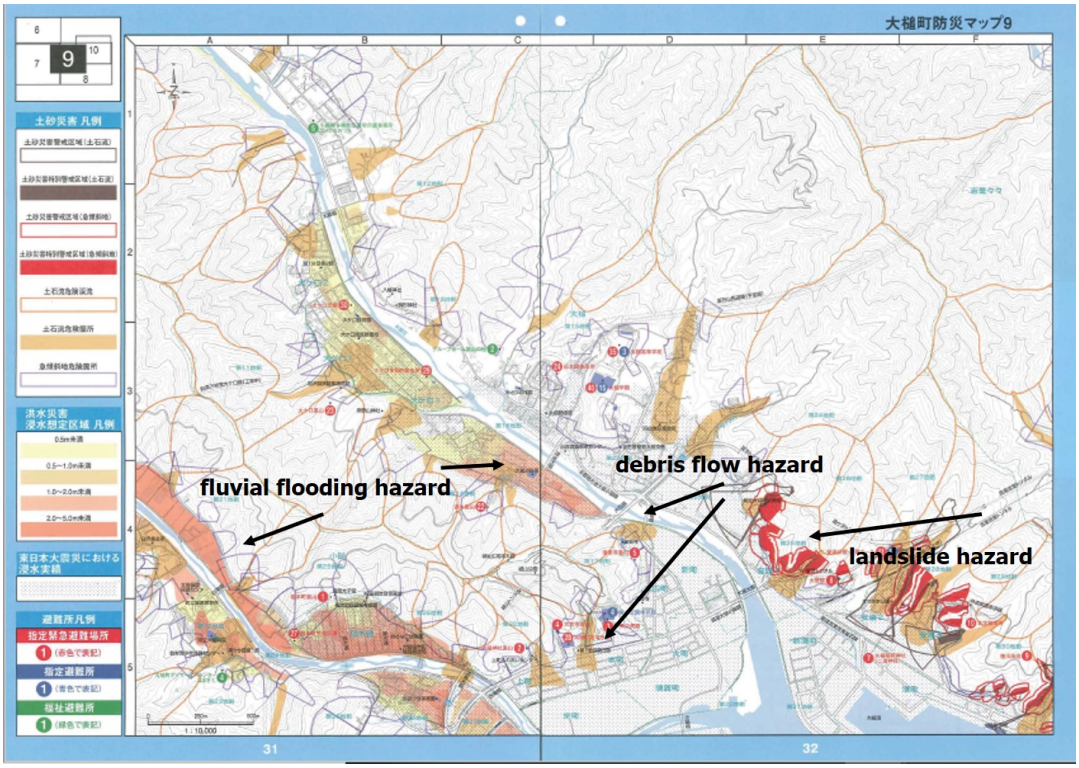

Figure A.4: Stormwater system layout

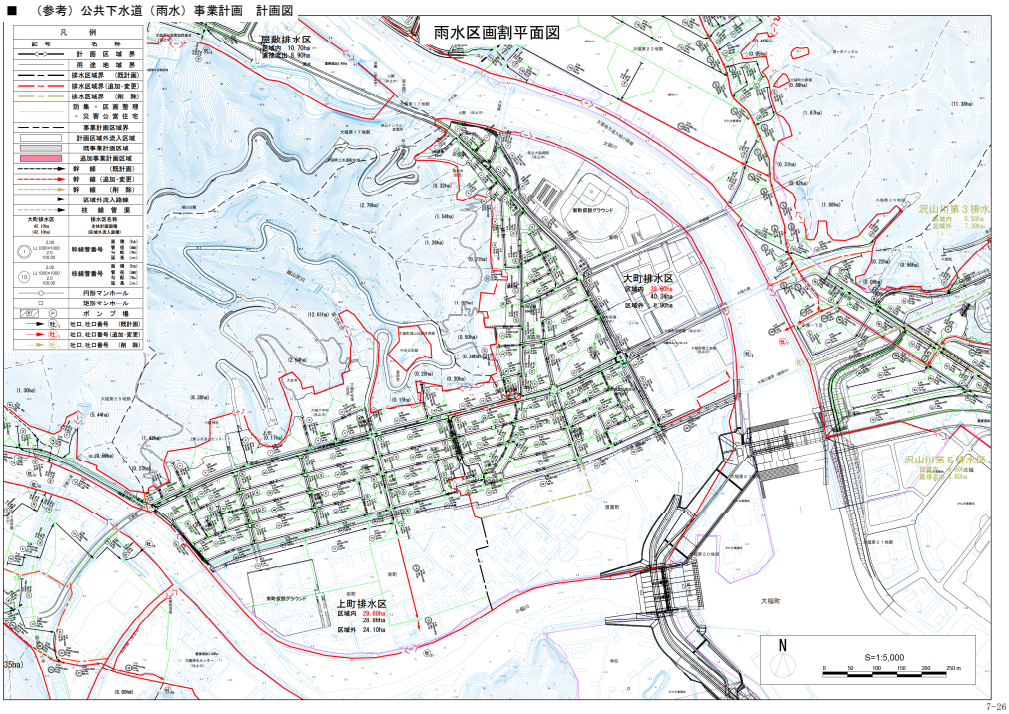

Source: Ötsuchi Town, https://www.town.otsuchi.iwate.jp/gyosei/docs/20160419000030/files/b008.pdf

Figure A.5: Location of natural spring wells

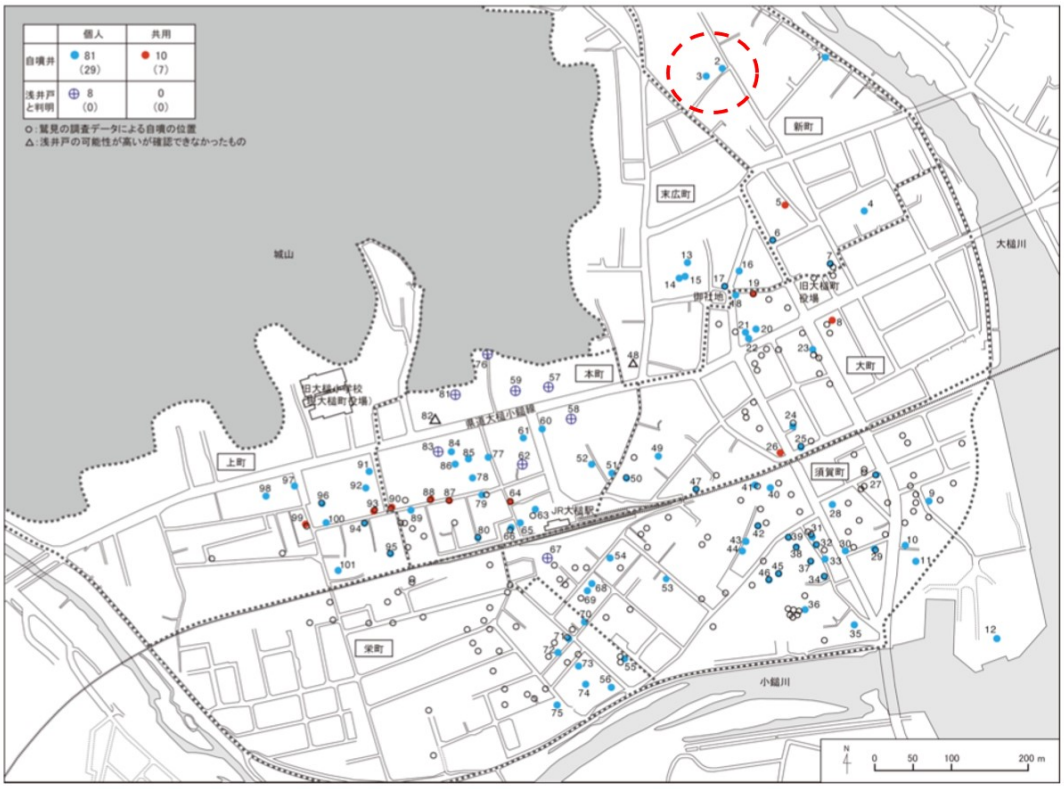

B

SWMM model characteristics

This section includes several maps of the swmm model to give information on the system characteristics, such as surface area, conduit dimensions and the specific hill slope subcatchment that has been selected to have a fixed runoff coefficient of C=0.7.

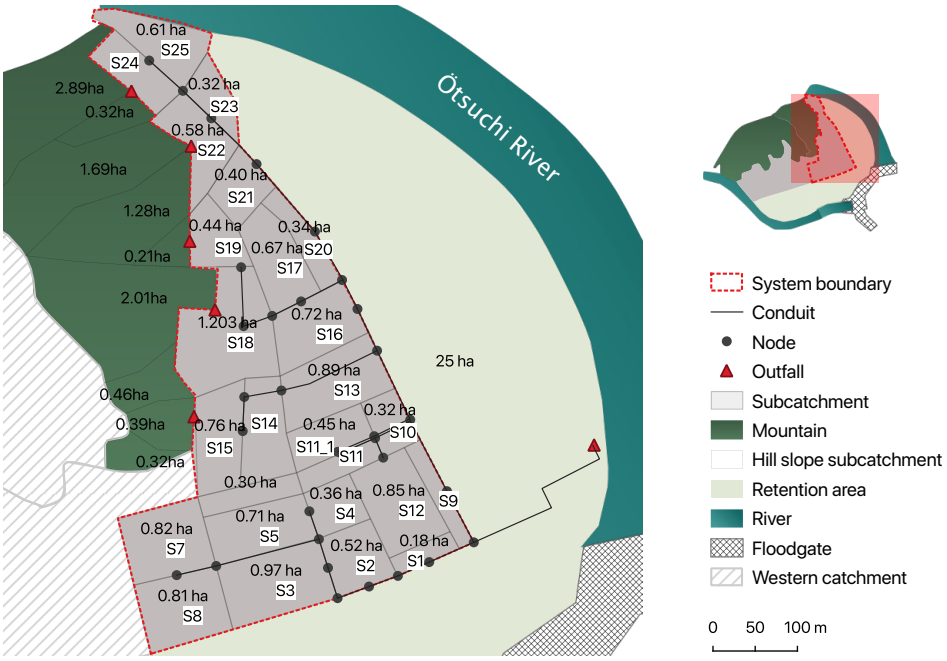

Figure B.1: Surface area in hectares

Table B.1: Area of external inflow subcatchments with corresponding receiving outalls based on mapA.4

Outfalls	Out15	Out18	Out22	Out24	Out19
Area [ha]	0.99	1.15 / 2.42* 0.7 + (1.27/2.42 * C)	2.8	3.08	0.21

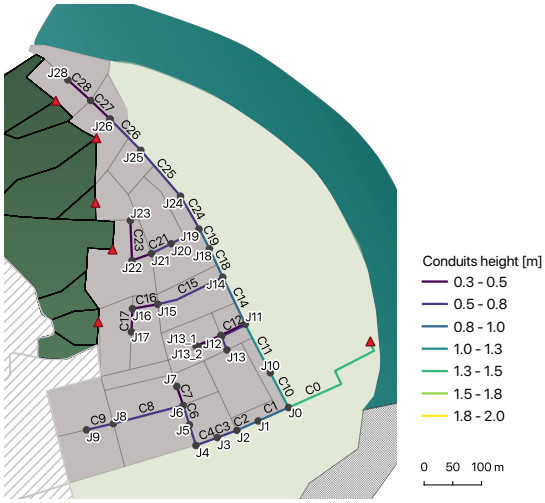

(a) height

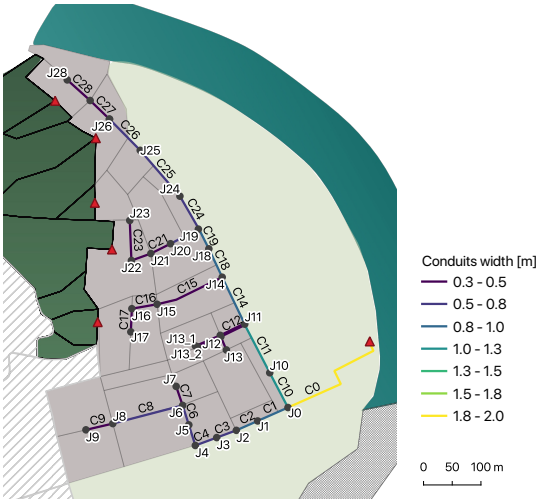

(b) width

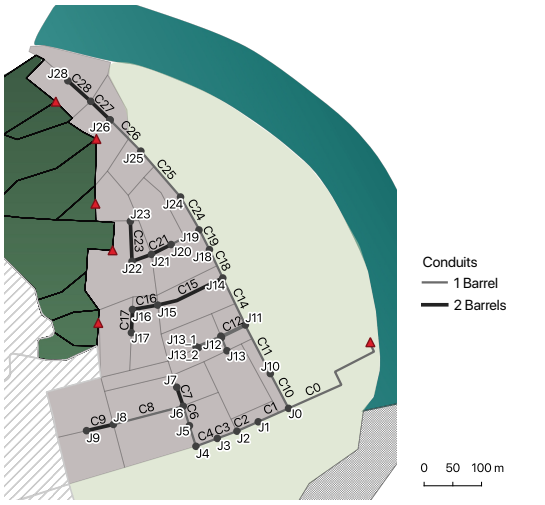

(c) barrels

Figure B.2: Conduits properties

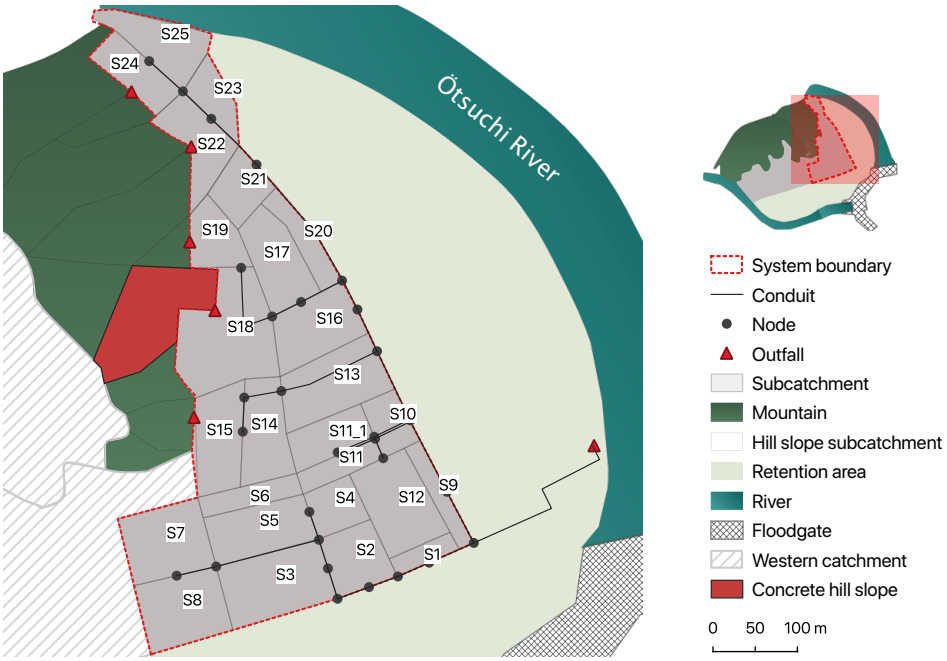

Figure B.3: Subcatchment external inflow with fixed coefficient of C=0.7

C

Additional results

C.1. Reference situation A0: examination of the current drainage system of Ötsuchi Town

Figure C.1: Preliminary visualisation of flooding occurrence - Run I for flood height thresholds 0.0 m and 0.2 m

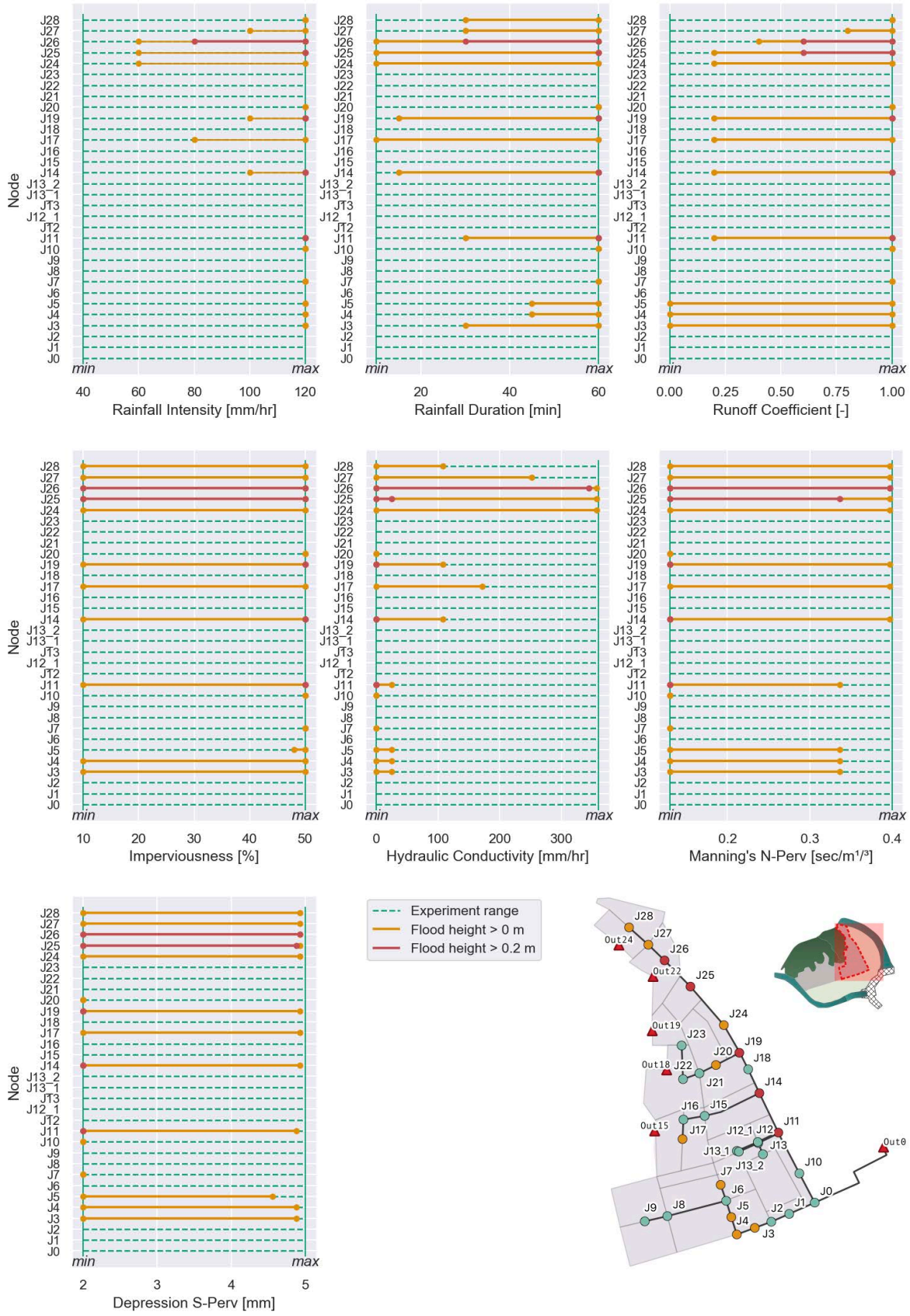

Figure C.2: Preliminary visualisation of flooding occurrence - Run II for flood height thresholds 0.0 m and 0.2 m

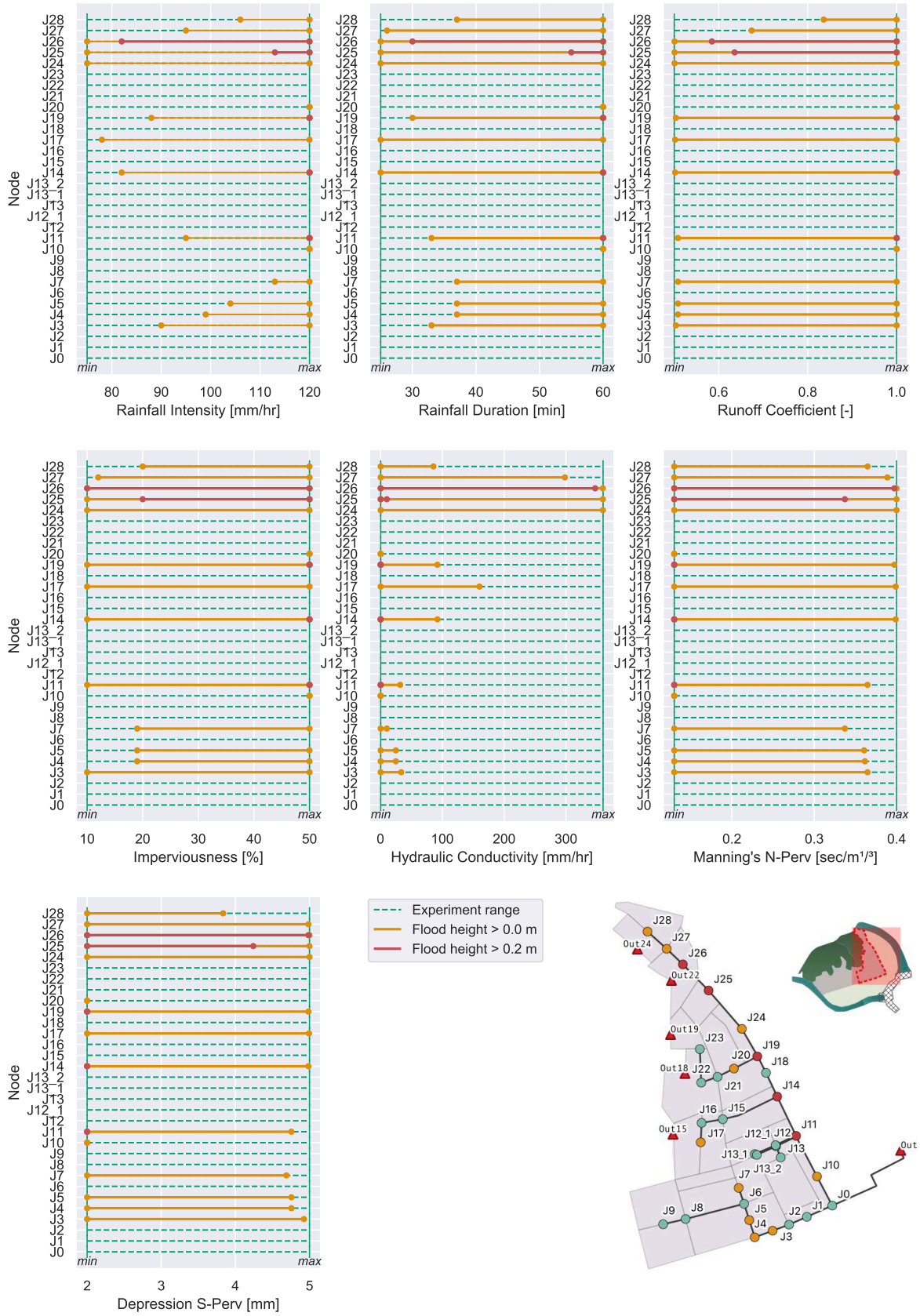

Table C.1: Selected experiments for PRIM - Run II - Parameter description of the selected experiments of X^{H0}, within the ranges of flooding occurrence of node J26 occurs

	Ri	Rd	C	Imp	k	n_p	s_p
count	2571.0	2571.0	2571.0	2571.0	2571.0	2571.0	2571.0
mean	101.038	45.016	0.793	30.42	174.404	0.263	3.483
std	11.272	8.886	0.119	11.795	100.271	0.077	0.858
min	82.0	30.0	0.585	10.0	0.36	0.13	2.0
25%	91.0	37.0	0.693	20.0	86.273	0.196	2.742
50%	101.0	45.0	0.792	30.0	177.575	0.262	3.487
75%	111.0	53.0	0.896	41.0	260.905	0.331	4.225
max	120.0	60.0	1.0	50.0	347.125	0.397	4.985

Figure C.3: Scatterplot node J19 - run II - threshold = 0.2m

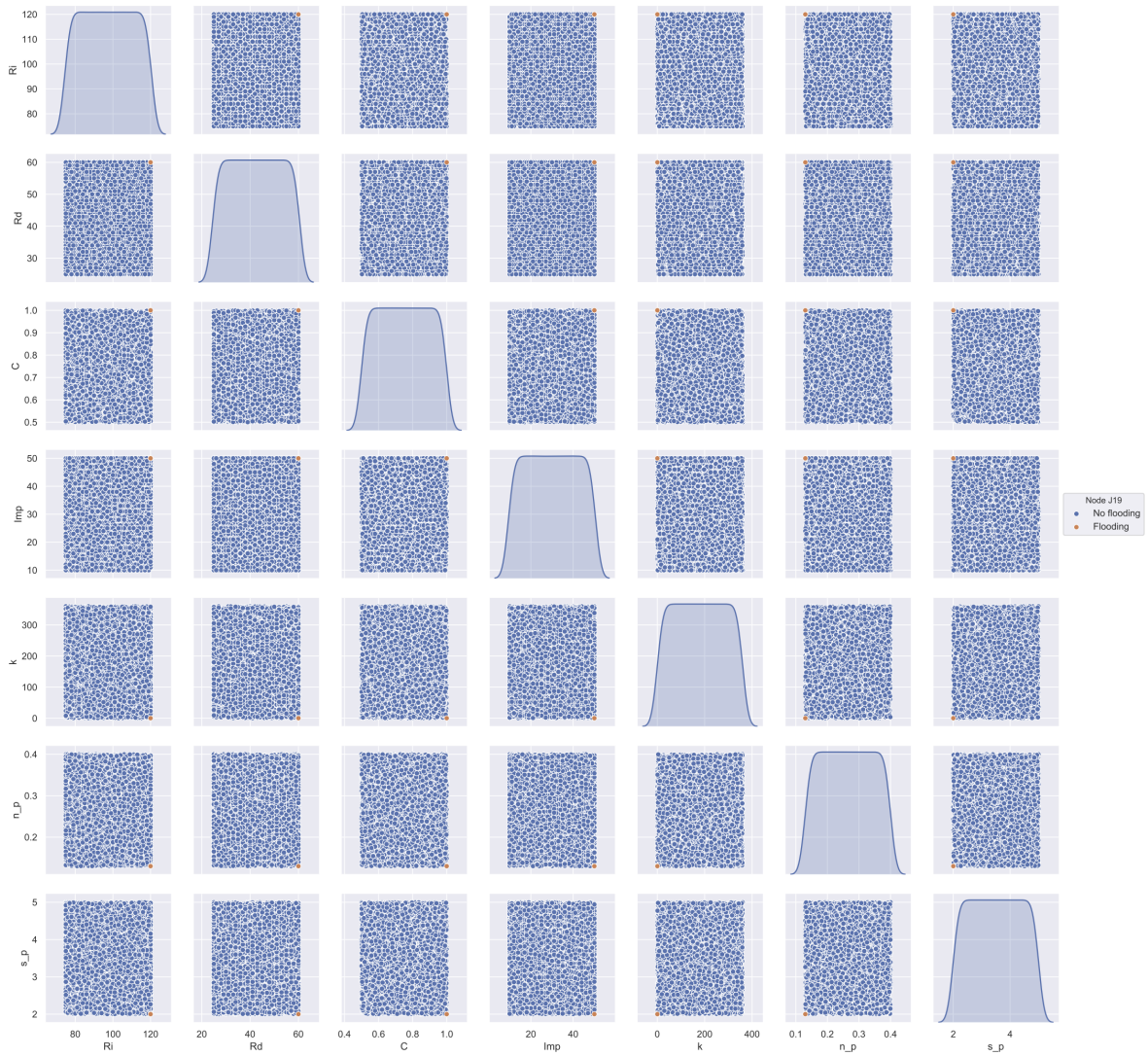

Table C.2: Run II - PRIM boxset description

	coverage	density	mass	res_dim	tradeoff_id	# cases of interest
box 1	0.506	0.6	0.084	4	37	129
box 2	0.275	0.314	0.087	5	45	70
box 3	0.153	0.048	0.315	5	-	56

Table C.3: Run II - PRIM boxset parameter ranges

	box 1				box 2				box 3			
	min	max	restricted	q-p	min	max	restricted	q-p	min	max	restricted	q-p
Ri	103.50	120	yes	5.00E-15	93.5	120	yes	0.029	86.5	120	yes	0.26
Rd	42.50	60	yes	2.00E-07	35.5	60	yes	0.084	41.5	60	yes	0.01
C	0.78	1.00	yes	5.00E-08	0.72	1	yes	0.029	0.64	1	yes	0.38
Imp	26.50	50	yes	5.00E-07	10	50	no	-	17.5	50	yes	0.092
k	0.36	347	no	-	0.36	86	yes	3.90E-18	0.36	347	no	-
n_p	0.13	0.4	no	-	0.13	0.4	yes	0.28	0.13	0.4	no	-
s_p	2.0	5.0	no	-	2.0	5.0	no	-	2.27	4.8	yes	0.029,0.52

Table C.4: Rotation matrix for run II ($y_j 26 = 1$)

	PC1	PC2	PC3	PC4	PC5	PC6	PC7
Ri	-0.01062	0.0163	0.16715	0.72782	0.07527	0.44159	0.49122
Rd	-0.06497	-0.2883	-0.00734	0.10317	-0.7435	-0.45322	0.37917
C	-0.01181	0.11868	0.20642	-0.64463	-0.23234	0.52728	0.44228
Imp	-0.32282	-0.02673	0.47093	-0.1469	0.51055	-0.4782	0.40297
k	-0.0874	0.09604	0.80065	0.12095	-0.30873	0.07416	-0.47608
n_p	-0.60461	-0.71139	-0.08213	-0.04289	0.05599	0.29514	-0.17187
s_p	0.71981	-0.6217	0.24462	-0.07774	0.1687	0.0167	0.02727

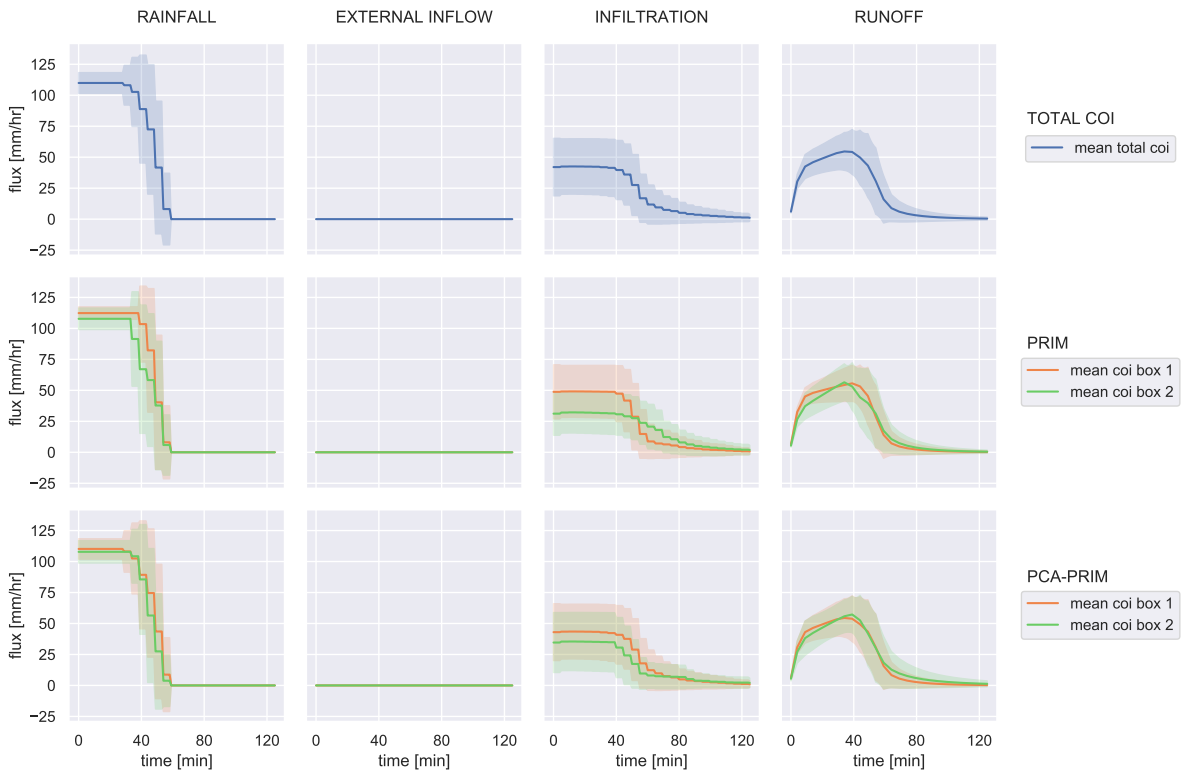

Figure C.4: Subcatchment S23 for PRIM and PCA-PRIM results

C.2. Policy A1

The scatterplot in figure C.5 shows all samples for which k is below 200 and $imp < 40$ %.

Figure C.5: A1: Scatterplot of samples Run II for k>200 and imp <40%

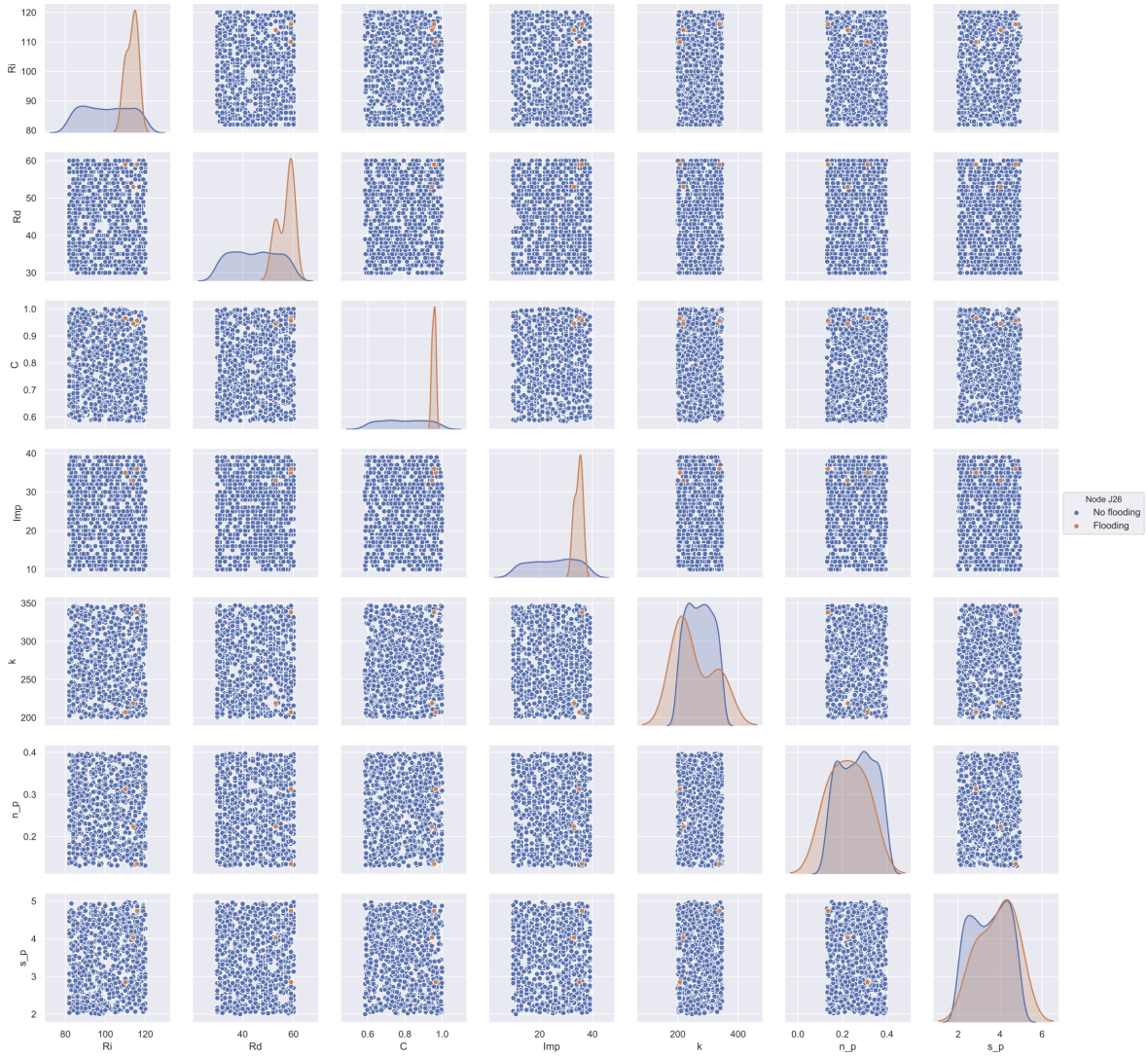

C.3. Policy A2

Table C.5: Settings for solution A2; vegetative swale + storage unit

LID vegetative Swale										
Conduit	From Node	To Node	Length	Roughness	Shape	Height	Width	Barrels	Left slope	Right slope
C26	J25	J24	105	0.01	Rect$_open$	0.7	0.7	2	-	-
C27	J26	J25	76	0.01	Rect$_open$	0.5	0.55	3	-	-
C28	J28	J27	47	0.01	Rect$_open$	0.55	0.55	3	-	-
C29	J25	1	58	0.035	Trapezoidal	0.7	1	1	3	3
Storage unit	Elevation	Max depth	Initial depth							
1	0	2.2	0							

Table C.5 shows the settings for policy A2.

The depth of the storage unit has been set to 2.2m, which is the elevation difference between the reclaimed land and the lower retention area. The surface area has been set to coarse value of 3000m2. No further specification of the dimensions have been explored, given the purpose of a preliminary investigation.

Figure C.6: Preliminary visualisation of flooding occurrence - Run III for flood height thresholds 0.0 m and 0.1 m

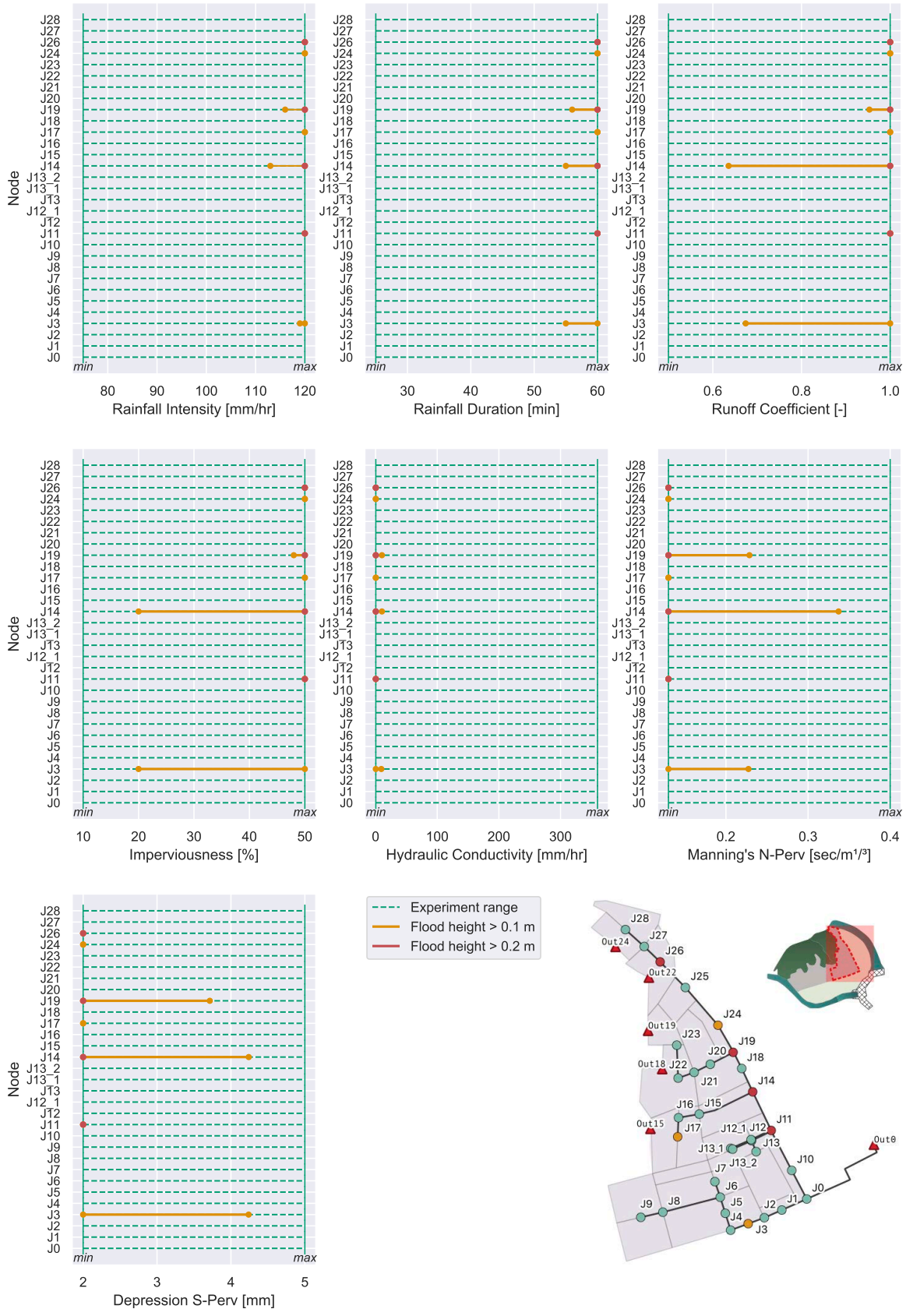

C.4. Policy A3

Table C.6: Settings for one infiltration trench unit

LID: Infiltration Trench									
Surface			Storage			Drain			
Berm Height	300	mm	Thickness	700	mm	Flow Coefficient	3	mm/hr	2D^0.5 / T
Vegetation Volume Fraction	0.05		Void Ratio (Voids/Solids)	0.75		Flow Exponent	0.5		
Surface Roughness (Manning's n)	1		Seepage Rate	0.5	mm/hr	Offset	6	mm	
Surface Slope	1	%	Clogging Factor	0					
Catchment	S24	S22							
Area of Each Unit	70	60	# length mountains towards conduit						
Number of Units	4	4							
% of Subcatchment Occupied	6.114	4.131							
Surface Width per Unit	1	1							
% initially Saturated	0	0							
% of Impervious Area Treated	50	50							
% of Pervious Area Treated	20	20							
send Drain Flow To	subcatchment outlet	subcatchment outlet							

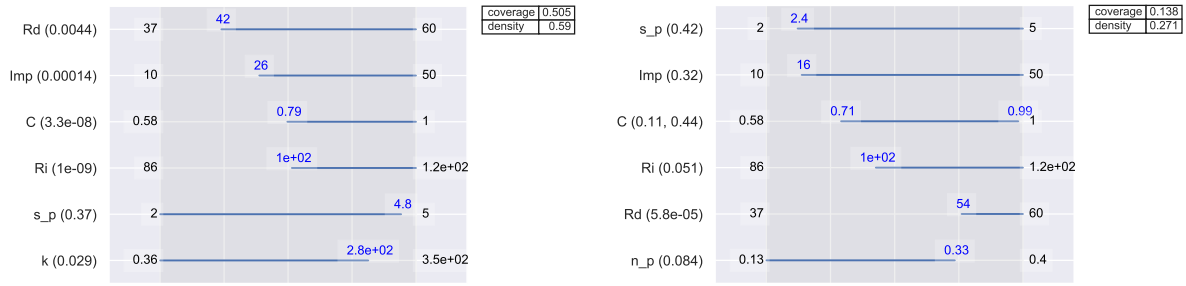

(a) Box 1 (b) Box 2

Figure C.7: PRIM outcome for J26, where cases of interest are the cases that are both flooded with policy A0 and A3

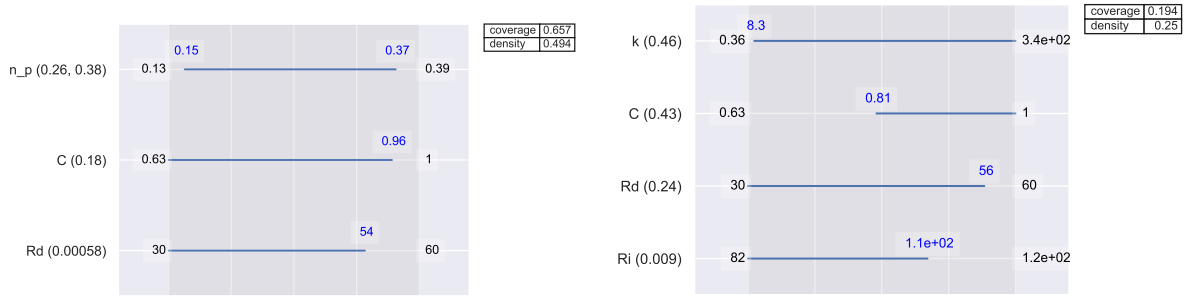

(a) Box 1 (b) Box 2

Figure C.8: PRIM outcome for J26, where cases of interest are the cases that are solved with A3

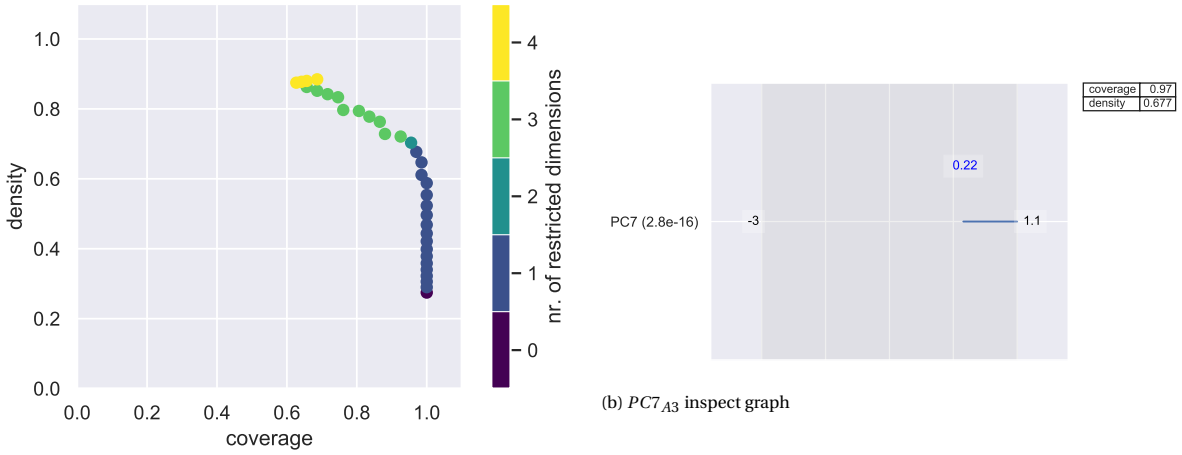

(a) PCA-PRIM J26, A3, tradeoff curve for solved cases as interest

(b) $PC7_{A3}$ inspect graph

Figure C.9: PCA-PRIM outcome for J26, where cases of interest are the cases that are solved A3

Figure C.10: Preliminary visualisation of flooding occurrence - Run IV for flood height thresholds 0.0 m and 0.1 m

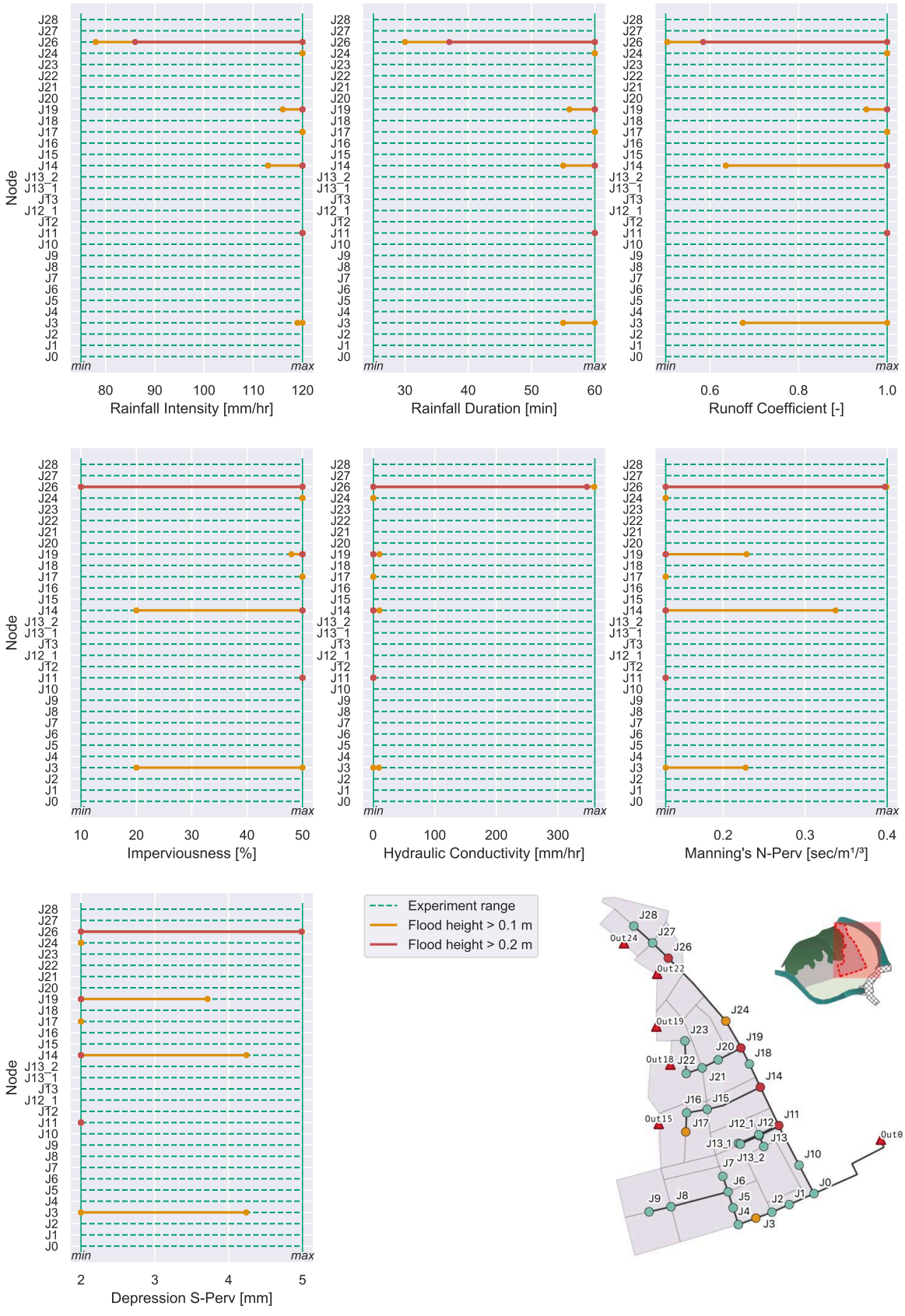

Table C.7: Run IV - PRIM boxset description for solved cases as interest

	coverage	density	mass	res_dim	tradeoff_id
box 1	0.656716	0.494382	0.364754	3	16
box 2	0.19403	0.25	0.213115	4	19

Table C.8: Run IV: PRIM boxset parameter ranges for solved cases as interest

	box 1				box 2			
	min	max	restricted	q-p	min	max	restricted	q-p
Rd	30	53.5	yes	0.26	30	56.5	yes	56
n_p	0.147053	0.369296	yes	0.96	0.13	0.394104	no	-
C	0.625146	0.959296	yes	54	0.805073	1	yes	0.43
k	0.36	340.1605	no	-	8.305472	340.1605	yes	0.46
Ri	82	120	no	-	82	107.5	yes	0.009

C.5. An example of a more simple SWMM model

Figure C.11 shows a previous simpler model that was examined prior to the final SWMM model template that has been used in this study. As can be seen the vulnerable region is the same as the region that appeared to be vulnerable in this study. However, the most upper node shows flooding here as well, due to an additional barrel conduit at C27 was missing in this specific model in figure C.11.

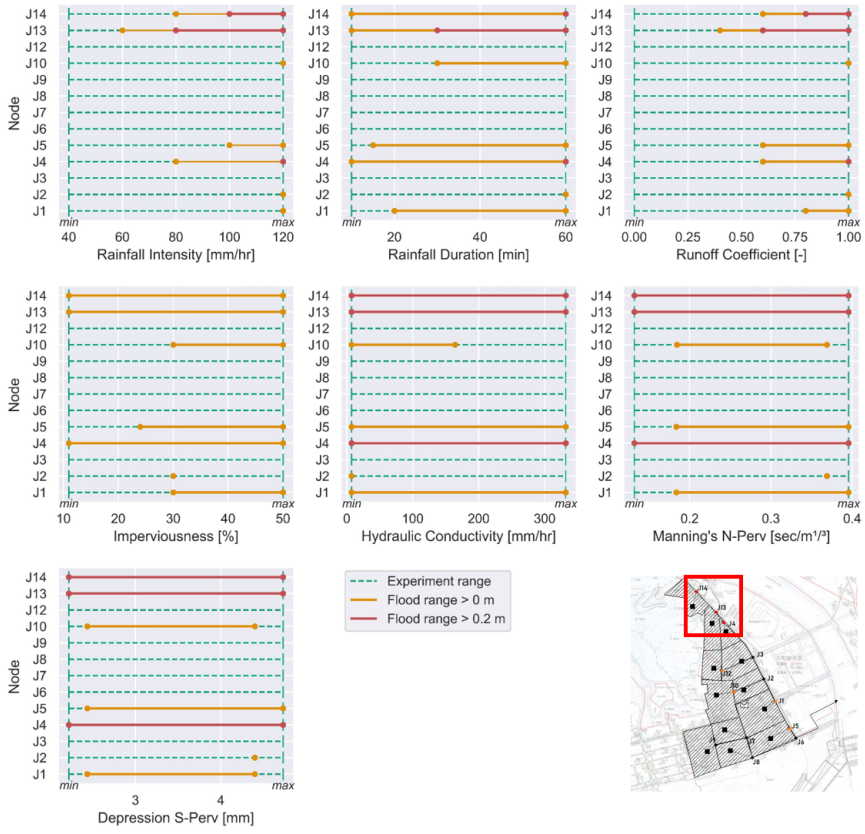

Figure C.11: Less complex model - same vulnerable area

References

ASCE. (1992). *Design & Construction of Urban Stormwater Management Systems*. New York, NY.

Astm, & International, A. (2006). Standard Practice for Classification of Soils for Engineering Purposes (Unified Soil Classification System). *ASTM Standard Guide*, *D5521-05*, 1–5. doi: 10.1520/D2487-11.

Babovic, F., Mijic, A., & Madani, K. (2018). Decision making under deep uncertainty for adapting urban drainage systems to change. *Urban Water Journal*, *15*(6), 552–560. Retrieved from `https://doi.org/10.1080/1573062X.2018.1529803` doi: 10.1080/1573062X.2018.1529803

Bankes, S. (n.d.). *Exploratory Modeling for Policy Analysis* (Vol. 41). INFORMS. Retrieved from `https://www.jstor.org/stable/171847` doi: 10.2307/171847

Bertilsson, L., Wiklund, K., de Moura Tebaldi, I., Rezende, O. M., Veról, A. P., & Miguez, M. G. (2019). Urban flood resilience – A multi-criteria index to integrate flood resilience into urban planning. *Journal of Hydrology*. doi: 10.1016/j.jhydrol.2018.06.052

Bryant, B. P., & Lempert, R. J. (2010). Thinking inside the box: A participatory, computer-assisted approach to scenario discovery. *Technological Forecasting and Social Change*, *77*(1), 34–49. Retrieved from `http://dx.doi.org/10.1016/j.techfore.2009.08.002` doi: 10.1016/j.techfore.2009.08.002

Butler, D., & Davies, J. (2011). *Urban Drainage* (Third ed.). London: Spon Press.

Butler, D., Farmani, R., Fu, G., Ward, S., Diao, K., & Astaraie-Imani, M. (2014). A new approach to urban water management: Safe and sure. *Procedia Engineering*, *89*(July), 347–354. doi: 10.1016/j.proeng.2014.11.198

Cheng, L., & Aghakouchak, A. (2014). Nonstationary precipitation intensity-duration-frequency curves for infrastructure design in a changing climate. *Scientific Reports*, *4*, 1–6. doi: 10.1038/srep07093

Chow. (1959). *Open-channel hydraulics*. McGraw-Hill.

Dalal, S., Han, B., Lempert, R., Jaycocks, A., & Hackbarth, A. (2013, oct). Improving scenario discovery using orthogonal rotations. *Environmental Modelling and Software*, *48*, 49–64. doi: 10.1016/j.envsoft.2013.05.013

de Graaf, R., & Matsushita, J. (2008). Stormwater management and multi source water supply in Japan: Innovative approaches to reduce vulnerability. In R. de Graaf & F. Hooimeijer (Eds.), *Urban water in japan* (pp. 143–173). London: Taylor & Francis.

Djordjević, S., Butler, D., Gourbesville, P., Mark, O., & Pasche, E. (2011). New policies to deal with climate change and other drivers impacting on resilience to flooding in urban areas: The CORFU approach. *Environmental Science and Policy*, *14*(7), 864–873. doi: 10.1016/j.envsci.2011.05.008

El Adlouni, S., & Ouarda, T. B. (2013). Frequency Analysis of Extreme Rainfall Events. *Rainfall: State of the Science*(January), 171–188. doi: 10.1029/2010GM000976

Esteban, M., Takagi, H., & Shibayama, T. (2015). *Handbook of Coastal Disaster Mitigation for Engineers and Planners*. Elsevier Inc. doi: 10.1016/C2013-0-12806-1

Fischbach, J., Siler-Evans, K., Tierney, D., Wilson, M., Cook, L., & May, L. (2017). *Robust Stormwater Management in the Pittsburgh Region: A Pilot Study*. RAND Corporation. doi: 10.7249/rr1673

Fitts, C. (2013). *Groundwater Science* (Second ed.). Elsevier Scienc ePublishing Co Inc.

Fletcher, T. D., Shuster, W., Hunt, W. F., Ashley, R., Butler, D., Arthur, S., ... Viklander, M. (2015). SUDS, LID, BMPs, WSUD and more – The evolution and application of terminology surrounding urban drainage. *Urban Water Journal*, *12*(7), 525–542. doi: 10.1080/1573062X.2014.916314

Fratini, C. F., Geldof, G. D., Kluck, J., & Mikkelsen, P. S. (2012). Three Points Approach (3PA) for urban flood risk management: A tool to support climate change adaptation through transdisciplinarity and multifunctionality. *Urban Water Journal*, *9*(5), 317–331. doi: 10.1080/1573062X.2012.668913

Friedman, J. H., & Fisher, N. I. (1999). Bump hunting in high-dimensional data. *Statistics and Computing*, *9*(2), 123–143. doi: 10.1023/A:1008894516817

Fukushima, H. (2017). Workshop Arrangement in Neighbor-Hood Communities for Residents' Participation in the Reconstruction Land Readjustment Project of Machikata District, Otsuchi Town, Kamihei County, Iwate Prefecture. *Journal of JSCE*, *5*(1), 190–205. doi: 10.2208/journalofjsce.5.1_190

Geldof, D.G., Kluck, J. (2008). The Three Points Approach. *Proceedings of 11th ICUD - international conference*

on urban drainage.

Goulden, S., Portman, M. E., Carmon, N., & Alon-Mozes, T. (2018). From conventional drainage to sustainable stormwater management: Beyond the technical challenges. *Journal of Environmental Management*, *219*, 37–45. Retrieved from https://doi.org/10.1016/j.jenvman.2018.04.066 doi: 10.1016/j.jenvman.2018.04.066

Greeven, S., Kraan, O., Chappin, É. J., & Kwakkel, J. H. (2016). The emergence of climate change mitigation action by society: An agent-based scenario discovery study. *Jasss*, *19*(3). doi: 10.18564/jasss.3134

Guivarch, C., Rozenberg, J., & Schweizer, V. (2016, jun). The diversity of socio-economic pathways and CO 2 emissions scenarios: Insights from the investigation of a scenarios database. *Environmental Modelling and Software*, *80*, 336–353. doi: 10.1016/j.envsoft.2016.03.006

Huang, J., Wu, P., & Zhao, X. (2013, may). Effects of rainfall intensity, underlying surface and slope gradient on soil infiltration under simulated rainfall experiments. *Catena*, *104*, 93–102. doi: 10.1016/j.catena.2012.10.013

IPCC. (2012). *Managing the risks of extreme events and disasters to advance climate change adaption* (Tech. Rep.). Intergovernmental Panel on Climate Change. Retrieved from https://www.ipcc.ch/report/managing-the-risks-of-extreme-events-and-disasters-to-advance-climate-change-adaptation/

Iwate Prefecture. (2011). *Iwate Prefecture Great East Japan Earthquake and Tsunami Reconstruction Plan: Basic Reconstruction Plan* (Tech. Rep.). Iwate Prefecture.

Iwate Prefecture sectie van de onderhoudsafdeling van het Prefectuur. (2015). *Iwate prefecture rainfall statistical analysis report, April 2015* (Tech. Rep.).

Jabareen, Y. (2013). Planning the resilient city: Concepts and strategies for coping with climate change and environmental risk. *Cities*. doi: 10.1016/j.cities.2012.05.004

JMA. (2018). *Precipitation: Japan*. Retrieved from https://www.jma.go.jp/en/amedas/000.html?elementCode=0

Kwakkel, J. H. (2017). The Exploratory Modeling Workbench: An open source toolkit for exploratory modeling, scenario discovery, and (multi-objective) robust decision making. *Environmental Modelling and Software*, *96*, 239–250. Retrieved from http://dx.doi.org/10.1016/j.envsoft.2017.06.054 doi: 10.1016/j.envsoft.2017.06.054

Kwakkel, J. H., & Cunningham, S. C. (2016). Improving scenario discovery by bagging random boxes. *Technological Forecasting and Social Change*, *111*, 124–134. Retrieved from http://dx.doi.org/10.1016/j.techfore.2016.06.014 doi: 10.1016/j.techfore.2016.06.014

Lempert, R. J. (2019). Robust Decision Making (RDM). In *Decision making under deep uncertainty* (pp. 23–51). Springer International Publishing. doi: 10.1007/978-3-030-05252-2_2

Lempert, R. J., Kalra, N., Peyraud, S., Mao, Z., Tan, S. B., Cira, D., & Lotsch, A. (2013). Ensuring Robust Flood Risk Management in Ho Chi Minh City. *World Bank*(May), 1–63. doi: 10.1596/1813-9450-6465

Lempert, R.J., Popper, S.W., Bankes, S. (2003). *Shaping the Next One Hundred Years: New Methods for Quantitative, Long-term Policy Anlaysis*. Santa Monica, CA: RAND Corporation.

Loucks, D. P., & van Beek, E. (2017). *Water Resource Systems Planning and Management*. Cham: Springer International Publishing. Retrieved from http://link.springer.com/10.1007/978-3-319-44234-1 doi: 10.1007/978-3-319-44234-1

Maeda Corporation. (2016). *Construction report*. Retrieved 2019, from https://www.maeda.co.jp/works/report/genba/56/56-1.html

Masatugu, I. (n.d.). *Rainfall-Runoff Relationship in Small Slope Drainge Area in Japan* (Tech. Rep.). Land Improvement, Dapartment of Land Improvement, Agricultural Engineering Research Station. Retrieved from https://www.jircas.go.jp/ja/file/7074/download?token=1w-DleTW.

McCuen, R. (1996). *Hydrology*. Washington, DC: Federal Highway Administration.

McDonnell, J. J. (2003, jun). Where does water go when it rains? Moving beyond the variable source area concept of rainfall-runoff response. *Hydrological Processes*, *17*(9), 1869–1875. doi: 10.1002/hyp.5132

Meerow, S., Newell, J. P., & Stults, M. (2016). *Defining urban resilience: A review*. doi: 10.1016/j.landurbplan.2015.11.011

Milly, P. C., Betancourt, J., Falkenmark, M., Hirsch, R. M., Kundzewicz, Z. W., Lettenmaier, D. P., & Stouffer, R. J. (2008, feb). *Climate change: Stationarity is dead: Whither water management?* (Vol. 319) (No. 5863). doi: 10.1126/science.1151915

MLIT. (2015a). *Materials for pavement and drainage design standards, 2015 edition* (Tech. Rep.). Author. Retrieved from http://www.mlit.go.jp/common/001157901.pdf

MLIT. (2015b). Rainwater management comprehensive plan development guidelines. Retrieved from http://www.mlit.go.jp/common/001193332.pdf

MLIT. (2016). *Current water reuse practices and challenges in Japan* (Tech. Rep.). Ministry of Land, Infrastructure, Transport and Tourism Government of Japan (MLIT). Retrieved from http://www.lis.edu.es/uploads/108954b0{_}11f9{_}4a8f{_}aca3{_}e56db0985905.pdf

Mori, S. (2018). Utilization of Environmental Water Resources in the Reconstruction of Otsuchi Town After the 2011 Tsunami. In (pp. 175–193). doi: 10.1007/978-981-10-7383-0_13

Mugume, S. N., Diao, K., Astaraie-Imani, M., Fu, G., Farmani, R., & Butler, D. (2015). Enhancing resilience in urban water systems for future cities. *Water Science and Technology: Water Supply*, *15*(6), 1343–1352. doi: 10.2166/ws.2015.098

Nakai, Y. (2013). Reconstruction Plan of Otsuchi Town, Kamihei County, Iwate Prefecture. *Journal of JSCE*, *1*(1), 242–250. doi: 10.2208/journalofjsce.1.1_242

of the Environment; Ministry of Education Culture Sports Science, M., of Agriculture; Forestry, T. M., of Land, F. M., Transport, A. I., & Meteorological, T. J. (2018). *Climate Change in Japan and Its Impacts: Synthesis Report on Observations, Projections and Impact Assessments of Climate Change, 2018* (Tech. Rep.). Retrieved from http://www.env.go.jp/

Otsuchi Town. (2014). *Machikata area, Kodamakura, Nobumatsu area: Reconstruction town development round-table conference* (Tech. Rep.). Reconstrution Bureau Urban Development Division.

Pianosi, F., Beven, K., Freer, J., Hall, J. W., Rougier, J., Stephenson, D. B., & Wagener, T. (2016, may). *Sensitivity analysis of environmental models: A systematic review with practical workflow* (Vol. 79). Elsevier Ltd. doi: 10.1016/j.envsoft.2016.02.008

River Port Section river sabo team. (2019). *River levels Otsuchi 2002-2018* (Tech. Rep.). Iwate Prefecture Coastal Area Promotion Bureau Public Works.

Rossman, L. A. (2006). *Storm Water Management Model* (Vol. I; Tech. Rep.). doi: 10.1145/948542.948544

Rozenberg, J., Guivarch, C., Lempert, R., & Hallegatte, S. (2014). Building SSPs for climate policy analysis: A scenario elicitation methodology to map the space of possible future challenges to mitigation and adaptation. *Climatic Change*, *122*(3), 509–522. doi: 10.1007/s10584-013-0904-3

Sumi, T. (2003). *Spring Water Environmental Survey Report of Ötsuchi (Water Circulation Survey)* (Tech. Rep.). Graduate School of Engineering, Nagoya University.

Takezawa, S., & Barton, P. T. (2016). *The aftermath of the 2011 East Japan earthquake and tsunami : living among the rubble*.

UNISDR. (2017). *Build Back Better - in recovery, rehabilitation and reconstruction* (Tech. Rep.). United Nations Office for Disaster Risk Reduction. Retrieved from https://www.unisdr.org/files/53213{_}bbb.pdf

United Nations General Assembly. (2016). *Report of the Open-Ended Intergovernmental Expert 2 Working Group on Indicators and Terminology Relating to disaster Risk Reduction.* (Tech. Rep.). United Nations General Assembly. Retrieved from https://www.unisdr.org/we/inform/publications/51748

Urban Renaissance Agency. (2013). *Otsuchi Town (Machikata) District Reconstruction and Maintenance Project.* Retrieved 2019, from https://www.ur-net.go.jp/saigai/letter/letter{_}iw201306.html

US EPA. (2015). *Storm Water Management Model User's Manual Version 5.1 Office of Research and Development Water Supply and Water Resources Division* (Tech. Rep. No. September).

van de Ven, F., Furumai, H., & Koga, K. (2008). Urban water in Japan: Introduction. In R. de Graaf & F. Hooimeijer (Eds.), *Urban water in japan* (pp. 1–15). London: Taylor & Francis.

Walker, W. E., Haasnoot, M., & Kwakkel, J. H. (2013). Adapt or perish: A review of planning approaches for adaptation under deep uncertainty. *Sustainability (Switzerland)*, *5*(3), 955–979. doi: 10.3390/su5030955

Wardekker, J. A., de Jong, A., Knoop, J. M., & van der Sluijs, J. P. (2010). Operationalising a resilience approach to adapting an urban delta to uncertain climate changes. *Technological Forecasting and Social Change*, *77*(6), 987–998. Retrieved from http://dx.doi.org/10.1016/j.techfore.2009.11.005 doi: 10.1016/j.techfore.2009.11.005

Weaver, C. P., Lempert, R. J., Brown, C., Hall, J. A., Revell, D., & Sarewitz, D. (2013). *Improving the contribution of climate model information to decision making: The value and demands of robust decision frameworks* (Vol. 4) (No. 1). Wiley-Blackwell. doi: 10.1002/wcc.202

Weibull, W. (1939). A statistical theory of strength of materials. *Ing. Vetensk. Akad. Handl.,*, *151*, 1–45.